Universidad Autónoma de Madrid

UNIVERSIDAD AUTÓNOMA DE MADRID

Programa de Doctorado en Biociencias Moleculares

UNRAVELING THE ROLE OF ARABIDOPSIS ALIX IN THE TRAFFICKING AND TURNOVER OF ABSCISIC ACID RECEPTORS

TESIS DOCTORAL

Marta García León

Madrid, 2019

UNIVERSIDAD AUTÓNOMA DE MADRID

Programa de Doctorado en Biociencias Moleculares

Unraveling the role of Arabidopsis ALIX in the trafficking and turnover of abscisic acid receptors

TESIS DOCTORAL

Marta García León

DIRECTOR

Dr. Vicente Rubio Muñoz

Centro Nacional de Biotecnología CNB, CSIC,

Madrid, 2019

ACKNOWLEDGEMENTS

ABSTRACT

The plant endosomal trafficking pathway controls the abundance of membrane-associated soluble proteins, as shown for ABA (abscisic acid) receptors of the PYR/PYL/RCAR (PYRABACTIN RESISTANCE1/PYR1-LIKE/REGULATORY COMPONENTS OF ABA RECEPTORS) family. ABA receptor targeting for vacuolar degradation occurs through the late endosome route and depends on FYVE1 (FYVE DOMAIN PROTEIN REQUIRED FOR ENDOSOMAL SORTING 1) and VPS23A (VACUOLAR PROTEIN SORTING 23A), components of the ESCRT-I (ENDOSOMAL SORTING COMPLEX REQUIRED FOR TRANSPORT) complexes. FYVE1 and VPS23A interact with ALIX (ALG-2 INTERACTING PROTEIN-X), an ESCRT-III-associated protein, although the functional relevance of such interactions and their consequences in cargo sorting are unknown. Here we show that *Arabidopsis thaliana* ALIX directly binds to ABA receptors in late endosomes, promoting their degradation. Impaired ALIX function leads to altered endosomal localization and increased accumulation of ABA receptors. In line with this, partial loss-of-function *alix-1* mutants display ABA hypersensitivity during growth and stomatal closure, unveiling a role for the ESCRT machinery in the control of water loss through stomata. ABA hypersensitive responses are suppressed in *alix-1* plants impaired in PYR/PYL/RCAR activity, in accordance with ALIX affecting ABA responses primarily by controlling ABA receptor stability. ALIX-1 mutant protein displays reduced interaction with VPS23A and ABA receptors, providing a molecular basis for ABA hypersensitivity in *alix-1* mutants. Our findings unveil a negative feedback mechanism triggered by ABA that acts via ALIX to control the accumulation of specific PYR/PYL/RCAR receptors. Finally, in this study we provide new evidences pointing to the participation of ALIX in other biological processes yet uncharacterized in plants.

RESUMEN

El tráfico endosomal permite a las plantas controlar la abundancia de proteínas transmembranales y proteínas solubles asociadas transitoriamente a la membrana plasmática, como es el caso de receptores de ácido abscísico de la familia PYR/PYL/RCAR (PYRABACTIN RESISTANCE1/PYR1-LIKE/REGULATORY COMPONENTS OF ABA RECEPTORS). La degradación vacuolar de estos receptores ocurre a través de la ruta endosomal y está mediada por las proteínas FYVE1 (FYVE DOMAIN PROTEIN REQUIRED FOR ENDOSOMAL SORTING 1) y VPS23A (VACUOLAR PROTEIN SORTING 23A), dos proteínas pertenecientes al complejo ESCRT-I (ENDOSOMAL SORTING COMPLEX REQUIRED FOR TRANSPORT). Tanto FYVE1 como VPS23A son capaces de interaccionar con ALIX (ALG-2 INTERACTING PROTEIN-X), una proteína asociada al complejo ESCRT-III. Sin embargo, la relevancia funcional de dichas interacciones y su implicación en la selección y tráfico de proteínas cargo se desconoce. En este trabajo mostramos cómo la proteína ALIX de *Arabidopsis thaliana* es capaz de interaccionar directamente con los receptors de ABA en endosomas tardíos, promoviendo su degradación. De hecho, alteraciones en la función de ALIX conducen a una acumulación de los receptores de ABA y a una localización subcelular alterada de los mismos. En línea con esto, los mutantes de pérdida de función *alix-1*, muestran hipersensibilidad al ABA durante el desarrollo y en el cierre estomático, revelando un nuevo papel de la maquinaria ESCRT en el control de la pérdida de agua a través de los estomas. Estas respuestas de hipersensibilidad al ABA que presentan los mutantes *alix-1* son suprimidas al eliminar parcialmente la actividad de los receptores de ABA, lo cuál apoya la idea de que ALIX afecta las respuestas al ABA controlando principalmente la estabilidad de sus receptores. La proteína mutante ALIX-1 muestra una menor interacción con VPS23A y con los receptores de ABA, proporcionando una base molecular que explica la hipersensibilidad al ABA observada en los mutantes *alix-1.* Nuestro estudio desvela por tanto un nuevo mecanismo de regulación negativa de la ruta del ABA, que a través de la proteína ALIX permite controlar la abundancia de PYR/PYL/RCAR específicos.

Además, nuestro trabajo proporciona nuevas evidencias que indican que la proteína ALIX está involucrada en otros procesos biológicos que aún no han sido caracterizados en plantas.

ABBREVIATIONS

ABA	Abscisic Acid
ABA-GE	ABA glucose-este
ABI	ABA insensitive
ALIX	ALG-2 INTERACTING PROTEIN-X
AMSH3	ASSOCIATED MOLECULE WITH THE SH3 DOMAIN OF STAM 3
AP1	ADAPTOR PROTEIN1
AP-2	adaptor protein 2
ARF	ADP-ribosylation factor
BAK1	BRI1 ASSOCIATED RECEPTOR KINASE 1
BAM	BARELY ANY MERISTEM
BAR	Bin-Amphiphysin-Rvs
BiFC	Bimolecular Fluorescence Complementation
BOR1	BORON TRANSPORTER 1
BR	Brassinosteroid
BRI1	BRASSINOSTEROID INSENSITIVE 1
BRM	BRAHMA
CAR	C2-domain ABA-related
CC	Coiled-Coil
CCV	clathrin-coated vesicles
CCVs	clathrin coated vesicles
CERK1	Quitin receptors 1
CHIP	Carboxyl terminus ofHsc70-interacting protein
CHMP4	Charged Multivesicular Body Protein 4
CHX	Cycloheximide
CLE25	CLAVATA3/EMBRYO-SURROUNDING REGION-RELATED 25
CME	Clathrin-mediated endocytosis
Col-0	Columbia-0
CPK	Calcium-Dependent Protein Kinase
CRLs	Cullin-RING ligases
C-t	C-terminal region
CYP707A	Cytochrome P450 707A subfamily monooxygenases
DDA1	DET1, DDB1-ASSOCIATED1
DPA	Dihydrophaseic acid
DUB	deubiquitinases
EDTA	EthyleneDiamineTetraAcetic
EE	Early Endosomes

EGFR	EPIDERMAL GROWTH FACTOR RECEPTOR
ESCRT	ENDOSOMAL SORTING COMPLEXES REQUIRED FOR TRANSPORT
FLS2	FLAGELLIN-SENSING 2
FREE1	FYVE-domain protein required for endosomal sorting 1
FYVE1/FREE1	Fab1b, YOTB, Vac1p, and EEA1/ FYVE DOMAIN PROTEIN REQUIRED FOR ENDOSOMAL SORTING 1
HECT	Homology to E6-Associated-Carboxyl-Terminus
ILV	Intraluminal Vesicles
IPTG	IsoPropyl-D-Thio-Galactopyranoside
IRT1	IRON-REGULATED TRANSPORTER1
K^+	Potassium
LB media	Luria Broth media
LeEix2	Eix receptor
LMB	Leptomycin B
LYK5	LYSIN MOTIF-CONTAINING RECEPTOR-LIKE KINASE5
MS media	Murashige Skoog media
MVB	Multivesicular Bodies
NP-40	Nonidet P-40
oeHAPYL4	overexpressing HA-tagged PYL4
OST1	OPEN STOMATA1
PA	Phaseic acid
PCR	Polymerase Chain Reaction
PHT1	High affinity Phosphate transporter 1
PI3P	phophatidilinositol 3 phosphate
PIN1	PIN-FORMED1
PIN2	PIN-FORMED2
PM	Plasma Membrane
PMSF	PhenylMethylSulfonyl Fluoride
PMSF	Phenylmethylsulfonyl fluoride
PP2C	2C protein phosphatases
Pro-r	Proline-rich
PROS	POSITIVE REGULATOR OF SKD1
PTM	Post-translational modifications
PUB12	plant U-box 12
PUB13	plant U-box 13
PYL1	PYRABACTIN RESISTANCE-LIKE1
PYL2	PYRABACTIN RESISTANCE-LIKE2
PYL3	PYRABACTIN RESISTANCE-LIKE3
PYL4	PYRABACTIN RESISTANCE-LIKE4

PYR/PYL/RCAR	PYRABACTIN RESISTANCE1/PYR1-LIKE/REGULATORY COMPONENTS OF ABA RECEPTORS
QUAC1	QUICKLY ACTIVATING ANION CHANNEL 1
RAE1	RNA EXPORT FACTOR 1
RBOHF	Respiratory Burst Oxidase HomologF
RGLG	RING DOMAIN LIGASE
RIFP1	RCAR3-INTERACTING F-BOX PROTEIN1
RIM20	Regulator of IME2 20
RING	Really Interesting New Gene
RLKs	receptor-like kinases
RLS1	RING FINGER OF SEED LONGEVITY1
ROS	Reactive Oxygen Species
RT-Qpcr	Reverse Transcription quantitative PCR
SH3P2	SH3 domain-containing protein 2
SH3P2	Src homology-3 (SH3) domain-cointaining protein 2
SLAC1	SLOW ANION CHANNEL-ASSOCIATED1
SNF7	SUCROSE NON-FERMENTING 7
SnRK2s	SNF1-RELATED PROTEIN KINASE2
TAP-tag	Tandem-affinity purification assays
TFs	Transcription factors
TGN	Trans Golgi Network
TOLs	TOM1-LIKE PROTEINS
TOR	Target of Rapamycin
UPS	Ubiquitin proteasome system
VIP1	VirE2-interacting protein 1
VPS2	VACUOLAR PROTEIN-SORTING-ASSOCIATED PROTEIN2
VPS2.1	VACUOLAR PROTEIN SORTING 2.1
VPS23A	VACUOLAR PROTEIN SORTING 23A
VPS25	VACUOLAR PROTEIN-SORTING-ASSOCIATED PROTEIN25
VPS36	VACUOLAR PROTEIN-SORTING-ASSOCIATED PROTEIN36
VSR1	VACUOLAR SORTING RECEPTOR1
VSR4	VACUOLAR SORTING RECEPTOR4
WM	Wortmannin
Y2H	Yeast two hybrid
YFP	Yellow Fluorescent Protein

LIST OF FIGURES

LIST OF TABLES

INDEX

1. INTRODUCTION

1.1. Plant proteostasis

In order to thrive and survive, both eukaryotic and prokaryotic cells have to be able to perceive and rapidly respond to internal and external stimuli. The capability to control the abundance, and therefore the activity of specific protein components at different compartments, is vital to maintain cell homeostasis and to trigger developmental and physiological responses that allow plants to adapt to the ever changing environment (Winter and Hauser, 2006). Distinct mechanisms, both specific and non-specific, allow plants to control the abundance of different sets of key proteins. Among them we can find the ubiquitin-proteasome system (UPS), endocytic degradation and autophagy (Kalinowska & Isono, 2017).

1.1.1. Ubiquitin proteasome system (UPS)

The UPS is the most important proteolytic system in eukaryotes and is responsible of the degradation of a myriad of key proteins involved in different processes. Inded, in *Arabidopsis thaliana* it has been estimated that 6% of its proteome corresponds to components of the UPS (Vierstra, 2009). The system consists in two consecutive steps: the first one attaches an ubiquitin chain to a target protein, tagging it for its degradation. In the second step, the tagged protein is recognized and degraded by the 26S proteasome, which is a mutiprotease complex composed by two subparticles, the 20S core protease (with the proteolytic activity) and the 19S regulatory particle (responsible of recognizing Ub-tagged proteins (Book et al., 2010)).

The process of tagging proteins with ubiquitin moeities is named ubiquitination. This process requires the concert activity of three enzymes: E1, E2 and E3. E1 enzymes activate ubiquitin, which is then transferred to the E2 conjugating enzyme. The final step is catalyzed by E3 ligases that provide target specificity and facilitate the transference of the ubiquitin from the E2 enzyme to the substrate, normally to a lysin (K) residue. The conjugative process can be repeated several times rendering polyubiquitin chains (Stone et al., 2019; Figure 1). The Arabidopsis genome codifies hundreds of E3 ligases that are able to target multiple specific substrates (Figure 2).

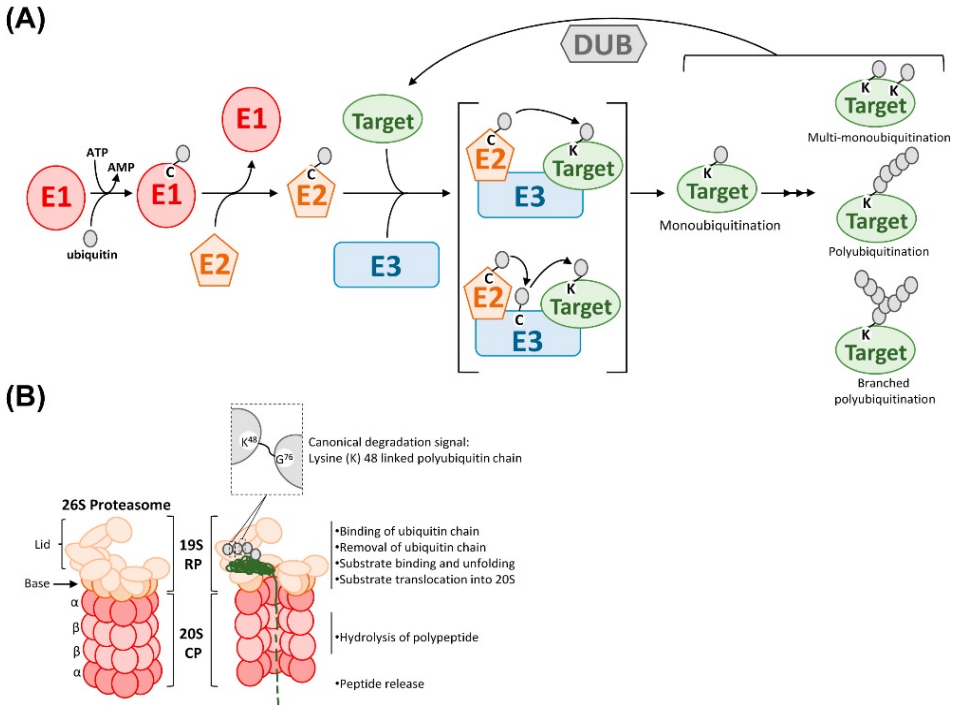

Figure 1. The UPS (Ubiquitin Proteasome System). Adapted from Stone 2019

(A) Scheme showing the E1, E2 and E3 ubiquitin enzymes working in concert in the process of ubiquitination.

(B) Representation of the 26S proteasome degrading a protein tagged with a Lys-48 linked ubiquitin chain

In plants, E3 ligases can be classified in four major groups depending on the presence of different domains: HECT (Homology to E6-Associated-Carboxyl-Terminus), RING (Really Interesting New Gene), U-box and Cullin-RING ligases (CRLs; which are the most abundant group; Figure 2; Stone et al., 2019). The location of the attachment and the extent of the polymer of ubiquitin molecules alters the fate of the ubiquitinated protein (Vierstra, 2009). For instance ubiquitin chains linked by the lysine 48 (Lys-48) direct proteins for their degradation in the 26S proteasome whereas ubiquitin chains linked to lysine 63 (Lys-63) are the most common signal to trigger vesicular trafficking (Paez-Valencia et al., 2016). Thus, different types of ubiquitination may alter the abundance, localization, activity and interaction ability of an ever growing number of targets. Indeed, over the last decades, it has been demonstrated the participation and relevance of the UPS in almost every key biological process in plants. It has an essential role in controlling plant growth, carbon and nitrogen metabolism (Sato et al., 2011),

abiotic and biotic responses, chromatin remodeling, hormone signaling and many others. Fine tune regulation of all these processes is vital for plants to cope with all the environmental changes they have to face (Vierstra, 2009; Sharma et al., 2016).

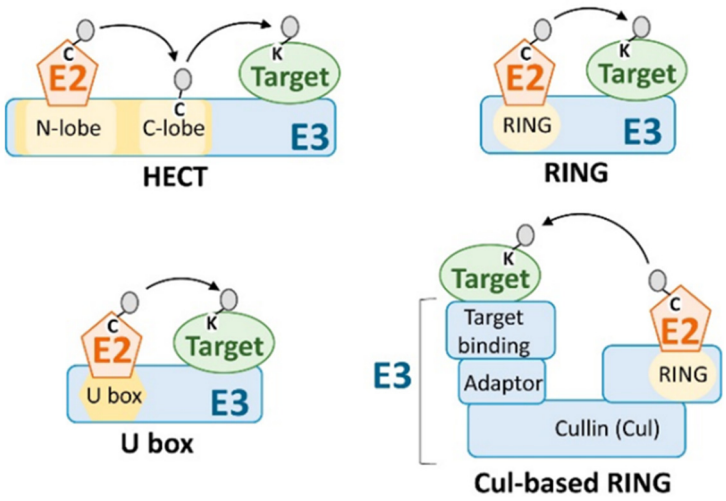

Figure 2. Scheme of the main families of ubiquitin E3 ligases. Adapted from Stone 2019

1.1.2. Autophagy

Autophagy is conserved in eukaryotes, from yeast and mammals to plants. Whereas autophagy is essential in other organisms, such as mammals, in which a lack of autophagy causes neurodegenerative diseases and cancer, in plants, autophagy seems to be dispensable under optimal growth conditions. However, under harsh environmental conditions, autophagy plays a key role removing protein aggregates and damaged or aging organelles. Indeed, it has been shown that plays a key role in embryogenesis, pollen germination and male gametogenesis in rice (Kalinowska & Isono, 2018).

There are two types of autophagy, selective and non-selective (also known as macroautophagy). In selective autophagy, whole damaged organelles, protein aggregates or pathogens are tagged with ubiquitin which is then recognized by ubiquitin-binding autophagic receptors. In non-selective autophagy, a nascent membrane (autophagosome membrane) grows to enclose a portion of cytoplasm that is delivered to the lytic vacuole for degradation.

Recent studies over the past years indicate that autophagy largely depends on the endosomal trafficking machinery and that both processes are functionally connected (Murrow et al., 2015). For instance, the specific plant component FYVE1/FREE1 (Fab1b, YOTB, Vac1p, and EEA1/ FYVE DOMAIN PROTEIN REQUIRED FOR ENDOSOMAL SORTING 1) plays dual roles, participating in both the MVB (multivesicular body) pathway and in autophagic degradation (Gao et al., 2015). Moreover, mutants in components of the ESCRT (ENDOSOMAL SORTING COMPLEXES REQUIRED FOR TRANSPORT) machinery produce defects in autophagy in plants, such as impairment in autophagosome biogenesis, transport, fusion and degradation or accumulation of autophagosomes (Gao et al., 2017; Kalinowska & Isono, 2018). Future studies will shed light on the precise molecular mechanisms and components that link both regulatory processes.

1.1.3. Endosomal sorting

The endomembrane system is conserved among eukaryotes and plays essential roles in controling abundance of membrane-associated proteins, exocytosis and storage of distinc molecules and substances as we describe in the following section.

1.2. Endocytosis and endosomal trafficking

Endosomal trafficking and endocytosis are vital proccesses to control the abundance of plasma membrane proteins and maintain cellular homeostasis. During endocytosis, patches of the PM (plasma membrane) containing cargo proteins and lipids, together with extracelular components are invaginated in endocytic vesicles. CME (Clathrin-mediated endocytosis) is the most prominent endocytic pathway in both plants and animals. CME occurs in five steps: nucleation, cargo selection, clathrin coat assembly, membrane scission and uncoating. Since clathrin can not directly interact with cargo proteins, there are different adaptor and accessory proteins that mediate the interaction among them, being the most important AP-2 (ADAPTOR PROTEIN 2). (McMahon et al., 2011; Paez-Valencia et al., 2016)

After endocytosis, plasma membrane proteins present at endosomes, can be recycled back to the plasma membrane, sorted for degradation to the lytic vacuole or even can be kept participating in downstream signaling pathways (Figure 3; Otegui & Reyes, 2010).

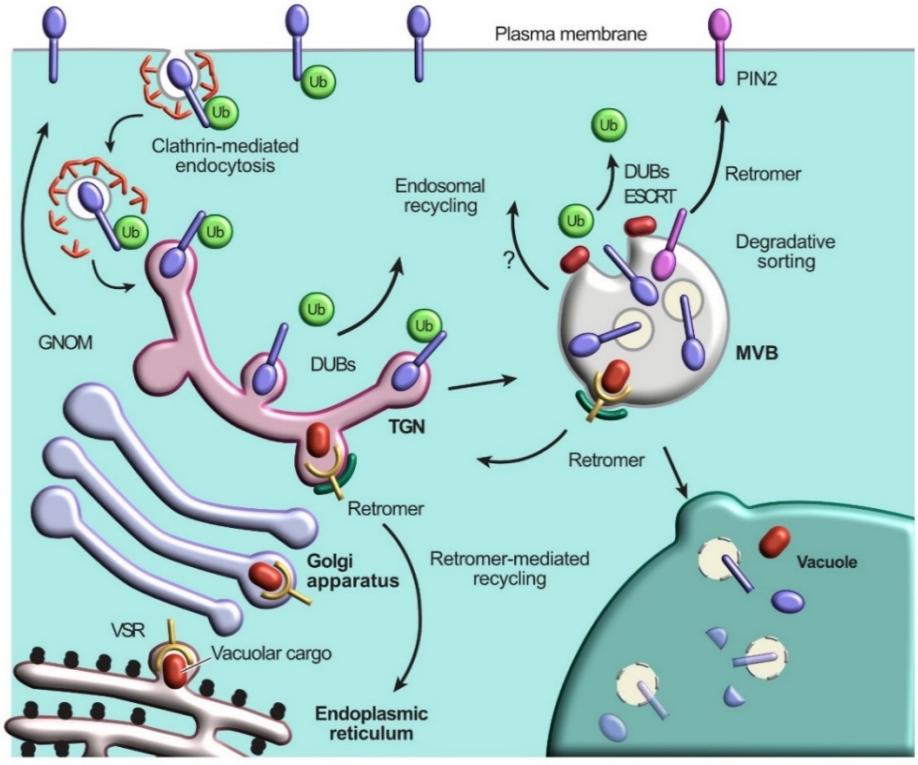

Figure 3. Representation of the plant endosomal trafficking system in plants. Adapted from Paez Valencia

Abbreviations: Ub, ubiquitin; DUBs, deubiquitinases; TGN, Trans-Golgi Network; MVB, Multivesicular Body; VSR, VACUOLAR SORTING RECEPTOR

1.2.1. Protein recycling

Some integral plasma membrane proteins are constitutively cycled in and out of the membrane to early endosomes close to it. This mechanism allows plants to rapidly control the composition of the plant PM since they have always available at the EE (early endosomes) a pool of PM proteins ready to be cycled back; some examples are the boron transporter BOR1 (BORON TRANSPORTER 1), the flagellin receptor FLS2 (FLAGELLIN-SENSING 2), the brassinosteroid receptor BRI1 (BRASSINOSTEROID INSENSITIVE 1), the auxin carrier PIN2 (PIN-FORMED2) or the potassium (K^+) channel KAT1 (Otegui & Reyes, 2010; Reyes et al., 2011; Paez-Valencia et al., 2016). As it occurs it animals, plant hormones can modulate the endocytosis rate, for instance auxins inhibits endocytosis (Paciorek et al., 2007) whereas abscisic acid promotes it.

There are two complexes involved in protein recycling not only back to the PM but also among other compartments of the endomembrane system. One of these complexes is the ARF (ADP-ribosylation factor) machinery which comprises two subfamilies in *Arabidopsis,* the BIG (Brefeldin A-inhibited GEF) and the GBF subfamily (Richter et al., 2007). The latter one includes the ARF-GEF (ARF GTPase) GNOM (that facilitated the exchange of GDP/GTP in ARF GTPases), which affects the recycling of some PM proteins such as the auxin carrier PIN1 (PIN-FORMED1). Lately, the subcellular localization of GNOM has been defined preferentially in the Golgi apparatus, and the exact mechanisms through which it participates in protein recycling are yet undefined (Paez-Valencia et al., 2016).

The other complex involved in recycling at endosomes is the retromer, a pentameric complex whose exact localization is not clear yet, as it could involve MVB or TGN (Trans Golgi Network), although recent studies support the presence of retromer subunits at MVBs (Hear et al., 2015). This complex has been involved in the recycling of biosynthetic receptors such as the vacuolar sorting receptor VSR1 (VACUOLAR SORTING RECEPTOR1) from MVBs back to the TGN, but also has an important role in the trafficking of proteins back to the PM, as it occurs with the auxin efflux carriers from the PIN family (PINFORMED) (Reyes et al., 2011). Nevertheless, as it occurs with the ARF small GTPases, further studies are needed to eventually understand the molecular details and the mechanisms by which the retromer acts.

1.2.2. Endosomes as signaling platforms

The endomembrane system is also a pivotal signalling platform. In mammals, some active receptors sorted and accumulated on the endosome surface such as the EGFR (EPIDERMAL GROWTH FACTOR RECEPTOR), are able to continue transducing signals. Indeed, they are even able to interact with specific signaling components present only at endosomes, generating signals different from the ones produced at the plasma membrane and continuing with the signaling cascades (Murphy et al., 2009). There are recent evidences showing that, as it occurs in mammals, plant endosomes likely act as signaling platforms. For instance, LeEix2 (Eix receptor), an ethylene responsive LRR (LEUCINE RICH RECEPTOR) that mediates plant defense, has been reported to signal at least partially from endosomes. Nevertheless, further studies are needed to provide irrefutable evidences showing that endosomes are signaling hubs also in plants (Bar et al., 2014).

1.2.3. Degradative sorting of cargo proteins

The attachment of an ubiquitin moiety (or chains of ubiquitin with specific configurations) to the cytosolic domain of cargo proteins is the most common signal to trigger their sorting into ILVs (Intraluminal vesicle; Gruenberg and Stenmark, 2004). At EE (also known as TGN), cargo proteins that have not been recycled are targeted for degradation to the vacuole via MVBs (also termed late endosomes, or prevacuolar compartments). The latter requires sorting and internalization of cargos into ILVs, which will be released into the vacuolar lumen upon fusion of the MVB with the tonoplast (Cui et al., 2016). Selective recognition and packaging of ubiquitinated cargos into ILVs is mediated by ESCRT protein complexes (Conibear, 2002; Winter and Hauser, 2006; Nickerson et al., 2007; Henne et al., 2011). Five ESCRT complexes have been described in eukaryotes; ESCRT-0-, -I, -II, -III, and the ESCRT-III-associated SKD1/Vps4 (SUPPRESSOR OF K+ TRANSPORT GROWTH DEFECT1/VACUOLAR PROTEIN SORTING4) complex (Table 1; Gao, 2017). In mammals and yeast it has been demonstrated that ESCRT-0 is able to interact with ESCRT-I subunits, leading to the recruitment of other ESCRT components to initiate ILV budding (Gao et al. 2017; Korbei et al., 2013). Moreover, recent studies in *Caenorhabditis* elegans have shown that ESCRT-0 is able to interact with clathrin adaptor proteins, such as members of the AP-2 complex, establishing a link between CME and ESCRT-mediated clustering of ubiquitinated cargos (Mayers et al., 2013). Plants lack canonical ESCRT-0 orthologs, however plant genomes codify nine TOLs (TOM1-LIKE PROTEINS) proteins that are able to bind ubiquitin. In fact, studies in *Arabidopsis thaliana* have demonstrated the capability of some TOL proteins to bind ubiquitin and regulate the internalization and sorting of specific cargo proteins, such as the auxin carrier PIN2 (Winter and Hauser, 2006; Richardson et al., 2011; Reyes et al., 2011; Paez-Valencia et al., 2016; Gao et al., 2017). Interestingly, a recent study proposed that the endosomal protein SH3P2 (Src homology-3 (SH3) domain-containing protein 2) may share main features with canonical ESCRT-0 proteins. Indeed, SH3P2 is able to bind ubiquitin and to associate with the ESCRT-I subunit VPS23A (VACUOLAR PROTEIN SORTING 23A), the deubiquitinase (DUB) AMSH3 (ASSOCIATED MOLECULE WITH THE SH3 DOMAIN OF STAM 3) and with CCVs (Clathrin Coated Vesicles). In this context, SH3P2 may act at the very early stages of cargo recognition as an ubiquitin adaptor in the ESCRT pathway (Nagel et al., 2017; Mosesso et al., 2019).

Table 1. ESCRT Components in yeast, human and Arabidopsis and their functions in plants. Adapted from Gao et al., 2017.

Abbreviations: AGI, Arabidopsis gene identifier number; At, Arabidopsis thaliana; Sc, Hs, Homo sapiens; N.I. Not identified; Saccharomyces cerevisiae.

Regulators	Yeast (Sc)	Human (Hs)	Arabidopsis (AGI of At)	Functional annotation in plants
ESCRT-0	VPS27	HRS	N.I.	
	Hse1	STAM1,2	N.I.	
Proteins show functional analogies to ESCRT-0	GGA1, 2	GGA1, 2, 3		
		TOM1 TOM1L1 TOM1L2 TOM1L3	TOL1 (At5g16880)	TOL-2, -3, -5, -6, -9 are involved in endosomal sorting of PIN2 and plant development
			TOL2 (At1g06210)	
			TOL3 (At1g21380)	
			TOL4 (At1g76970)	
			TOL5 (At5g63640)	
			TOL6 (At2g38410)	
			TOL7 (At5g01760)	
			TOL8 (At3g08790)	
			TOL9 (At4g32760)	
ESCRT-I	VPS23	TSG101	VPS23A/ELC (At3g12400)	Endosomal sorting, viral replication, cytokinesis, endosomal trafficking of ABA receptors
			VPS23B (At5g13860)	Viral replication
	VPS28	hVPS28	VPS28-1 (At4g21560)	Endosomal sorting
			VPS28-2 (At4g05000)	Endosomal sorting, immune response against bacterial pathogens
	VPS37	VPS37 A, B, C, D	VPS37-1 (At3g53120)	Endosomal sorting, immune response against bacterial pathogens
			VPS37-2 (At2g36680)	
	MVB12	hMVB12A, B	N.I.	
	N.I	N.I	FREE1/FYVE (At1g20110)	MVB and vacuole biogenesis, endosomal sorting of integral membrane proteins such as PIN2 and IRT1, endosomal sorting of the non-integral membrane proteins that are ABA receptors, autophagic degradation
ESCRT-II	VPS22	EAP30	VPS22 (At4g27040)	MVB biogenesis
	VPS25	EAP20	VPS25 (At4g19003)	MVB biogenesis
	VPS36	EAP45	VPS36 (At5g04920)	MVB biogenesis, endosomal sorting

Regulators	Yeast (Sc)	Human (Hs)	Arabidopsis (AGI of At)	Functional annotation in plants
ESCRT-III and accessory proteins	VPS20	CHMP6	VPS20-1 (At5g63880)	MVB biogenesis, endosomal sorting
			VPS20-2 (At5g09260)	
	SNF7 (VPS32)	CHMP4A, B, C	SNF7-1 (At2g19830)	MVB biogenesis, endosomal sorting, viral replication
			SNF7-2 (At4g29160)	Viral replication
	VPS24	CHMP3	VPS24-1 (At5g22950)	MVB biogenesis, endosomal sorting, viral replication
			VPS24-2 (At3g45000)	
	VPS2	CHMP2A, B	VPS2-1 (At2g06530)	MVB biogenesis, endosomal sorting, autophagic degradation
			VPS2-2 (At5g44560)	
			VPS2-3 (At1g03950)	
	Did2	CHMP1,5, CHMP1A, CHMP1B	CHMP1A (At1g73030) CHMP1B (At1g17730)	MVB biogenesis, endosomal sorting, chlorophagy
	VPS60	CHMP5	VPS60-1 (At3g10640)	MVB biogenesis, endosomal sorting
			VPS60-2 (At5g04850)	
	IST1		ISTL1 (At1g34220)	MVB biogenesis, plant immunity, and cell death
	Cmp7	CHMP7	CHMP7 (At3g62080)	Senescence, abiotic stress
				responses
VPS4 and accessory proteins	VPS4	VPS4/SKD1	VPS4/SKD1 (AT2G27600)	MVB biogenesis, endosomal sorting, viral replication, plant immunity, cytokinesis
	VTA1	LIP5	LIP5 (AT4g26750)	MVB biogenesis, endosomal sorting, plant basal immunity, abiotic stress responses
	N.I	N.I	PROS (At4g24370)	Regulate SKD1 ATPase activity and plant cell expansion
Other ESCRT-related proteins	BRO1	ALIX	BRO1/ALIX (AT1G15130)	MVB and vacuole biogenesis, endosomal sorting, viral replication
			Bro1L1 (AT1G17940)	
			Bro1L2 (AT5g14020)	
	Doa4	AMSH	AMSH1 (AT1G48790)	Autophagic degradation, plant immune response to mildew infection
			AMSH2 (AT1G10600)	
			AMSH3 (At4g16144)	Vacuole biogenesis, endosomal sorting, autophagic degradation

On the contrary to what occurs with ESCRT-0, specific plant ESCRT components have been characterized, such as FREE1/FYVE protein, which participates in MVB formation and sorting of transmembrane and non-transmembrane cargos. Another plant specific component is PROS (POSITIVE REGULATOR OF SKD1), which regulates the activity of the ATPase SKD1 (Gao et al., 2014; Reyes et al., 2014; Gao et al., 2015; Kolb et al., 2015; Belda-Palazon et al., 2016).

In the current model, ubiquitinated cargo proteins are recognized at the plasma membrane or early after their internalization by the TOL-like proteins, which would act as members of the ESCRT-0; afterwards protein cargos would be transferred to the ESCRT-I and -II thanks to the ubiquitin-binding activity of FREE1/FYVE1, VPS23 (ESCRT-I) and VPS36 (VACUOLAR PROTEIN-SORTING-ASSOCIATED PROTEIN 36; ESCRT-II), that will cluster them on the MVB surface (Shields and Piper, 2011; McGurn et al., 2012; Henne et al., 2013; Gao et al., 2017). Additionally, ESCRT-I and -II complexes associate to trigger membrane deformation and initiate ILV formation (Katzmann et al., 2001; Babst et al., 2002a). This process is further continued thanks to the ESCRT-II subunits VPS25 (VACUOLAR PROTEIN-SORTING-ASSOCIATED PROTEIN25) and VPS20 (VACUOLAR PROTEIN-SORTING-ASSOCIATED PROTEIN20), that recruit and activate the polymerization of ESCRT-III subunits (including SNF7 and VPS2; VACUOLAR PROTEIN-SORTING-ASSOCIATED PROTEIN2). The later enable cargo concentration and engulfment inside ILVs, avoiding their diffusion out of ILVs (Babst et al., 2002b; Wemmer et al., 2011). Prior to the scission of the ILV, protein cargos are deubiquitinated by AMSH-type DUBs to recycle the ubiquitin moieties (Swaminathan et al., 1999; Reggiori and Pelham, 2001; Kyuuma et al., 2007; McNatt et al., 2007; Isono et al., 2010; Katsiarimpa et al., 2011; Wright et al., 2011). For this, Bro1-domain containing proteins (Bro1 in yeast and ALIX in plants and animals) associate to ESCRT-III subunit Vps32/SNF7 and recruit the deubiquitinases to the MVBs to remove ubiquitin from ubiquitinated cargos (Missotten et al., 1999; Luhtala and Odorizzi, 2004; Cardona-López et al., 2015; Kalinowska et al., 2015; Shen et al., 2016). Last step involves disassembly and dissociation of the ESCRT machinery from the MVB surface by SKD1/Vps4 (Figure 4; Babst, 2005).

The overall sequence of events of the ESCRT machinery in cargo sorting is well established, however, due to the high dynamism and constant maturation of the endocytic system, the details underlying how exactly the ESCRT machinery binds

cargos and how they orchestrate the ILV formation remains unknown and will require further investigation.

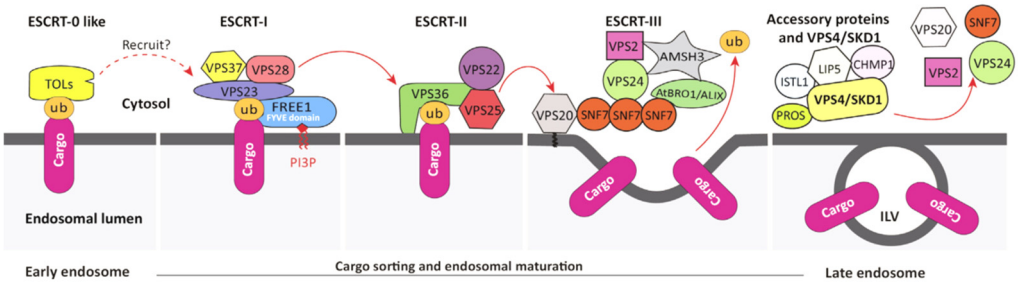

Figure 4. ESCRT-mediated sorting of cargo proteins. Adapted from Gao et al., 2017

During all this process MVB mature, acquiring the capacity to fuse to the tonoplast, releasing the ILV into the vacuolar lumen, where they are degraded together with their cargos.

1.3. Signals for cargo selection

The selection of the PM proteins that will to undergo endocytosis depends on the existance of different types of signals that tag them as endocytic cargos. Overall, signals can be classified in: linear amino acid and conformational motifs and posttranslational modifications (ubiquitination and phosphorylation; Paez-Valencia et al., 2016), nevertheless there can be more than one sorting signal in the same cargo protein. These signals are directly recognized by adaptor proteins, which mediate the interaction with the clathrin coat, or by members of the ESCRT machinery.

1.3.1. Linear amino acid and conformational motifs

In animals, it has been described that the adaptor protein AP-2 contains specific pockets in its structure, capable of recognizing two amino acidic motifs in cargo proteins, a di-Leu based motif and a Tyr-based motif (Kelly et al., 2011). However to date, the knowledge about the motifs involved in the sorting of plant protein cargos into CCV is very limited. Some reports have shown that the sorting of BOR1 (the borate transporter), LeEix2 (the tomato ethylene responsive leucine rich receptor) and KORRIGAN (an endoglucanase necessary for cell wall remodeling) depends on Tyr-

based motifs located in their cytosolic domains (Paez-Valencia et al., 2016). Nevertheless, only a few studies demonstrate the interaction of protein adaptors with specific motifs present in cargo proteins. One of them, has shown that the residue Phe-165 located in the cytosolic loop in the auxin transporter PIN1 is necessary for the binding to subunits of the AP-3 complex that is necessary for the correct trafficking of PIN1 (Sancho-Andrés et al., 2016). Another study published in 2016 discovered a tyrosine-sorting motif (YMPL) in the vacuolar sorting receptor VSR4 (VACUOLAR SORTING RECEPTOR4) able to interact with a subunit of the AP-1 (ADAPTOR PROTEIN1) complex (Nishimura et al., 2016). Altogether, these studies support the notion that similarly to animals systems, it is very likely the existence of sorting signals in plant protein cargos that determine their endocytosis.

1.3.2. Post-translational modifications (PTM)

The most common signal to trigger endocytosis and sorting of protein cargos into ILV is ubiquitination. E3 ubiquitin ligases involved in the ubiquitination of cargo proteins to tag them for endocytosis contain transmembrane domains or can associate to the plasma membrane. For example, PUB13 (plant U-box 13) lacks a transmembrane domain, but can interact with phospholipids embedded in membranes (Antignani et al., 2015) and together with PUB12 (plant U-box 12) ubiquitinate RLKs (RECEPTOR-LIKE KINASES), such as BRI1 and FLS2. Other E3 ligases, such as IDF1 (IRT1 DEGRADATION FACTOR1) or RSL1 (RING FINGER OF SEED LONGEVITY1) contain transmembrane domains and are located at the PM, where they ubiquitinate IRT1 (IRON-REGULATED TRANSPORTER1), and PYL4 (PYRABACTIN RESISTANCE-LIKE4), respectively. Until recently, all identified protein cargos of the ESCRT machinery in plants corresponded to integral proteins. However the report of PYL4, which is a soluble protein, as cargo of the MVB route widens the landscape of possible cargos of the plant endocytic pathway (Belda-Palazon et al., 2016; Yu et al., 2016).

Other important PTM (Post-translational modification) that affects the endocytosis of many PM proteins is phosphorylation. For instance LYK5 (LYSIN MOTIF-CONTAINING RECEPTOR-LIKE KINASE5), a receptor-like kinase involved in chitin signaling, is phosphorylated by chitin-activated CERK1 (CHITIN ELICITOR RECEPTOR KINASE1) inducing its endocytosis (Erwig et al., 2017). In many cases, phospho/dephosphorilation and ubiquitination are both necessary to trigger endocytosis of certain receptors, such as BRI1 (Zhou et al., 2018).

1.4. Functional relevance of the MVB pathway in protein cargo trafficking in plants

The MVB pathway is essential to switch off the signaling or activity from transmembrane and membrane-asssociated proteins, since their constitutive activity may have deleterious effects for plant fitness. In other cases, vacuolar degradation of cargos may serve as a mean to modulate the distribution of phytohormones or nutrients (Marhavy et al., 2011; Yoshinari et al., 2016)

PM proteins that undergo endocytosis and vacuolar degradation can be divided into three groups. First group corresponst to PM localized PRR (PATTERN RECOGNITION RECEPTORS) that, upon binding of its ligand, undergo endocytosis to control plant immune responses. An example is the flagellin receptor FLS2. The second category includes nutrient/ion and water transporters whose regulation plays a key role in plant cell homeostasis. Among them are the boron transporter BOR1, the iron transporter IRT1 or the phosphate transporter PHT1 (HIGH AFFINITY PHOSPHATE TRANSPORTER1). Finally, the last group are hormone transporters and receptors, such as PIN auxin transporters, the brassinosteroid receptor BRI1 or the fraction of soluble PYR/PYL/RCAR (PYRABACTIN RESISTANCE1/PYR1-LIKE/REGULATORY COMPONENTS OF ABA RECEPTORS) ABA receptors that can transiently bind to membranes.

1.4.1. Boron transporter BOR1

Boron uptake has to be tightly regulated since it is an essential nutrient. However, excessive levels are toxic for the cell. For this reason, plant cells control the abundance of the boron transporter BOR1 at their plasma membranes. The presence of high boron levels induces the ubiquitination of the transporter BOR1 with Lys-63 ubiquitin chains (Kasai et al., 2011) which together with a Tyr-based motif in its cytosolic domain (Takano et al., 2010), triggers its vacuolar degradation in order to avoid the excessive uptake of boron. As it occurs with PIN proteins, endocytosis and vacuolar degradation of this transporter is also essential to modulate its polar distribution (Figure 5A).

1.4.2. Iron transporter IRT1

Similarly to what occurs with boron, excessive iron levels are toxic for cells since they produce oxidative stress. For this reason, IRT1 levels at the plasma membrane are highly controlled to ensure an optimal iron uptake. It has been demonstrated that IRT1

is monoubiquitinated and constantly cycled in and out of the PM to maintain proper transporter levels at the PM. However, a fraction of the endocytosed Ub-IRT1 is sorted for vacuolar degradation to keep the turnover (Figure 5B; Barberon et al., 2011).

1.4.3. BRI1

Arabidopsis BRI1 encodes a LRR RLK (RECEPTOR LIKE KINASE) that upon brassinosteroid (BR) perception through its extracellular domain, it associates to another RLK, BAK1 ((BRI1)-ASSOCIATED KINASE 1), and they transphosphorylate each other amplifying the downstream signaling in response to BR (Eckardt et al., 2005; Wang et al., 2008). In addition, after BR perception, BRI1 associates to the E3 ligases PUB12 and 13. BRI1 activates PUB13 by directly phosphorylating it. In turn, PUB12 and PUB13 ubiquitinate the brassinosteroid receptor, tagging it for its subsequent endocytosis and degradation at the vacuole (Figure 5C).

1.4.4. Flagellin receptor FLS2

FLS2 is a receptor-like kinase (RLK) present at the plasma membrane that recognize flagellin (flg22), a highly conserved peptide present in bacterial flagella, triggering several defense responses to allow plants to fight infections. Similarly to what occurs with IRT1, FLS2 is constantly cycled from the plasma membrane to early endosomes. However, upon flg22 perception, FLS2 associates with the kinase BAK1. BAK1 recruits the E3 ubiquitin ligases PUB12 and 13 (shared with BRI1) to the receptor complex, phosphorylating them, and in turn, PUB12 and 13 polyubiquitinate FLS2 promoting its vacuolar degradation (Figure 5D; Robatzek et al., 2013; Lu et al., 2011; Spallek et al., 2013).

1.4.5. Phosphate transporter PHT1

The phosphate transporters allow phosphate uptake at the roots and its distribution accross the plant organs and tissues. The levels of PHT1 at the PM are tightly regulated at both transcriptional and post-translational levels. PHT1 is highly induced under phosphate starvation conditions, and newly synthesized proteins are transported from the ER (endoplasmic reticulum) to the PM. However, when phosphate levels are high, PHT1 is retained at the ER and PM-located PHT1 is endocytosed and sorted for degradation to the vacuole in order to reduce PHT1 abundance at the plasma membrane (Bayle et al., 2011; Cardona-López et al., 2015).

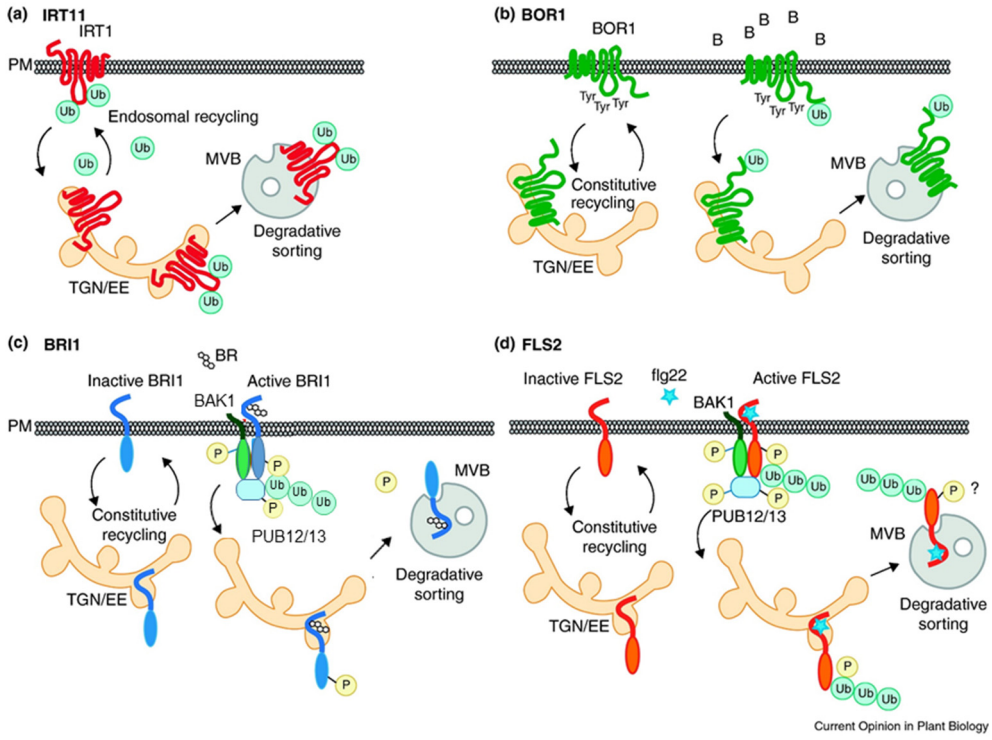

Figure 5. Examples of cargo proteins in the MVB pathway. Adapted from Reyes et al., 2011

1.4.6. PIN auxin transporters

PIN auxin efflux carriers are one of the best characterized cargos of the endomembrane system. Thanks to the subcellular trafficking of PINs, they are polarly distributed at PM domains, allowing auxin fluxes intra and extracellularly. As it occurs with other cargos, PINs dynamically cycle from the PM to early endosomes to maintain the polarized location of PINs at the PM. Polar sorting of specific PINs for their degradation in the vacuole depends on ubiquitination with Lys-63 ubiquitin chains as it has been seen for PIN2 (Leitner et al., 2012).

1.4.7. PYL ABA receptors

PYR/PYL/RCAR ABA receptors (named as PYLs hereafter for simplicity) are encoded by a multigenic family with different subcellular localizations. They can perceive ABA intracellularly or close to the PM, initiating signaling cascades to this hormone. Until

recently, all the mechanisms described to control ABA receptor abundance invoked the 26S proteasome system. However, very recent studies have demonstrated that PYLs can bind to the PM, and there they can be ubiquitinated, entering in the endosomal pathway for their vacuolar degradation (Belda-Palazón et al., 2016). This mechanism should limit plant responses to ABA when the stress conditions turn back to be optimal.

1.5. Abscisic acid (ABA)

Abscisic acid (ABA) is one of the most important phytohormones that regulates many developmental and growth processes (including embryo maturation, dormancy, seed germination, cell division and elongation and floral induction) and responses to abiotic and biotic stresses (such as water deprivation, high salinity, cold, UV radiation and pathogen attacks) (Finkelstein et al., 2013; Nakashima et al., 2013). In fact, in *Arabidopsis thaliana* ABA regulates the expression of approximately 10% of protein coding-genes, a much larger subset than those controlled by other phytohormones (Nemhauser et al., 2006). As well, ABA has a key role in controlling stomatal movements which is essential to help plants to fight drought and pathogen attack (Munemasa et al., 2015).

1.5.1. ABA signaling pathway

In *Arabidopsis thaliana*, ABA is perceived by a family of 14 receptors known as PYR/PYL/RCAR (named hereafter as PYLs) that can be classified in 3 phylogenetically different subfamilies. All the receptors that belong to the PYR1 subfamily (PYR1, PYL1, PYL2 and PYL3) are dimeric, whereas the other 10 receptors are monomeric and display higher ABA affinity (Figure 6A; Helander et al., 2016). Despite they display functional redundancy, they likely have certain specificity since they show differential subcellular localizations, including the cytoplasm, the nucleus, like PYL8, or close to the PM, like PYL4 (Belda-Palazón, et al., 2016; Yu et al., 2016).

PP2Cs (TYPE 2C PROTEIN PHOSPHATASES) are negative regulators of the ABA pathway. In the absence of ABA, PP2Cs dephosphorylate members of the SnRK2s (SNF1-related protein kinase 2) family of kinases (including SnRK2.2, 2.3. and 2.6/OST1) inhibiting its kinase activity. When ABA is present, PYLs bind it and as a result, they form ternary complexes with PP2Cs repressing them (Ma et al., 2009; Archana et al., 2011). Since PP2Cs remain now sequestered, SnRK2s are free to self-activate them, and

phosphorylate specific protein targets (Sheard et al., 2009). Downstream targets include TFs (transcription factors), mainly belonging to the bZIP family of TFs, such as AREB/ABFs and ABI5 (Fujita et al., 2011). SnRK2s can also phosphorylate PM proteins such as the potassium channel KAT1 (Sato et al., 2009), the ion channel SLAC1 (SLOW ANION CHANNEL-ASSOCIATED1; phosphorylated by SnRK2.6/OST1, which is very important in guard cell responsiveness to ABA; Geiger et al., 2009) or the anion/proton exchanger CLCa that has dual activity in controlling stomatal movements (Figure 6B; Wege et al., 2014; Yang et al., 2017). SnRK2s can also act on chromatin-remodeling proteins, such as BRM (BRAHMA), which is inactivated by SnRK2s and activated by PP2C-mediated dephosphorylation (Peirats-Llobet et al., 2016).

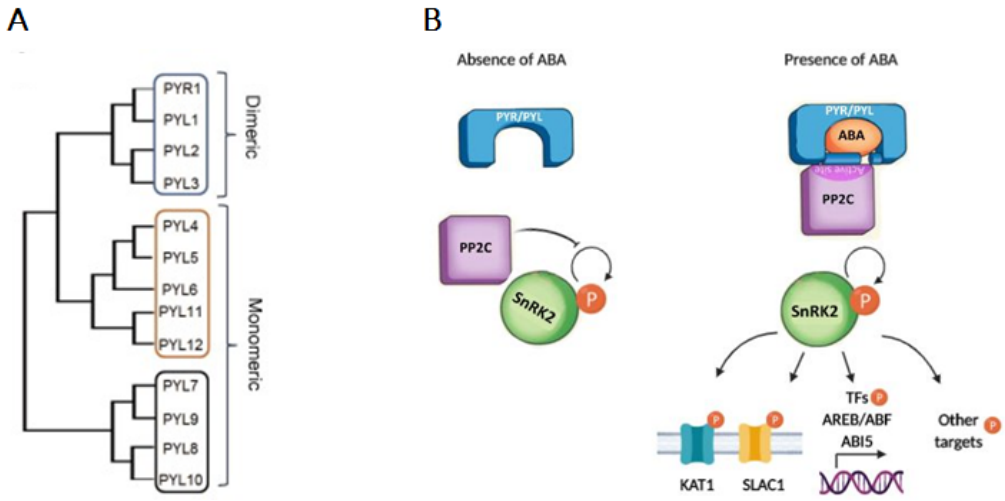

Figure 6. ABA core signaling components.
(A) Phylogenetic tree of PYR/PYL ABA receptor family. **(B)** Schematic representation of the ABA mechanism of action. Adapted from Sheard et al., 2009

A recent study has shed light on the mechanisms that allow plants to repress ABA signaling under normal growth conditions. In unstressed conditions, the protein kinase TOR (TARGET OF RAPAMYCIN) phosphorylates PYLs in a conserved serine located in the ABA binding pocket, disrupting the interaction with ABA and PP2C phosphatases. When ABA levels increase, SnRK2 kinases are active, phosphorylating a subunit of the TOR complex, RAPTOR. This phosphorylation triggers the disassembly of the TOR complex, leading to its inactivation (Wang et al., 2018).

1.5.2. Stomatal movements

Stomata are pores located in the leaf and stem epidermis that allow plants to incorporate CO_2 for photosynthesis, however in exchange, plants lose over 95% of their water via transpiration. Stomata are flanked by two guard cells, mostly occupied by a big vacuole, that control opening or closing of the stomatal pores depending on changes in vacuolar volume. For stomatal opening, guard cells accumulate anions, potassium and sucrose; this produces osmotic water uptake, swelling the guard cells and opening the stomata. Light, reduced CO_2 levels in the leaves and increased relative air humidity, trigger stomatal opening. On the contrary, during stomatal closure, there is an efflux of anions and K^+ from guard cells; that drives water out of the guard cells decreasing turgor pressure and therefore, closing the stomata. Some stimuli that promote stomatal closure are ABA, darkness, high CO_2 levels in the leaves and reduced relative humidity (Schroeder et al., 2001; Hsu et al., 2018). The regulation of stomatal movements is essential for plants to acclimate and adapt to the always changing environmental conditions.

Role of ABA in stomatal movements

ABA biosynthesis, followed by downstream signaling via PYL receptors has been shown to be essential for ABA-induced stomatal closure. A recent study has demonstrated that guard cells are even able to autonomously synthesize ABA (Bauer et al 2013). Although the exact sequence of events that lead to stomatal closure is not completely clear yet, the current model proposes that ROS (Reactive Oxygen Species) and calcium act as second messengers. Block of ROS production of calcium influx leads to inhibition of ABA-inducted stomatal closure. In guard cells, in the absence of ABA, PP2Cs block SnRK2 kinases and the slow-sustained anion channel (S-type) SLAC1 (SLOW ANION CHANNEL-ASSOCIATED1) to prevent its non-specific activation. In the presence of ABA, SLAC1 and SnRK2 kinases (such as OST1; OPEN STOMATA1) are released from PP2C-dependent inhibition. Active OST1 SnRK2 is now able to phosphorylate downstream targets, among them the NADPH oxidase RBOHF (RESPIRATORY BURST OXIDASE HOMOLOGF), which produces a ROS burst. ROS activates ICa L-type calcium channel, producing an increase in cytoplasmic Ca^{2+} that turns on CPKs (Ca^{2+}-DEPENDENT PROTEIN KINASES), and also is perceived by the receptor like kinase GHR1 (GUARD CELL HYDROGEN PEROXIDE-RESISTANT1). GHR1 together with OST1 and CPKs phosphorylate SLAC1 anion channel, producing anion efflux. OST1 also activates another anion channel, QUAC1 (QUICKLY ACTIVATING ANION CHANNEL 1) increasing

the exit of anions from the cell. The efflux of anions causes the depolarization of the membrane that, in turn, activates voltage-dependent K^+ channels (K_{+out}) and deactivates inward-rectifying K^+ (K^+_{in}) channels (Schroeder et al., 1987). The reduction of cytosolic levels for both anions and K^+ increase the water potential inside the cell, causing an efflux of water that eventually leads to a reduction in the turgor pressure producing the stomatal closure (Figure 7; Munemasa et al., 2015; Mäser et al., 2003; Sierla et al., 2016; Hua et al., 2012).

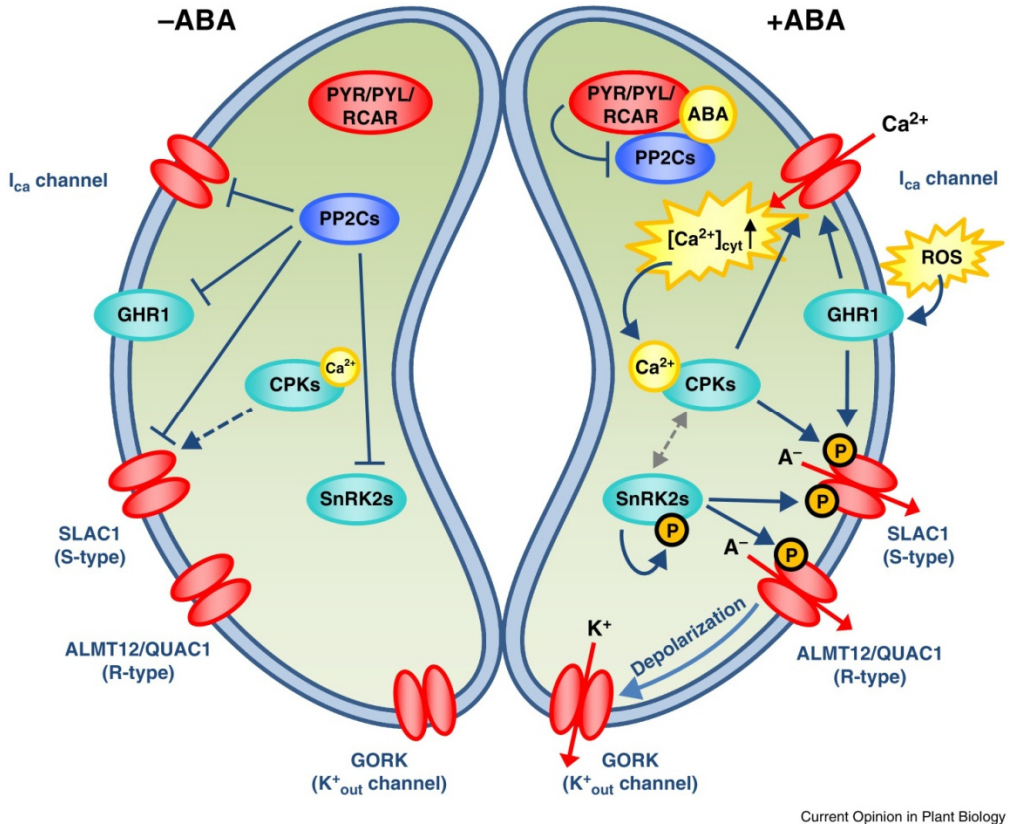

Figure 7. Diagram that depicts the molecular events that lead to stomatal closure

1.5.3. Mechanisms to control the ABA pathway

ABA participates in many different processes essential for plant life. To maintain plant homeostasis to this hormone, ABA levels and abundance of key components involved in biosynthesis, catabolism, perception and signaling have to be tightly controlled.

ABA biosynthesis: control of biosynthetic enzymes

A balance between ABA biosynthesis and catabolism is essential to maintain ABA homeostasis. Abiotic stresses such as drought, cold or salinity induce de novo ABA biosynthesis (Tuteja, 2007). Among all the biosynthetic enzymes that participates in the process, NCEDs (9-CIS-EPOXYCAROTENOID DIOXYGENASES) are the key enzymes that limit the biosynthetic rate, being NCED3 the most important in conditions of water deprivation. A study published in 2018 has described for the first time in plants, the existence of a mobile peptide, CLE25 (CLAVATA3/EMBRYO-SURROUNDING REGION-RELATED 25) that triggers ABA synthesis in leaves and affects stomatal movements. Under water deficient conditions, *CLE25* is highly expressed in roots and vascular tissues; the resulting peptide is able to move from roots to the leaves thanks to its association with two RLKs BAM1 and BAM3 (BARELY ANY MERISTEM). In the leaves, the CLE25-BAM pair induces the expression of *NCED,* which produces an increase in ABA and eventually triggers stomatal closure (Ma et al., 2018; Takahashi et al., 2018).

ABA degradation is mainly catalyzed by enzymes of the family CYP707A (CYTOCHROME P450 707A SUBFAMILY OF MONOOXYGENASES). When the stress conditions are relieved, the content of ABA needs to be reduced to return to homeostatic conditions. It has been demonstrated that during rehydration, there is a rapid accumulation of the bZIP TF VIP1 (VirE2-INTERACTING PROTEIN 1). This TF directly binds to the promoters of *CYP707A1* and *CYP707A3* inducing their expression, which leads in turn to a reduction in ABA when the stress conditions are gone (Ma et al., 2018).

ABA signaling: control of phosphatases

The tight control over the ABA pathway also spans to PP2C phosphatases, which can be ubiquitinated to repress or promote their activity. For instance, it has been reported that when the PP2C ABI1 (ABA INSENSITIVE 1) is forming a ternary complex with ABA and PYLs, it can be ubiquitinated by the E3 ligases PUB12 and PUB13 to be degraded in the 26S proteasome (Kong et al., 2015). Similarly, it has been described that the RING E3 ligases RGLG 1 and 5 (RING DOMAIN LIGASE) ubiquitinate ABI2 (ABA INSENSITIVE 2) and HAB2 targeting them for degradation in the proteasome (Wu et al., 2016). These mechanisms allow plants to potentiate ABA signaling by reducing the availability of PP2Cs to inhibit their targets. In the contrary, monoubiquitination of other family of phosphatases that mediate ABA responses, the PP2As, by the E3 ligase CHIP (CARBOXYL TERMINUS OFHSC70-INTERACTING PROTEIN) enhances their phosphatase activity (Luo et al., 2006).

ABA perception: control of PYLs levels

ABA receptors act at the core of the ABA perception and signaling pathway. Therefore, their abundance and hence their function is subjected to a tight control. The ubiquitination system plays an essential role in controlling PYL abundance at different subcellular compartments by means of specific E3 ubiquitin ligases. Thus, in the nucleus, CULLIN4-RING E3 ligases containing either DDA1 (DET1, DDB1-ASSOCIATED1) or the DWD protein RAE1 (RNA EXPORT FACTOR 1) as the substrate adapter, and the CULLIN1- E3 ligases containing the F-box protein RIFP1 (RCAR3-INTERACTING F-BOX PROTEIN1) are able to target PYL receptors for degradation at the 26S proteasome as a way to desensitize plants against ABA (Irigoyen el al., 2014; Li et al., 2016; Li et al., 2018).

Targeted ubiquitination of PYLs can be promoted by additional PTMs that help to locally control ABA perception, such as NO (nitric oxide)-mediated PYLs nitration at specific tyrosine (Tyr) residues, that produces PYL inactivation. There is a preferential ubiquitination of Lys residues located in close proximity of nitrated Tyr residues. Therefore, in the presence of NO, specific PYL nitration produces a rapid reduction in ABA responsiveness, that followed by polyubiquitination and 26S proteasome degradation of these nitrated receptors leads to a reduction in the ABA signaling (Castillo et al., 2015).

An additional mechanism for targeted degradation of PYLs involves the vesicle trafficking machinery. Thus, PYL receptors are known to associate with membranes by their physical interaction with members of the CAR (C2-domain ABA-related) protein family (Rodriguez et al., 2014). CAR proteins can transiently bind to phospholipids in a Ca^{2+}-dependent manner, increasing the abundance of PYLs associated to membranes, likely facilitating the formation of active signaling ternary PYL-ABA-PP2C complexes at the plasma membrane. Thus, CAR proteins have been reported to act as positive regulators of many ABA responses, including ABA-mediated inhibition of seedling establishment and shoot and root growth. Membrane-bound PYL levels are regulated by the RING-type E3 ligase RSL1, which is anchored to the plasma membrane via its C-terminal transmembrane domain. Interaction of RSL1 with PYL receptors (i.e., PYR1 and PYL4) promotes their ubiquitination and subsequent sorting, together with RSL1, through the endosomal pathway for vacuolar degradation (Bueso et al., 2014; Belda-Palazon et al., 2016). Involvement of the ESCRT machinery in this process was evidenced by physical interaction of PYL receptors with ESCRT-I subunits FYVE1 (also termed FREE1) and VPS23A (also termed ELC) in vesicle-like structures (Belda-Palazon

et al., 2016; Yu et al., 2016). FYVE1 is the only representative of class IV of FYVE-domain-containing proteins in Arabidopsis whereas VPS23A is a homologue of mammalian TSG101 and yeast Vps23a proteins, which contain a ubiquitin conjugating enzyme variant domain likely used for binding and sorting of ubiquitinated protein cargos (Spitzer et al., 2006; Gao et al., 2014, 2015; Kolb et al., 2015; Yu et al., 2016). Within ESCRT-I complexes, FYVE1 and VPS23A proteins are known to interact with each other and are required for recognition and internalization of cargo proteins into ILVs (Shen et al., 2016). According to their role in cargo trafficking through MVBs and their interaction with PYL receptors, partial loss of function of FYVE1 and VPS23A led to altered subcellular localization and accumulation of PYL proteins. As a consequence, weak Arabidopsis *fyve1* and *vps23a* mutants displayed increased sensitivity to ABA at the seedling stage (Belda-Palazon et al., 2016; Yu et al., 2016). FYVE1 and VPS23A also participate in ILV formation, trafficking to the vacuole, and vacuolar biogenesis (Gao et al., 2014, 2015; Kolb et al., 2015), functions that also require the activity of the ESCRT-III-associated protein ALIX (APOPTOSIS-LINKED GENE-2 INTERACTING PROTEIN X; also termed AtBRO1). Indeed, loss of function mutants of ALIX displayed defects in vacuolar biogenesis and protein cargo trafficking. For instance, the phosphate receptor PHT1 appears mislocated in *alix-1* mutants, and instead of being degraded in the vacuole it accumulates in the tonoplast (Cardona-López et al., 2015; Kalinowska et al., 2015; Shen et al., 2016). Interestingly, ALIX, as occurs with FYVE1, physically interacts with VPS23A (ESCRT-I) and with SNF7 (ESCRT-III), suggesting that these two proteins might act as a bridge between ESCRT-I and –III complexes and thereby coordinate cargo protein sorting and vacuolar targeting. Yet, such a functional relationship has not been fully demonstrated (Shen et al., 2016; Gao et al., 2017).

Besides perceiving ABA, a subset of specific PYLs is able to perceive PA (phaseic acid), an oxydative catabolite of the ABA. PA retains ABA-like hormonal activity, triggering typical ABA responses, being especially relevant in the control of stomatal movements and in the inhibition of seed germination. However, PA is a less potent hormone than ABA, it acts in the submicromolar to micromolar range whereas ABA acts in the nanomolar range. Among the whole ABA-receptor family members, PYL2 has a prominent role at perceiving PA, which elicitates physiological growth responses and stomatal closure in response to prolonged water deprivation (Rodríguez, 2016; Weng et al., 2016; Dittrich et al., 2019).

1.6. ALIX

1.6.1. ALIX is conserved among eukaryotes

ALIX is a cytosolic protein originally described in mammals, which is highly conserved among eukaryotes. Arabidopsis ALIX (AtALIX) amino acid sequence shows greater homology with *Dictyostellium* ALIX (30% of identity), *Aspergillus* PalA (22% of identity) and mammalian ALIX (21% of identity) than with yeast Bro1p (BCK1-LIKE RESISTANCE TO OSMOTIC SHOCK 1P) and Rim20 (REGULATOR OF IME2 20) with whom AtALIX displays only a 13 and 19% of sequence identity, respectively (Cardona-López et al., 2015). In mammals there are other ALIX paralogues that share similar protein structure and that have been recently involved in the endosomal trafficking such as BROX and HD-PTP (Ichioka et al., 2007 and 2008). The Arabidopsis genome does not contain AtALIX homologues but encodes another 4 Bro1-domain containing proteins: BRAF (Bro1-domain protein As FREE1 suppressor), AT1G13310, AT1G17940, and AT1G73990. BRAF has been described to participate in the MVB pathway, repressing the formation of ILV by competing with VPS23A for the interaction with FYVE1 within the ESCRT-I complex (Shen et al., 2018).

AtALIX has similar protein size and domain organization to that shown by its homologues from other species (Figure 8):

- All of them have a Bro1 domain in the N terminal part that has a boomerang shape and spans from the 1 to 367 amino acid (in Arabidopsis from 1 to 377; Kim et al., 2005). The whole Bro1 domain is composed by 14 α helices and three β sheets, and the entire assembly is stabilized by extensive hydrophobic interactions and two polar clusters. The residues Arg-51, Tyr-70, Trp-94, and Glu-116 in the first cluster and Glu-197 and Lys-246 in the second cluster of mammalian ALIX, are highly conserved among ALIX homologues (Kim et al., 2005). Moreover, it has been described that the region comprising the residues 118-316 in the Bro1 domain can be considered a TPR (tetratricopeptide repeat) domain with 3 TPR repeats that conforms a cleft, in which the α7 forms the floor of the pocket, the α5, α9 forms the walls and the α10-α11 are linkers (Kim et al., 2005).

  The Bro1 domain has been described to be responsible of the interaction with the ESCRT-III subunit CHMP4/SNF7 (which polymerizes into spirals mediating ILV budding; Henne et al., 2012) in all organisms tested so far (view table 1; Fisher et

al., 2007; McCullough et al 2008; Wemmer et al., 2011; Cardona-López et al., 2015).

- In the middle region has a V-shaped domain with one (PalA, Dd-ALIX, Bro1p and Rim20) or two coiled-coil domains (AtALIX and mammalian ALIX). Although ALIX proteins lacks a canonical Ub-binding domain, it has been extensively demonstrated that ALIX V-domain is able to directly bind mono-Ub and Lys63-linked polyUb chains (Pashkova et al., 2013; Dowlatshahi et al., 2012; Kalinowska et al., 2015; Mosesso et al., 2019). This domain is essential and sufficient for the interaction between AtALIX with the deubiquitinase AMSH3. Mammalian viruses such as VIH (Human Immunodeficiency Virus) can hijack ALIX to parasite the MVB pathway for viral budding. It has been described that HIV viral proteins can interact with both the Bro1 domain (nucleocapsid Gags) and the V-domain (p6 region of Gag) to engage the MVB pathway (Popov et al., 2007).

- The C terminal part of most ALIX proteins contains a proline-rich (Pro-rich) domain, absent in the yeast homologue Rim20 (regulator of IME2 20) but present in *Aspergillus* PalA, mammalian ALIX, yeast Bro1p, *Dictyostellium* ALIX (Mattei et al., 2006) and Arabidopsis ALIX. In mammals it has been described that this region mediates the interaction with SETA proteins, endophilins and the ESCRT-I subunit TSG101 (view table 1; Kim et al., 2005) In Arabidopsis, this domain is essential for the interaction with FYVE1 (Shen et al., 2016). Presumably the Pro-rich domain of AtALIX also modulates the interaction with Vps23A (TSG101) since in mammals it occurs through this region.

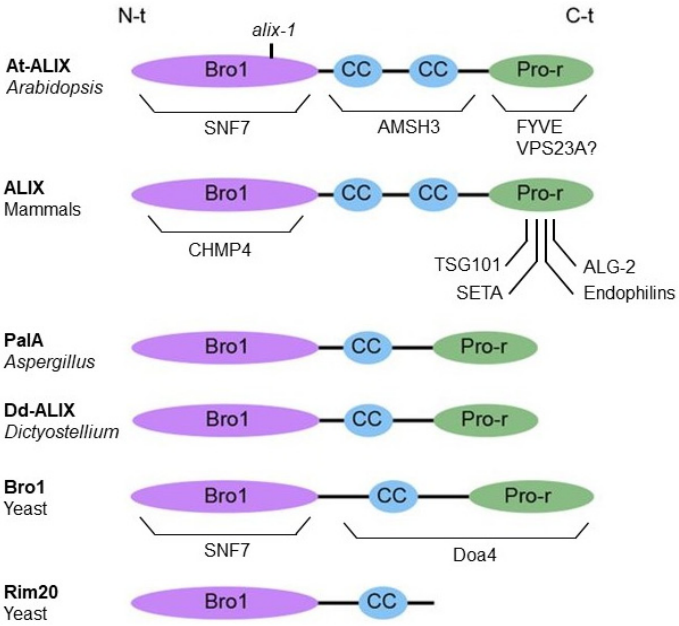

Figure 8. Diagrams depicting the domain organization of different ALIX homologues
ALIX-related proteins comprise a Bro1 domain (Bro1) in the N-terminal region (N-t), followed by one or two coiled-coil (CC) domains and a proline-rich (Pro-r) motif in the C-terminal region (C-t). Protein interactors and the position of the *alix-1* mutation in the Bro1 domain of At-ALIX protein are indicated. Adapted from Odorizzi et al., 2006 and Cardona-López et al., 2015

1.6.2. ALIX is a multifunctional protein

ALIX is a multi-faceted protein that has been described to participate in many ESCRT-mediated processes. In mammals, ALIX participates in MVB sorting of PM proteins, viral budding, exosome biogenesis, load of extracellular vesicles (EV) with miRNAs, autophagy and membrane scission at the end of cytokinesis (Murrow et al., 2015; Sun et al., 2016; Iavello et al., 2016). In Arabidopsis, the processes in which AtALIX is involved are less characterized, so far it is known that participates in vacuolar biogenesis and trafficking of PM located cargos for their vacuolar degradation, such as PHT1 and BRI1 (Cardona-López et al., 2015; Kalinowska et al., 2015). Additionally, ALIX homologues in mammalian and yeast systems, have an important role controlling cytokinesis (Spitzer et al., 2006). In plants the secretory pathway has been reported to be essential for plant cell division, as Arabidopsis *vps23a* mutants show increased ploidy levels that can be visualized by the appearance of aberrant trichomes with multiple branches. In this context, it is very likely that AtALIX may also have a role in

controlling cell division since partial loss of AtALIX function produces altered trichome morphology (Dr. Cardona-López thesis).

1.6.3. ALIX is essential for plant life: *alix* mutants

AtALIX, as other components of the ESCRT machinery, is an essential protein for plants. For instance, knockout (KO) mutants for AMSH3, VPS2.1 (VACUOLAR PROTEIN SORTING) or double mutant *vps23.1-3 vps23.2-1* are lethal (Ibl et al., 2012; Cai et al., 2014; Kalinowska et al., 2015; Nagel et al., 2017). Similarly, ALIX null alleles such as *alix-2* and *alix-3* display embryolethality (Cardona-López et al., 2015). Different attemtps to develop artificial microRNA lines against ALIX have been carried out, however lines with significantly reduced ALIX levels could not be obtained (Kalinowska et al., 2015).

Fortunately, in our laboratory we obtained a weak mutant allele for *AtALIX*, termed *alix-1,* which harbors a point mutation in the second exon of the *AtALIX* gene. Such mutation produces a substitution in the Gly260 (an hydrophobic amino acid) for an Asp (which is polar and negatively charged). This mutation localizes in the in 9th alpha helix of ALIX, which conforms one of the walls of the TPR pocket, and also it localizes in the proximity of one of the conserved amino acids of the second polar cluster (Lys 246). It is very likely that the negatively charged Asp disturbs the 3D conformation of the whole Bro1 domain reducing its functionality (Figure 9). The use of this mutant allele has enable us to functionally characterize AtALIX.

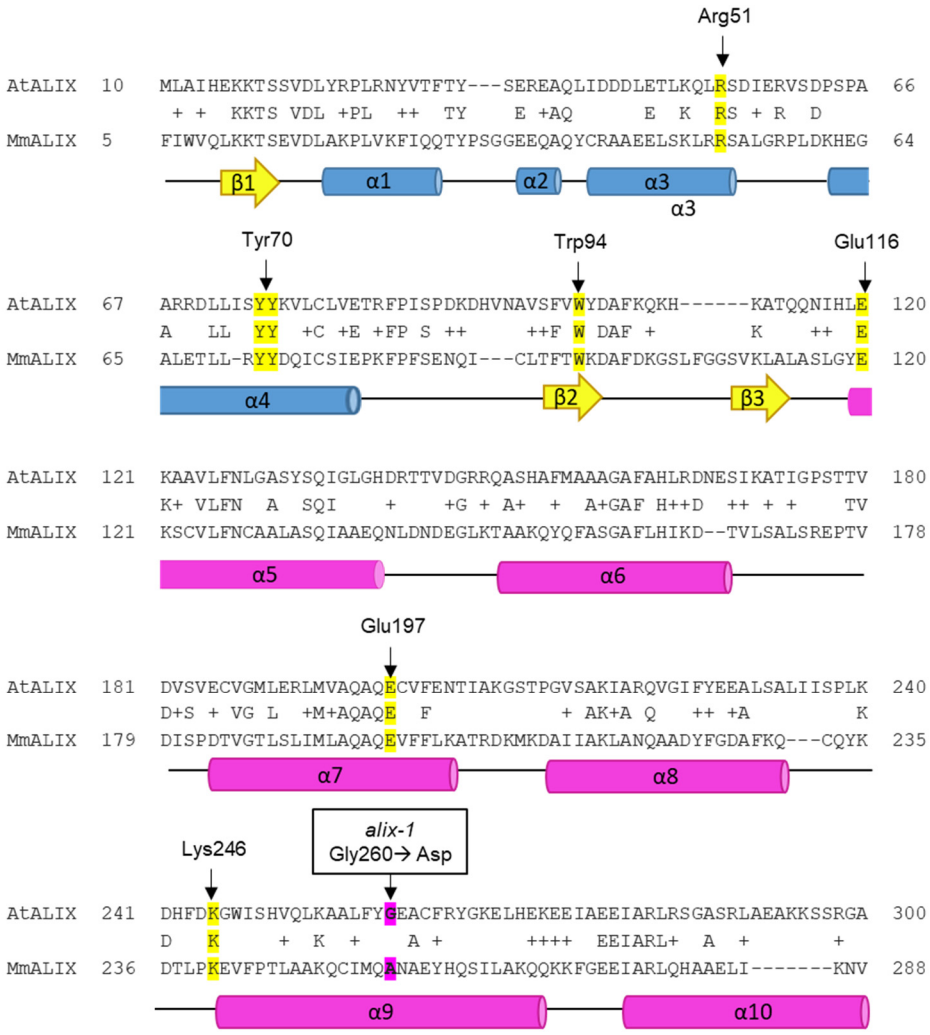

Figure 9. Alligment of the Bro1 domains of mammalian and Arabidopsis ALIX.
The regions corresponding to the alpha helixes and beta sheets of the secondary structure of the Bro1 domain are shown. Arrows indicate conserved amino acids belonging to the polar cluster 1 and 2 and the *alix-1* mutation in position 260.

1.6.4. Arabidopsis ALIX interactors

Although the interactors of ALIX in other species are well characterized, in plants only a few number have been described yet. So far, it is known that ALIX interacts with different components of the ESCRT machinery and participates in the trafficking of different cargos.

ESCRT components

- SNF7: In mammals and yeast, ALIX/Bro1 interacts with the ESCRT-III subunit CHMP4 (Charged Multivesicular Body Protein 4)/SNF7 to mediate ILV formation (McCullough et al 2008; Wemmer et al., 2011). Similarly, Arabidopsis ALIX interacts with SNF7, and mutations in the Bro1 domain, such as the *alix-1* mutation, disrupt the interaction between them (Cardona-López et al., 2015).
- AMSH3: In yeast, Bro1p is able to interact with the deubiquitinating enzyme Doa4 (Luthala et al., 2004), whereas AtALIX interacts with another type of DUB, AMSH3, through its V domain (Kalinowska et al., 2015). ALIX recruits AMSH3 to the MVBs to recycle ubiquitin moieties prior to the incorporation of protein cargos to the ILVs.
- ALIX is also able to interact with members of the the ESCRT-I complex, VPS23A and FYVE1/FREE1 through its proline-rich domain. Therefore ALIX associates not only to the ESCRT-III complex but also to the ESCRT-I, where it may help to remove ubiquitin from endocytosed cargos (via AMSH DUBs) allowing their recycling to the PM (Shen et al., 2016; Gao et al., 2017).

Protein cargos

- ALIX participates in the sorting of both PHT1 and BRI1, although a direct interaction for them has not been reported. However, since ALIX has been described in other species as an ubiquitin receptor for protein cargo sorting into the MVB pathway (Pashkova et al., 2013), it is very likely that Arabidopsis ALIX is able to recognize ubiquitinated BRI1 and PHT1 to facilitate their sorting.
- Recent studies have revealed that FYVE1 and VPS23A are able to directly interact with ABA receptors to mediate their endosomal trafficking. In this work we have demonstrated that ALIX, as part of the ESCRT machinery, mediates an ABA-enhanced negative feedback mechanism that promotes the turnover of specific ABA receptors through the MVB pathway. This regulatory process allows plant adaptation to ABA-mediated stresses such as water deprivation, modulating plant growth, development and stomatal closure.

2. OBJECTIVES

This PhD thesis is intended to reveal the role and the physiological implications of the *Arabidopsis thaliana* protein ALIX in the ABA signaling pathway. To accomplish this goal, the following specific objectives are proposed:

I. Search for new interactors of ALIX

II. Evaluation of the physiological relevance of ALIX within the abscisic acid (ABA) plant response.

III. Characterization of the physical interaction of ALIX with the PYR/PYL/RCAR ABA receptors

IV. Unraveling the molecular basis underlying ABA response defects in *alix-1* mutants.

3. MATERIALS AND METHODS

3.1. Plant Materials

Arabidopsis plants used in this study, including mutants and transgenic plants (table 1), were of the Columbia-0 (Col-0) ecotype.

Table 2. Arabidopsis mutant alleles and transgenic lines used in this study

STABLE LINE	REFERENCES	OBSERVATIONS
alix-1	Cardona-López et al., 2015	
cra1	Fernández-Arbaizar et al., 2012	
pyr1 pyl4 pyl5 pyl8 (quadruple pyl mutant*)*	Gonzalez-Guzman et al., 2012	
pyr1 pyl1 pyl4 pyl5 pyl8 (*pentuple pyl* mutant)	Antoni et al., 2013	
pyr1 pyl1 pyl4 pyl5 pyl8 alix-1 (*pentuple alix*)	García-León et al., 2019	
pyl4	Park et al., 2009	
pyr1-1	Park et al., 2009	
ost2-2	Merlot et al., 2007	
hab1-1 abi 1-2	Saez et al., 2006	
ALIXpro: GFP-gALIX / alix-1	Cardona-López et al., 2015	pBIB binary vector (Becker, 1990)
ALIXpro: gALIX/ alix-1	Cardona-López et al., 2015	pBIB binary vector (Becker, 1990)
oeHA-PYL4	Pizzio et al., 2013	ALLIGATOR2 vector (Bensmihen et al., 2004)
35S:GFP-PYL4	Belda-Palazon et al., 2016	pMDC43 vector (Curtis and Grossniklaus, 2003)
35S:GFP-PYL4 / alix-1	García-León et al., 2019	pMDC43 vector (Curtis and Grossniklaus, 2003)

3.2. Growth conditions

3.2.1. In vitro growth conditions

For *in vitro* plant growth, seeds were surface sterilized for 7 minutes in 70% (v/v) bleach and 0,01% (v/v) Tween-20, and washed 3 times with Milli-Q sterile water, under sterile conditions in a laminar flow hood. The sterilized seeds were sown in Murashige Skoog (MS) solid media plates (Duchefa, Holland) (Murashige and Skoog, 1962) with 1% sucrose; stratified for 3 days at 4°C and then grown in phytochambers under a 16-h-light/8-h-dark photoperiod using cool white fluorescent light conditions (100 mmol m^{-2} s^{-1}) at a constant temperature of 21°C. Bactoagar concentration was 0,7% (w/v; 6g/L) for horizontal growth and 1% (w/v; 10g/L) for vertical growth. Specific treatments were performed as stated in each experiment.

For drug treatments, plants were transferred to MS 1X liquid media and incubated under continuous 100µmol/(m^2*s) light at 21°C on shakers at 45 rpm.

3.2.2. Soil growth conditions

Arabidopsis seedlings were transplanted to a mix of soil and vermiculite (ratio 3:1) and grown in the green house or phytochambers at 22°C with a 16-h-light/8-h-dark photoperiod in long-day conditions, or 10-h-light/14-h-dark in short-day conditions.

For Bimolecular Fluorescent Complementation (BiFC) experiments, *N. benthamiana* plants were grown in soil in the green house at 22°C under 16-h-light/8-h-dark photoperiod during 3 weeks prior to agroinfiltration of leaves with the corresponding constructs.

3.3. Physiology

3.3.1. Growth analyses and water loss measurements

For seed germination, seedling establishment and root growth assays, conditions were as described in Irigoyen et al., 2014. To do so, seeds were sterilized and grown in horizontal MS plates supplemented or not with 0.5µM or 1µM of abscisic acid (ABA, Sigma Aldrich). The percentage of germination was evaluated 3 days after sowing as the number of seeds with emerged roots. Seedling establishment was recorded as the number of seeds that developed the first pair of true leaves at 7 days after sowing. For

the root growth assays, seedlings were grown on vertical MS plates for 5 days and then transferred to MS plates lacking or supplemented with 10 µM ABA. Root length was analyzed with ImageJ freeware (https://imagej.net/Fiji).

Water loss assays in 15-d-old seedlings were performed as described in Belda-Palazon et al., 2016. For this, seedlings were grown in horizontal MS plates and 15 seedlings per genotype with similar growth, in three independent experiments, were submitted to the drying atmosphere of a flow laminar hood. Kinetic analysis of water loss was performed and represented as the percentage of initial fresh weight at each scored time point.

3.3.2. Stomatal aperture measurements

Stomatal aperture was measured from epidermal strips of abaxial leaf faces of 4-week-old plants grown under short day conditions. Epidermal strips were incubated in KCl buffer (50 mM KCl, 10 mM MES-KOH pH 6.0) during 1.5 h in darkness and then transferred to white light (250 100 mmol m^{-2} s^{-1}) to measure stomatal aperture at different time points as indicated. For ABA treatments, epidermal peels were placed in KCl buffer with different ABA concentrations (ranging from 0 to 1 µM) for 2.5 h under dark or light conditions. For fusicoccin (FC; Sigma-Aldrich) treatment, epidermal peels were maintained for 1.5 h in darkness in the above-mentioned buffer and then transferred to buffer plus 5 µM fusicoccin or an equivalent volume of ethanol, and maintained for 2.5 h under dark or light conditions. Stomata were visualized in an optical microscope (Optiphot; Nikon) and apertures were measured with ImageJ freeware (https://imagej.net/Fiji). All the experiments were performed as blind and repeated at least three times independently.

3.3.3. Thermal Infra-Red Imaging

Arabidopsis seeds were directly sown on 7 cm x 7 cm pots containing a mixture of 1/3 sand (2-3 mm particles) and 2/3 horticultural compost (v/v). Pots were incubated in the dark at 4°C for 2 days to break seed dormancy. Plants were then grown in growth chambers under an 8-hour light photoperiod and the following conditions. Day conditions: 22°C, 55% relative humidity, daily watering and cool white fluorescent light conditions (100 mmol m^{-2} s^{-1}). Night conditions: 18°C and 60% relative humidity. Thermal images of 3 to 4 week old plants were obtained using a FLIR A655sc infrared camera (FLIR Systems) equipped with a 24.6 mm focal length lens and FLIR ResearchIR max software (version 4.20.2.74).

3.4. ABA concentration measurements

The measurements in ABA content were performed in collaboration with the laboratory of Dr. García-Mina (Department of Environmental Biology, Agricultural Chemistry and Biology Group, Faculty of Sciences, University of Navarra). ABA levels were analyzed using high-performance liquid chromatography-electrospray ionization-high-resolution accurate mass spectrometry (HPLC-ESI-HRMS). The extraction and purification were performed using the following method: 250 mg of frozen tissue from roots or shoots (previously ground to a powder in a mortar with liquid N2) was homogenized with 2.5 mL of pre-cooled methanol:water:HCOOH (90:9:1, v/v/v with 2.5 mM Na-diethyldithiocarbamate) and 25 µL of a stock solution of 1000 ng/mL of deuterium-labelled internal standard D-ABA. The mixture was shaken for 60 min at room temperature. After extraction, solids were separated by centrifugation at 20.000 RCF for 10 min using a Sigma 4-16K Centrifuge (Sigma Laborzentrifugen gmbH), and re-extracted with an additional 1.25 mL of extraction mixture followed by shaking for 20 min and centrifugation. A 2 mL aliquot of pooled supernatants was taken and dried at 40°C using a RapidVap Evaporator (Labconco Co.). The residue was dissolved in 500 µL of methanol:0.133 % acetic acid (40:60, v/v) and centrifuged (20.000 g, 10 min) before being injected in an HPLC-ESI-HRMS system. ABA was quantified using a Dionex Ultimate 3000 UHPLC device coupled to a Q Exactive Focus Mass Spectrometer (Thermo Fisher Scientific), equipped with an HESI(II) source, a quadrupole mass filter, a C-Trap, a HCD collision cell and an Orbitrap mass analyzer (Orbitrap-Focus, Thermo Scientific). A reverse-phase column (Synergi 4 mm Hydro-RP 80A, 150 2 mm; Phenomenex) was used. A linear gradient of methanol (A), water (B) and 2 % acetic acid in water (C) was used: 38 % (v/v) A for 3 min, 38 % (v/v) to 96 % (v/v) A in 12 min, 96 % (v/v) A for 2 min and 96 % (v/v) to 38 % (v/v) A in 1 min, and kept for 4 min. C remains constant at 4 %. The flow rate was 0.30 mL/min, the injection volume was 40 µL and column and sample temperatures were 35°C and 15°C, respectively. The detection and quantification were performed using a Full MS experiment with tandem mass spectrometry (MS/MS) confirmation in the negative-ion mode. Instrument control and data processing were performed by TraceFinder 3.3 EFS software.

3.5. Cloning procedures

All genes of interest that were not previously cloned in the laboratory were amplified from purified Arabidopsis cDNAs by Polymerase Chain Reaction (PCR) using Pwo DNA

polymerase (Roche) and specific primers with the Gateway *attB1 / attB2* sites (*attb1*: 5'-GGGGACAAGTTTGTACAAAAAA GCAGGCTAT-3' / *attb2* 5'-GGGGACCACTTTGTACAAGAAAGCTGGGTA-3'). *attB*-PCR products were purified from agarose gels using the Qiaquick Gel Extraction Kit (QIAGEN) and subsequently cloned into the entry vector pDONR207 gentamycin^{R} using Gateway BP Clonase II enzyme (Invitrogen). BP reactions were transformed in 35aSilva-competent *E. coli* DH5α cells (see 2.6.1 Transformation of *E. coli* and *A. tumefaciens*). Transformant cells were selected using the corresponding antibiotic. Isolated colonies were grown overnight in liquid Luria Broth (LB) media and their plasmidic DNA was extracted using QIAPrep Spin Miniprep kit (QIAGEN) (See 2.8.1 Plasmid isolation from bacteria). Positive clones were confirmed by sequencing. Then the different genes of interest were transferred from pDONR to empty Gateway-compatible destiny vectors for yeast two hybrid (Y2H), BiFC and protein expression using LR clonase enzyme (Table 2).

Table 3. Constructs used for protein fusion expression in Y2H, recombinant protein expression in E. coli BL21, BiFC and TAP assays

VECTOR	CONSTRUCT	ANTIBIOTIC	OBSERVATIONS
pGADT7	AD-PYR1	Ampicillin	Irigoyen el al., 2014
pGADT7	AD-PYL4	Ampicillin	Irigoyen el al., 2014
pGADT7	AD-PYL8	Ampicillin	Irigoyen el al., 2014
pGADT7	AD-PYL9	Ampicillin	Irigoyen el al., 2014
pGBKT7	BD-Bro1	Kanamycin	Cardona-López et al., 2015
pGBKT7	BD-Δbro1	Kanamycin	Cardona-López et al., 2015
pGBKT7	BD-Bro1mut	Kanamycin	Cardona-López et al., 2015
pETM11	His-PYL4-His	Kanamycin	Kindly provided by Dr. Pedro Rodríguez
pETM11	His-PYL5-His	Kanamycin	Kindly provided by Dr. Pedro Rodríguez
pET28a	His-PYL8-His	Kanamycin	Kindly provided by Dr. Pedro Rodríguez
pET28a	His-PYL9-His	Kanamycin	Dr. Pedro Rodríguez
pMAL-c2X	3xGly-ALIX	Ampicillin	García-León et al., 2019
pBIFP-2	PYR1	Spectinomycin	García-León et al., 2019
pBIFP-2	PYL4	Spectinomycin	García-León et al., 2019

VECTOR	CONSTRUCT	ANTIBIOTIC	OBSERVATIONS
pBIFP-2	PYL5	Spectinomycin	García-León et al., 2019
pBIFP-2	PYL8	Spectinomycin	Irigoyen el al., 2014
pBIFP-2	PYL9	Spectinomycin	García-León et al., 2019
pBIFP-2	VPS23A	Spectinomycin	García-León et al., 2019
pBIFP-2	ALIX	Spectinomycin	Cardona-López et al., 2015
pBIFP-3	ALIX	Spectinomycin	Cardona-López et al., 2015
pBIFP-3	ALIX-1	Spectinomycin	Cardona-López et al., 2015
pKNGSrhino	ALIX	Spectinomycin	This work

3.6. Transformation methods

3.6.1. Escherichia coli and Agrobacterium tumefaciens transformation

Transformation of competent DH5α, DB3.1 or BL21 pLysS *E. coli* cells was carried out by heat-shock as described in Sambrook, et al., 1989.

Agrobacterium tumefaciens (C58C1 strain) cells were transformed using the method described in Weigel & Glazebrook, 2002. For PSB-D culture transformation, the strain C58C1 RifI pMP90 was used.

After transformation, *E. coli* and *A. tumefaciens* cells were plated onto selective media (LB with corresponding antibiotics) and incubated overnight at 37°C or 48h at 28°C, respectively.

3.6.2. Saccharomyces cerevisiae transformation

S. cerevisae cells (AH109 strain) were transformed as it is described in Matchmaker Gal4 Two-Hybrid User Manual (CLONTECH Laboratories, Inc.)

3.7. Yeast two- hybrid experiments

In a previous study, Dr. Laura Cuyas performed a yeast two hybrid screen to seek putative interactors of ALIX. To confirm those potential protein-protein interactions, positive clones were cotransformed into *Saccharomyces cerevisiae* AH109 cells,

following standard heat shock protocols (Cardona-López et al., 2015). Successfully transformed colonies were identified on yeast synthetic dropout media (SD) lacking Leu and Trp (SD-WL; Clontech). These colonies were resuspended in water and transferred to selective media lacking Ade, His, Leu, and Trp (SD-WLHA) (supplemented or not with 0.5 mM, 3-amino-1,2,4-triazole, 3-AT, Sigma). Yeast cells were incubated at 28°C for 3 days. Empty vectors were co-transformed as negative controls. To test the effect of ALIX-1 mutation on the interaction with PYL proteins, an ALIX-1 1-413 (an ALIX 1-413 version containing the *alix-1* mutation) version was also used. For figure preparation, representative colonies for each bait:prey construct combination from independent plates were used.

3.8. Nucleic acid extraction and analysis

3.8.1. Plasmid isolation from bacteria (miniprep)

For plasmid isolation, 5mL of liquid culture were grown overnight. The following day cells were pelleted and plasmids were isolated using QIAPrep Spin Miniprep kit (QIAGEN) in which plasmidic DNA binds to silica gel membrane in a spin column.

3.8.2. Genomic DNA extraction from Arabidopsis

Arabidopsis genomic DNA was extracted following the method described by Aitchitt et al., 1993 with small changes.

1. Grind frozen tissue to powder using glass beads and add approximately 1 volume of extraction buffer (1.4 M NaC1, 20 mM EDTA, 100 mM tris HCI pH 8.0, 3% w/v CTAB, 1% v/v 2-mercaptoethanol) per 1 volume of powder tissue. Vortex vigorously and incubate 30 minutes at 65°C.
2. Add 1 volume of chloroform isoamyl alcohol to the sample and vortex vigorously. Centrifuge at 16000g for 10 minutes at 4°C. Transfer the upper aqueous phase to a new tube and add 0.7 volumes of isopropanol to precipitate the DNA. Mix well and store for 1h at -20°C.
3. Centrifuge at 16000grpm for 10 minutes at 4°C, discard the supernatant and wash the pellet with 0.7mL of 70% ethanol. Repeat the wash with 100% ethanol
4. Let dry the pellet for 5 minutes to evaporate the ethanol and resuspend the pellet in 50-100 µl of sterile milliQ water.

3.8.3. Genotyping of the sextuple *pyr1 pyl1 pyl4 pyl5 pyl8 alix-1* mutant line

To generate *pyr1 pyl1 pyl4 pyl5 pyl8 alix-1* mutants (*pent alix-1* for simplicity) pentuple *pyr1* (*pyr1-1) pyl1* (SALK_054640) *pyl4* (SAIL_517_C08) *pyl5* (SM3_3493) *pyl8* (SAIL_1269_A02) mutants were crossed with *alix-1* mutants and selected in MS plates supplemented with 15µM of ABA. ABA-insensitive mutants were then identified by PCR using specific primers for the target gene and for the T-DNA insertion (Table 3). In the case of *pyr1* point mutants, the resulting PCR amplification product was sent for sequencing to detect the mutation.

Table 4. List of primers used in the genotyping of pent alix-1 mutants

NAME	SEQUENCE (5'-3')
PYR1 Fw	ATG CCT TCG GAG TTA ACA CCA
RV PYR1	TCA CGT CAC CTG AGA ACC ACT
Fw PYL1	ATG GCG AAT TCA GAG TCC TCC
Rv PYL1	TTA CCT AAC CTG AGA AGA GTT
LBb1.3 SALK	ATT TTG CCG ATT TCG GAA C
PYL2 Fw	ATG AGC TCA TCC CCG GCC GTG
PYL2 RV	TTA TTC ATC ATC ATG CAT AGG TG
DS5-insert	GTT CGA AAT CGA TCG GGA TAA AAC
FPYL4	ATGCTTGCCGTTCACCGTCCTTCTTCCGC
RPYL4	CAGAGACATCTTCTTCTTGCTCTCAGCCGC
LB3SAIL	TAG CAT CTG AAT TTC ATA ACC AAT CTC GAT ACA C
FPYL5	ATG AGG TCA CCG GTG CAA CT
RPYL5	TTA TTG CCG GTT GGT ACT TCG A
Spm3	ACC GTC GAC TAC CTT TTT TCT TGT AGT G
FPYL8	ATG GAA GCT AAC GGG ATT GAG
RPYL8	TTA GAC TCT CGA TTC TGT CGT

3.8.4. RNA extraction and cDNA synthesis

RNA extraction, cleanup and Dnase treatment were carried out using Direct-zol RNA MiniPrep Plus (Zymo Research). Following RNA isolation, RNA concentration was examined by measuring absorption A260 with a NanoDrop® ND-1000 UV-VIS

spectrophotometer. cDNA was synthesized from 400 ng of total RNA using qScriptTM XLT cDNA SuperMix (Quanta Biosciences) and was diluted 1/20 prior to use it for RT-qPCR experiments.

3.8.5. Reverse transcription quantitative PCR (qRT-PCR)

qRT-PCR experiments were performed using SYBR Green I Master (Roche) and 2 µL of the diluted cDNA obtained from Col-0 wild-type, *alix-1* and GFP-ALIX/*alix-1* plants. To check *ABI1* and *MYB60* levels, three biological replicates, consisting each of tissue pooled from shoots of three 45-day- old-day plants growing on soil, were taken. For *PYL4* levels analysis, three biological replicates were prepared using seedlings grown in 0.5x MS supplemented or not with 0.3 µM ABA for 6 days. *ACTIN8* and *TUBULIN* were used as housekeeping reference genes. Primers used are shown in table 4.

Table 5. List of primers used in qRT-PCRs

NAME	SEQUENCE (5'-3')
ABI1_F	GAGGCAGAGAGGGTCCTTTT
ABI1_R	AGCCCGGGAAGAAAAATACA
MYB60_F	CCTTCTTGAGGGTTGGATGA
MYB60_R	GTCATCATCCCCGTTAGTTC
TUB_F	GAGCCTTACAACGCTACTCTGTCTGTC
TUB_R	ACACCAGACATAGTAGCAGAAATCAAG
PYL4_F	ATGCTTGCCGTTCACCGTCCT
PYL4_R	CGAGCGGCCGTGGAGTCGCGTG
ACTIN8_F	GACTCAGATCATGTTTGAGACCTTT
ACTIN8_R	ACCGGTTGTACGACCACTGG

Quantitative PCRs were performed in 384-multiwell optical plates in a Light Cycler 480 Real Time PCR system (Roche). The PCR conditions were as follows: 10 min at 95°C and 40 cycles of 15 s at 95°C and 60 s at 60°C.

3.9. Protein technology

3.9.1. Protein Extraction and Immunoblots

For protein extraction from seedlings, proteins were extracted in buffer containing 50 mM Tris-HCl, pH 7.4, 150 mM NaCl, 10 mM $MgCl_2$, 10% Glycerol, 1 mM phenylmethylsulfonyl fluoride (PMSF), 0.1% Nonidet P-40 (NP-40) and 1x complete protease inhibitor (Roche). After centrifugation at 14.000 rpm for 10 min at 4°C, the supernatants were collected. This step was repeated twice. Protein concentration in the final supernatants was determined using the Bio-Rad Protein Assay kit. In the case of PYL4 immunoblots, proteins were extracted using 50 mM Tris-MES pH 7.4, 0.5 M sucrose, 1 mM $MgCl_2$, 10 mM ethylenediaminetetraacetic acid (EDTA), 5 mM dithiotreitol, 0.2% NP-40 and 1x complete protease inhibitor (Roche). Subcellular fractionation assays were performed as described in Cardona-López et al., 2015. Nuclear protein extractions were performed as previously described (Liu et al., 2001).

For immunoblots, protein samples were denatured, separated on SDS-PAGE gels, and transferred onto polyvinylidene difluoride membranes (Millipore). Membranes were probed with different antibodies: Living ColorsTM polyclonal anti-GFP at 1:1000 dilution (for detection of BiFC fusions; BD Biosciences; Catalog No. 632593), anti-His at 1:10000 dilution (for His-PYL fusions; BD Biosciences; Catalog No. 552565), anti-PYL4 at 1:2000 dilution (Yu et al., 2016), anti-MBP at 1:10000 dilution (Abcam; Catalog No. ab9084), and anti-MYC-HRP at 1:2000 dilution (Santa Cruz Biotechnology; Catalog No. sc-40). For immunodetection of 3HA-PYL fusions, anti-HA-HRP (Roche; Catalog No 11667475001) was used at 1:1000 dilution. To confirm equal protein loading, membranes were immunoblotted using anti-RPT5 at 1:10000 dilution (Abcam; Catalog No ab22676) or stained with Ponceau staining (Sigma).

3.9.2. Protein Extraction from yeasts

Protein extracts from yeast cells were prepared using a trichloroacetic acid protein extraction technique (Foiani et al., 1994). For immunodetection of baits (pGBKT7 constructs) anti-MYC-HRP at 1:2000 dilution (Santa Cruz Biotechnology; Catalog No. sc-40) was used. For immunodetection of preys (pGADT7 constructs) anti-HA-HRP (Roche; Catalog No 11667475001) was used at 1:1000 dilution.

3.9.3. Protein Extraction from *N. benthamiana*

For protein extraction from infiltrated *N. benthamiana* leaves, 4 leaf-discs per infiltration were collected and frozen in liquid nitrogen. Powdered tissue was homogenized with 150 µL of cracking buffer (75mM Tris pH: 6.8, 6% SDS, 26% glycerol, 250mg bromophenol blue per 50mL and freshly added 7.5% β-mercaptoethanol) per 100 µL of powdered tissue. Samples were boiled 10 minutes at 95°C, and centrifuged 5 minutes at room temperature. Supernatant was collected and stored at -20°C.

For immunoblots, 20 µL of sample (extracted as described above) were loaded on SDS-PAGE gels, transferred onto PVDF (polyvinyl; Millipore) membranes and immunoblotted with the corresponding antibodies as follows:

The N- and C- terminal fragments of the yellow fluorescent protein (YFP) fused to the BiFC partner proteins were immunodetected using the polyclonal antibody Living ColorsTM anti-GFP at 1:1000 dilution (BD Biosciences; Catalog No. 632593).

3.9.4. Purification of Recombinant Proteins and Pull-Down Experiments

Recombinant His-PYL, MBP alone and MBP-ALIX fusions were expressed in *Escherichia coli* BL21 (DE3) strain carrying pET28 or pETM11-HisT7PYL (Pizzio et al., 2013), empty pMAL-c2X and pMAL-c2X-ALIX constructs, respectively. The pMAL-c2X-ALIX construct was prepared by transferring the ALIX cDNA from a pDONR207 (Invitrogen) plasmid to a Gateway-adapted pMAL-c2X plasmid (Austin et al., 2012). Bacteria were cultured in LB at 37°C to an optical density at 600 nm of 0.5, at which time protein expression was induced with 0.1 mM isopropyl-D-thio-galactopyranoside (IPTG; Sigma) for 6 hours at room temperature. Cell lysis was performed using a sonicator (Labsonic U, B.Braun; 5 pulses of 15-seconds each at low intensity on ice) and lysates were clarified by centrifugation at 16.000 g for 30 min at 4°C. His-PYL and MBP or MBP-ALIX protein were purified from lysates with Ni-NTA-agarose (Qiagen) or Amylose resin (New England Biolabs) beads, respectively, under native conditions. His-PYLs were eluted with 250 mM imidazole (Sigma), as described by the manufacturers, whereas MBP-ALIX or MBP were left bound to the amylose resin. Eluted samples were dyalized overnight in dyalisis buffer (20mM Tris pH=7.4 and 10% v/v glycerol) using “Slide-A-Lyzer Dialysis cassette” 3,5kDa of pore size (Life technologies). Protein concentration in dialyzed final eluates was determined using a Bio-Rad Protein Assay kit.

For in vitro pull-down assay, 5 µg of His-PYLs were incubated with mild rotation with 10 µg of either purified MBP-ALIX or MBP alone on amylose resin for 1 hour at 4°C in 500 µL of binding buffer (50 mM Tris-HCl, pH 7.5, 100 mM NaCl, 10% Glycerol, 0.1% Tween-20, 1 mM PMSF, 1x EDTA free-Complete Protease Inhibitor Cocktail [Roche]). After washing three times with binding buffer, the beads were resuspended in 50 µL loading buffer, boiled for 5 min and 40 µL was analyzed by protein gel blotting using anti-His at 1:10000 dilution (BD Biosciences; Catalog No. 552565) and anti-MBP antibody at 1:10000 dilution (Abcam; Catalog No. ab9084). For semi in vivo pull-down assays, protein extracts from oeHA-PYL4 plants were incubated with rotation with 10 µg of either MBP-ALIX or MBP alone on amylose resin for 1 hour at 4°C in 500 µL of above-mentioned binding buffer. Washing and elution were as before. 30 µL and 5 µL were analyzed by protein gel blotting using anti-HA (1:1000 dilution; Roche; Catalog No 11667475001) and anti-MBP (1:10000 dilution; Abcam; Catalog No. ab9084) antibodies, respectively.

3.10. Tandem affinity purification (TAP)

The cDNA of *ALIX* was transferred from pDONR plasmid (Cardona-López et al., 2015) to the destination vector pKNGsrhino (Van Leene et al., 2008; García-León et al., 2019) using Gateway system (Invitrogen) and transformed into *Agrobacterium tumefaciens* (*A.* tumefaciens) C58C1 PMP90 competent cells. *Arabidopsis* cell 42aSilva42on cultures PSB-D (ABRC clone no. CCL84840) were transformed with the *A.* tumefaciens carrying the pKNGsrhino-ALIX construct. Growth of PSB-D suspensions and TAP purification was performed as described in García-León et al., 2019 (See annexes, Tandem Affinity Purification of Protein Complexes from Arabidopsis Cell Cultures).

3.11. Confocal imaging

3.11.1. Bimolecular Fluorescence Complementation assays (BiFC)

The cDNA of *ALIX, ALIX-1, PYR1, PYL4, PYL5, PYL8, PYL9* and *VPS23A* genes were transferred from pDONR plasmids (Irigoyen et al., 2015; Cardona-López et al., 2015; Yu et al., 2016) to destination vectors of the pBiFP series (To et al., 2006) using the Gateway system (Invitrogen) and transformed into *A.* tumefaciens C58C1 competent cells. Different combinations of (*A.* tumefaciens) clones expressing fusion proteins as indicated were coinfiltrated into the abaxial surface of leaves from 3-week-old *N.*

benthamiana plants (Sparkes et al., 2006). Leaves were also coinfiltrated with p19-expressing *A. tumefaciens*, which suppresses gene silencing (Voinnet, 2003). Empty vectors were used as negative controls. Fluorescence was visualized in epidermal cells of leaves 3 days after infiltration using a Leica TCS SP8 confocal microscope (Leica).

3.11.2. Tracer and Drugs, Microscopy, and Image Processing

Seedlings visualized in live imaging experiments were grown for 3 days in MS vertical plates and transferred to 0.5x MS liquid medium supplemented or not with specific drugs at concentrations and periods described as follows: For LysoTracker Red (Thermo Fisher Scientific) treatments, seedlings were incubated for 30 min with 1 µM LysoTracker Red. For WM (Invitrogen) treatments, seedlings were incubated with 33 µM WM for 30 min under dark conditions. WM stock was at 50 mM in DMSO.

Confocal laser scanning microscopy was performed on two different inverted microscopes: Leica TCS SP8 (CNB-CSIC, Madrid, Spain), and Zeiss LSM 780 (CEA-Cadarache, Saint-Paul-lès-Durance, France). Image processing was done with Fiji software from the National Institutes of Health (https://imagej.net/Fiji).

3.12. Accession numbers

Sequence data from this article can be found in the Arabidopsis Genome Initiative database under the following accession numbers: ALIX (At1g15130), FYVE1/ FREE1, (At1g20110), VPS23A/ELC (At3g12400), PYR1 (At4g17870), PYL4 (At2g38310), PYL5 (At5g05440), PYL8 (At5g53160), PYL9 (At1g01360).

4. RESULTS

4.1. Identification of new protein interactors

To identify new functions for ALIX in plants, as well as the regulatory mechanisms that control its activity, a former member of the lab, Dr. Laura Cuyas, sought for proteins that physically interact with ALIX. To do so, she carried out yeast two-hybrid (Y2H) screens, using as baits full-length ALIX as well as two truncated versions corresponding to its N-terminal Bro1 domain (aas 1-413) and the C- terminal portion (ΔBro1; aas 405-846), containing two coiled coil domains and a proline rich (Pro-rich) region. After confirming that the three baits were unable to activate reporter gene expression alone, we used them to screen an *Arabidopsis* cDNA library (Puga et al., 2014). Transformant colonies were grown in media lacking different amino acids alone or supplemented with 0.5 mM, 3-amino-1,2,4- triazole, 3-AT. Yeast colonies able to grow in the strictest conditions and displaying β-galactosidase activity were selected for DNA sequencing of prey plasmids. Dr. Cuyas identified a total of 65 different proteins as potential ALIX interactors that are shown in Table 1. Among them, she found one clone corresponding to a truncated version of the ABA receptor PYL9 (amino acids 75 to 188) and two C2-domain containing proteins belonging to the CAR family that recruits PYLs to phospholipidic vesicles in a Ca^{2+}-dependent manner (Rodriguez et al., 2014). In order to validate these results and to find proteins that interact with ALIX in vivo we followed another approach, by performing tandem-affinity purification (TAP) assays. To do so we cloned the full length version of ALIX (with 3xGly as linker) into the TAP vector pKNGSrhino and we agrotransformed *Arabidopsis thaliana* cell cultures (PSB-D). Then, we performed TAP assays as described in Van Leene et al., 2008 and 2011; García-León et al., 2018. (Annex 2). Among the proteins identified in the mass spectrometry analysis we could find an enrichment in proteins related to mRNA biology and the endomembrane system, such as SNF7.2 or SH3P2.

Altogether, these results indicate that ALIX is a key protein involved in many biological processes that we expect to address in the future. For this study we focused in the potential functional relationship between ALIX and the ABA signaling pathway. In this context, it has been previously shown the involvement of the endosomal trafficking in the control of the abundance of the ABA receptors, although a potential implication of ALIX in such regulatory mechanism had not been reported yet. The following sections describe the different approaches that were undertaken to characterize, both at the

molecular and physiological level the function of ALIX in the control of plant responses to ABA.

4.2. ALIX physically interacts with PYL ABA receptors in MVBs

Data from the Y2H screen (Dr. Laura Cuyas' thesis) showed that ALIX interacted with PYL9 and 2 members of the CAR protein family. We aimed to validate whether ALIX interacts with PYL9 and other Arabidopsis PYLs and whether these interactions are exclusively mediated by the Bro1 domain. We made this study extensive to members of the CAR and PP2C families, since it has been proposed that, in the presence of ABA, PYLs and PP2Cs form ternary complexes (Archana et al., 2011) that ALIX could be controlling.

To do so we performed Y2H experiments using the Bro1 and the ΔBro1 domains of ALIX. Our results showed that both Bro1 and ΔBro1 are able to bind to full-length versions of different PYLs (both dimeric; i.e. PYR1, and monomeric types; PYL4, 8 and 9) (Figure 10).

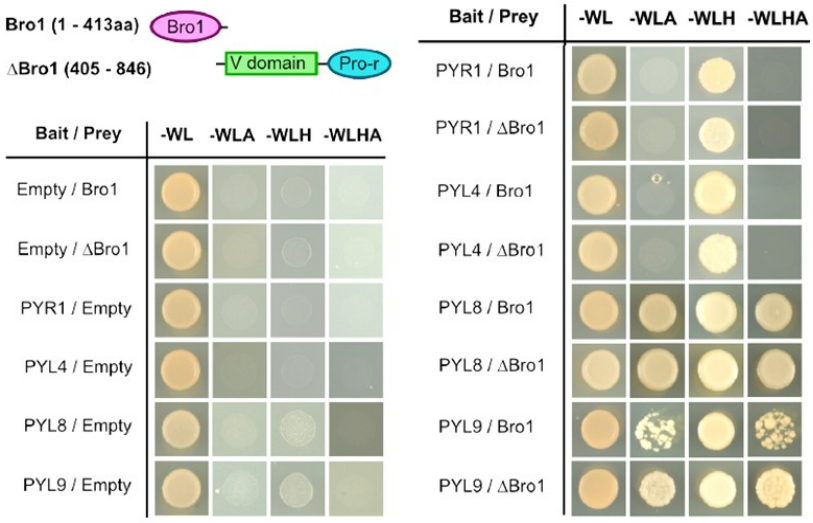

Figure 10. ALIX interacts with ABA receptors by Y2H

The structure of ALIX showing the Bro1 domain (Bro1; aas 1 to 413) and the coiled coils (V-domain) plus the Pro-rich (Pro-r) region (ΔBro1; aas 405 to 846) are shown in the upper panel. Yeast two-hybrid assays showing interaction of PYL ABA receptors with either Bro1 or ΔBro1 domains. Transformed yeast cells were grown in SD-WL medium as a transformation control and in SD-WL media lacking adenine (-WLA), histidine (-WLH) or both (-WLHA) for interaction assays. Cotransformation with empty plasmids was used as negative control.

In addition we found direct interaction between ALIX domains and a representative member of the CAR family, CAR1 (At5G37740) that showed interaction in our Y2H screen and had been reported to interact with PYLs, attaching them to membranes (Rodríguez et al., 2014) For this assay, a CAR1 version lacking the first 21 amino acids was used to avoid autoactivation (Δ21-CAR1). Very interestingly ALIX showed interaction with ABI1, a member of the PP2C family which can control many ABA responses and has a role controlling stomatal movements by directly dephosphorylating SLAC1 channel (Brandt et al., 2012; Munemasa et al., 2015; Figure 11). Altogether these results support a role of ALIX in the control of the whole ternary CAR-PYL-ABA-PP2C complexes associated to membranes.

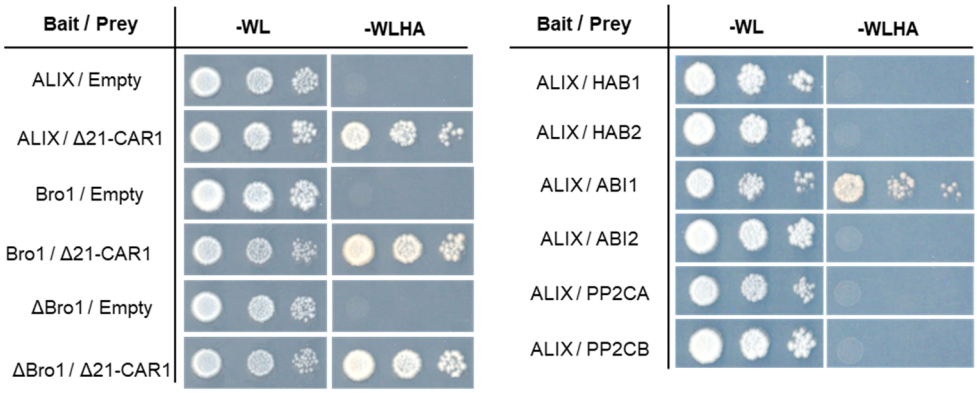

Figure 11. ALIX interacts with CAR proteins and with ABI1 PP2C
Yeast two-hybrid assays showing interaction of CAR1 with Bro1 and ΔBro1 domains, and ABI1 with full length ALIX. Transformed yeast cells were grown in SD-WL medium as a transformation control and in SD-WL media lacking adenine and histidine (-WLHA) for interaction assays. Cotransformation with empty plasmids was used as negative control.

As a first approach to dissect the potential involvement of ALIX in the control of ABA components, we first concentrated in the main players of ABA perception, the ABA receptors. As part of our efforts towards this goal, interaction of ALIX with PYLs was further substantiated by in vitro pull downs in which bacterial purified recombinant His-PYLs (PYL4, 5, 8 and 9) and MBP-ALIX bound to amylose resin, were co-precipitated upon incubation. Although all PYLs showed ability to interact with ALIX, their interaction occurred at different rates for each receptor, where His-PYL4 showed the strongest with ALIX (Figure 12A).

Semi-in-vivo pull down experiments, in which protein extracts from *Arabidopsis* lines overexpressing HA-tagged PYL4 (oeHAPYL4; Pizzio et al., 2013) were incubated with

amylose resin-bound MBP-ALIX, also showed co-purification of both protein fusions, providing additional support to the ALIX-PYL interaction (Figure 12B).

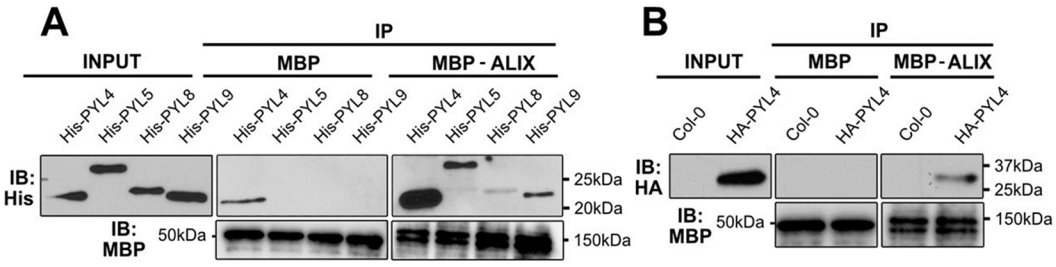

Figure 12. ALIX interacts with ABA receptors as shown by in vitro and semi-in vivo pull down assays

(A) Bacteria-purified PYL proteins fused to a 6xHis tag (His-PYL) were pulled down upon incubation with recombinant MBP-ALIX or MBP bound to amylose resin. Anti-His was used in immunoblots (IB) to detect His-PYL fusions, and anti-MBP for MBP-ALIX and MBP.

(B) HA-PYL4 was pulled down upon incubation of oeHA-PYL4 plant extracts with recombinant MBP-ALIX or MBP bound to amylose resin. Protein extracts from wild-type (Col-0) plants were used as negative control. Anti-HA was used to detect HA-PYL4 and anti-MBP for MBP-ALIX and MBP.

To confirm that ALIX interacts with PYR/PYL ABA receptors in planta, we performed bimolecular fluorescence complementation (BiFC) assays. For this, we coinfiltrated *Nicotiana benthamiana* leaves with *Agrobacterium tumefaciens* cells carrying constructs for expression of ALIX and full-length ABA receptors fused to the N- or C-terminal portions of the yellow fluorescent protein (YFP). The infiltrated leaves were analyzed by confocal fluorescence microscopy 3 d after agro-infiltration. We could observe reconstitution of YFP fluorescence in cells that were coinfiltrated with constructs corresponding to YFPC-ALIX and YFPN-PYL (PYR1, PYL4, 5, 8 and 9), revealing a physical interaction between ALIX and the five ABA receptors; however expression of empty vectors combined with ALIX or receptor constructs did not restore the YFP fluorescence (Figure 13A). As observed in Supplemental Movies 1 to 5 (Supplementary Material), the reconstituted signal appeared into small and very mobile vesicles, likely endosomes. To date, all the reported interactions with ALIX occur at the MVBs, therefore to check if the BiFC vesicles corresponded to MVB, we coinfiltrated the leaves with the MVB marker ARA7 fused to mCherry (Geldner et al., 2009). As it can be observed in figure 13A and Supplemental Movie 1, the fluorescent BiFC signal colocalized with the signal from the mCherry-ARA7 marker indicating that ALIX-PYL4 interaction occurs in MVBs. Such localization was further substantiated by

quantification of the number of punctae displaying colocalization between the YFP and the mCherry fluorescent signal (Figure 13B).

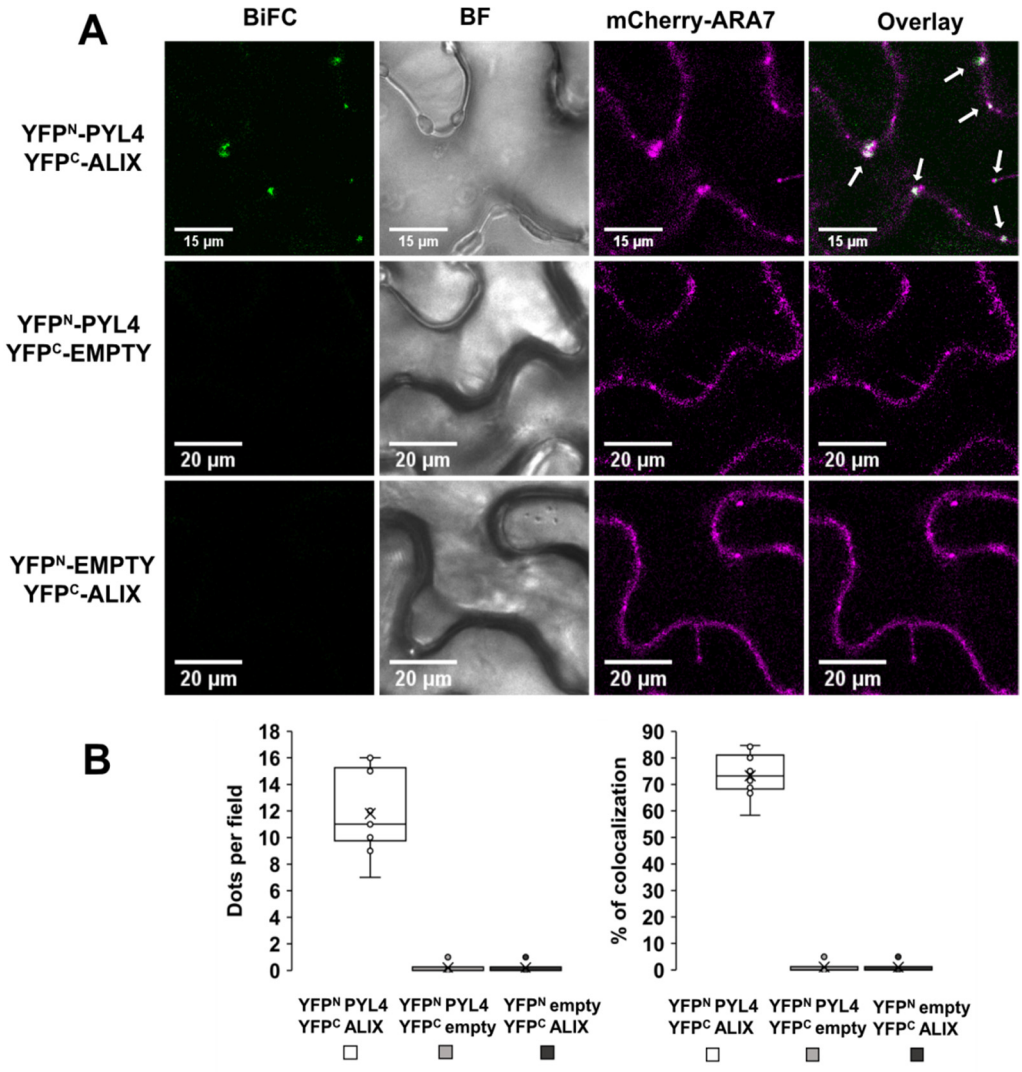

Figure 13. ALIX interacts with ABA receptors in vivo at MVBs

(A) In vivo interaction of ALIX with PYL4 assessed by BiFC. Confocal images were taken of *N. benthamiana* leaf epidermal cells expressing different BiFC construct combinations together with mCherry-ARA7, a MVB marker. Reconstitution of YFP fluorescence shows that ALIX and PYL4 constructs directly interact in mCherry-ARA7-labelled MVBs (i.e. punctae indicated by arrows in Overlay image). Bright-field (BF) images of the leaf areas are shown. Bars= 15 and 20 µm.

(B) The numbers of intracellular punctae per leaf section agroinfiltrated (y-axis; dots per 50x50 µm field) as well as the percentage of colocalization of YFP-fluorescent and mCherry-ARA7 labelled vesicles (y-axis; %

of colocalization) with each construct combination (x-axes) are quantified below the micrographs. Results were obtained from 10 fields from five biological replicates (2 fields/replicate)

4.3. *alix-1* mutant seedlings display increased sensitivity to ABA

Previous studies have reported that protein levels of several PYL receptors are regulated by proteolysis at both the proteasome and the vacuolar compartment (Bueso et al., 2014; Irigoyen et al., 2014). The later, involving the endosomal trafficking pathway, is mediated by members of the ESCRT machinery (i.e. FYVE1/FREE1 and VPS23A/ELC) and seems to modulate abundance of ABA receptors associated to membranes, as it is the case of PYL4, as a means to limit ABA responses. In fact, weak mutant alleles *fyve1/free1* and *vps23a/elc* showed hypersensitivity to ABA (Belda-Palazon et al., 2016; Yu et al., 2016).

ALIX also belongs to the ESCRT machinery, working as an accessory protein; since we have demonstrated that ALIX is able to interact with PYL ABA receptors, we hypothesized a similar function for ALIX, working as a negative regulator in ABA signaling. To test this, we characterized several ABA responses in weak *alix-1* mutant plants (note that null ALIX mutants are embryolethal; Cardona et al., 2015), including ABA-mediated inhibition of seed germination, seedling establishment, and root growth (Figure 14A, 14B and 14C). As controls, we used wild-type (Col-0) plants, a complemented line GFP-ALIX/*alix-1* (named GFP-ALIX for simplicity; Cardona-López et al., 2015), *cra1* (as ABA insensitive control; Fernández-Arbaizar et al., 2012), and *hab1-1 abi1-2* mutants (as ABA hypersensitive control; Saez et al., 2006). As it can be observed in figure 14, in all cases *alix-1* plants showed increased responses to ABA when compared to wild-type and GFP-ALIX controls. This was particularly significant in the case of ABA-mediated inhibition of seedling establishment (figure 14C) and root growth (figure 14D) in which *alix-1* plants were extremely hypersensitive to ABA, at a level comparable to the double mutant *hab1-1 abi1-2*. In agreement with previous reports, Arabidopsis transgenic lines overexpressing PYL4 (oeHA-PYL4) showed increased sensitivity to ABA (Pizzio et al., 2013), although not at the same extent than the *alix-1* line.

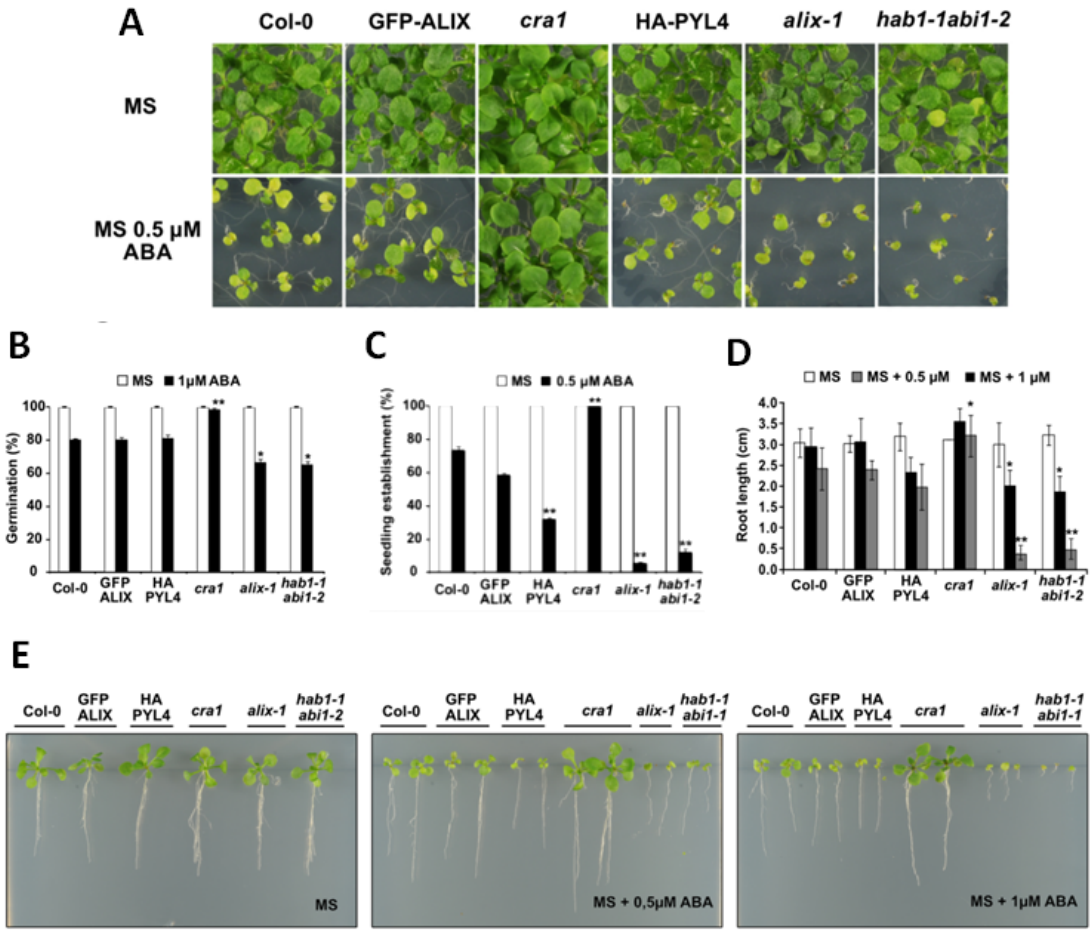

Figure 14. *alix-1* mutants display hypersensitivity to ABA

(A) Representative photographs of 12-d-old wild-type (Col-0), complemented line GFP-ALIX/*alix-1* (labelled as GFP-ALIX), oeHA:PYL4 (HA-PYL4), *alix-1*, ABA insensitive *cra1* and ABA hypersensitive *hab1-1 abi1-2* mutants grown in the presence of 0.5 µM ABA.

(B) Percentage of seeds germinated (radicle emergence) in the presence of 1 µM ABA at 3 d after sowing. Genotypes analyzed were as in (A).

(C) ABA-mediated inhibition of seedling establishment (emergence of the first true green leaves) of the same genotypes analyzed in (A) that were grown in medium lacking or supplemented with 0.5µM ABA.

(D) and (E) Root length measurements of seedlings germinated in the presence or absence of 0.5 µM ABA after 12 d, or in the presence of 1 µM ABA after 15 d. Genotypes were as in (A).

Photographs of representative plants analyzed in (D).

$p < 0.05$; $^{**}p < 0.01$ (Student's t-test) with respect to the wild –type in the same experimental conditions. In all cases, data are means of three biological replicates (n=20 in each replicate). Error bars represent SD. MS medium (MS) was used as a control in all assays.

Next, we tested the possibility that defective ALIX function could be leading to increased accumulation of ABA that could explain the ABA hypersensitivity phenotype of *alix-1* mutants. For this reason, we analyzed the concentration of this hormone in roots and shoots of wild-type, GFP-ALIX, *hab1-1 abi1-2* and *alix-1* plants. We found significantly higher ABA levels in *alix-1* samples in both roots and shoots, compared to wild-type controls (Figure 15). However, since increased ABA concentration was also observed in the GFP-ALIX line, which behaves as wild-type controls in response to ABA, higher ABA concentration is not sufficient to explain ABA hypersensitivity shown by *alix-1* mutants. Besides ABA, we also measured different ABA catabolites such as ABA-GE (ABA glucose-ester), 7'-hydroxy-ABA, PA and DPA (Dihydrophaseic acid; supplemental figure 1). As in the case of ABA content, we could observe higher levels of ABA catabolites both in *alix-1* and GFP-ALIX complemented lines, which may correlate with higher ABA levels in these lines.

Therefore, additional factors such as altered ABA-perception and/or signaling may be the responsible of the ABA hypersensitivity displayed by the *alix-1* mutants.

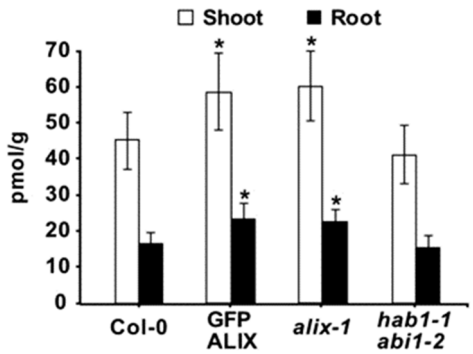

Figure 15. *alix-1* mutants display increased endogenous ABA levels
ABA concentration (pmol/g) in shoot and roots of 14-d-old seedlings for wild-type (Col-0), GFP-ALIX and *alix-1* mutant. *Hab1-1 abi1-2* mutants were used as the ABA hypersensitive control.
$*p < 0.05$; $**p < 0.01$ (Student's t-test) with respect to the wild –type in the same experimental conditions. Error bars represent SD.

4.4. Reduced function of ALIX decreases water loss and stomatal aperture

ABA is known to control water loss in plants by inducing stomatal closure (Munemasa et al., 2015). To test whether ALIX participates in this adaptive response against desiccation, we analyzed the kinetics of water loss over time in *alix-1* mutants compared to those of wild-type (Col-0), GFP-ALIX, oeHA-PYL4, *cra1* (ABA insensitive) and *hab1-1 abi1-2* (ABA hypersensitive) mutants (Figure 16). As observed in Figure 16A, *alix-1* seedlings lost less water than all controls, including the ABA hypersensitive mutant *hab1-1 abi1-2*. It has been previously described that the rate of water loss positively correlates with that of heat dissipation (Merlot et al., 2002). Consequently, when we analyzed foliar temperature by thermal infra-red (IR) imaging, we could observe higher leaf temperature in *alix-1* mutants (up to 1°C difference) compared to wild-type and GFP-ALIX controls. On the contrary, *open stomata 2-2* (*ost2-2*), a mutant with defective stomatal closure, displayed colder leaf temperature due to increased water loss through stomata (Merlot et al., 2007; Figure 16B)

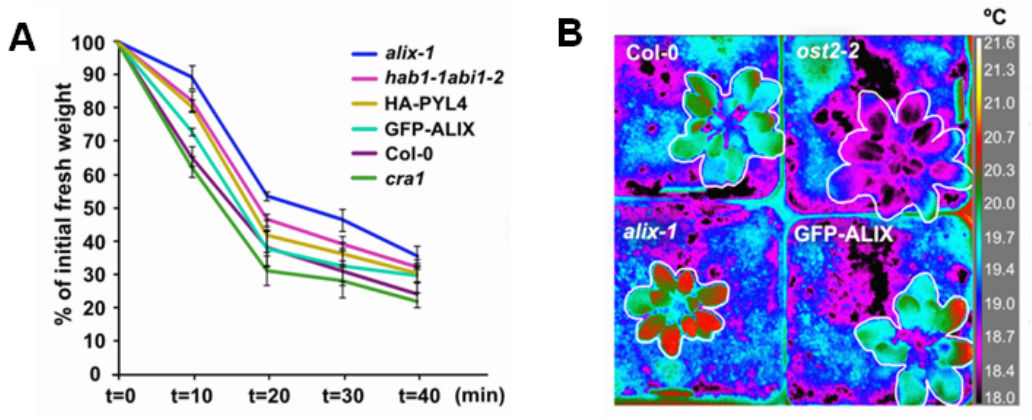

Figure 16. Reduced water loss in alix-1 mutants

(A) Kinetics of the loss of fresh weight in 15-day-old seedlings of wild-type (Col-0), complemented line GFP-ALIX, oeHA-PYL4 (HA-PYL4) and *alix-1* genotypes. *Cra1* and *hab1-1 abi1-2* mutants were used as ABA insensitive and hypersensitive controls, respectively. Plants were exposed for 40 minutes to the drying environment of a laminar flow hood. Values shown are averages ± SE from three replicates (n=15 in each replicate).

(B) Infra-red (IR) imaging was used to analyze foliar temperature in wild-type (Col-0), complemented line GFP-ALIX, and *alix-1* plants. The *ost2-2* mutant, that displays constitutively open stomata, was used as a control. Correspondence between false colors and temperatures (°C) in IR images is shown.

Next, we tested whether reduced water loss and heat dissipation in *alix-1* mutants were due to a defect in regulation of stomatal opening. To do so, we measured the kinetics of stomatal aperture in response to light (which is a stimulus that promotes stomatal opening) in leaves of wild-type Col-0, GFP-ALIX, and *alix-1* plants. As shown in figure 17, we could observe clear differences in stomata responsiveness to light just after 30 min of leaf illumination, with *alix-1* stomata being markedly closer than those of controls (33.8% less open than wild-type control). Indeed, even after 2 h of light treatment, *alix-1* stomata were not able to open as much as those in controls (44.5% less opened than the wild-type control), suggesting that reduced stomata openness in *alix-1* mutants leads to decreased water loss and reduced heat dissipation.

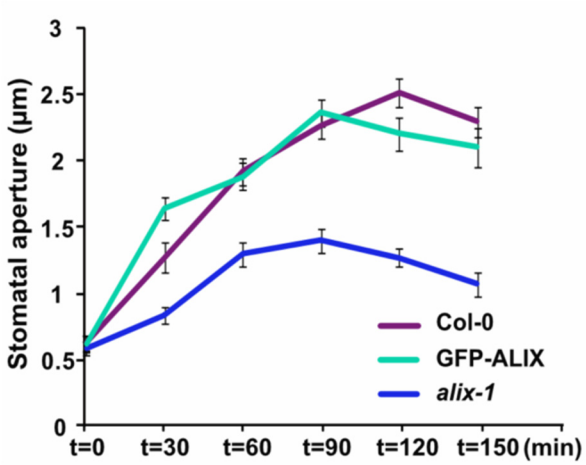

Figure 17 - *alix-1* mutants display reduced stomatal openness
Kinetics of stomatal aperture in response to light in leaves of wild-type (Col-0), GFP-ALIX/alix-1, and alix-1 plants. Values shown are averages ± SE from three replicates (n=70 in each replicate).

The mechanism through which stomatal aperture is achieved depends on changes in vacuolar volume at guard cells. Rapid fluxes of potassium and other osmolytes lead to an increase in vacuolar volume that eventually produces the opening of the stomata (Kim et al., 2010; Santelia and Lawson, 2016). To test whether impaired stomatal openness displayed by *alix-1* mutants could be due to altered vacuolar morphology, we used confocal microscopy to visualize fluorescence from a tonoplast marker (YFP-VAMP711; Geldner et al., 2009) in *alix-1* and wild-type plants. We could observe that

whereas wild-type guard cells were filled with a large vacuole, 2 or 3 smaller vacuoles could be visualized in the *alix-1* samples (Figure 18). This alteration should reduce the vacuole volume and pressure required for stomata openness.

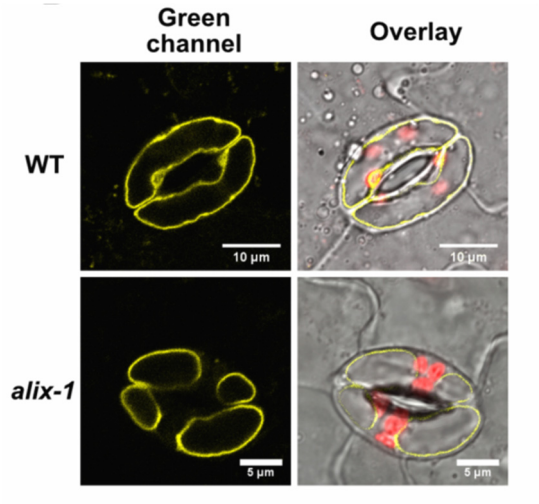

Figure 18. Altered vacuolar morphology in alix-1 mutants
Confocal imaging was used to visualize vacuolar morphology in guard cells of wild-type (Col-0) and *alix-1* plants expressing the tonoplast marker YFP-VAMP711. Plants were grown under short days for 21 days before leaves were collected. Bars = 10 and 5 µm, respectively.

Previous reports showed that loss of ALIX function leads to defects in vacuole biogenesis (Cardona-López et al., 2015; Kalinowska et al., 2015). To evaluate whether a general mechanical failure occurs in *alix-1* guard cells, due to altered vacuolar morphology, we analyzed the effect of fusicoccin (FC; a potent fungal activator of stomatal aperture; Squire and Mansfield, 1972) on their stomata opening. As shown in Figure 19, FC treatments greatly recovered *alix-1* defects in stomatal aperture, however they still displayed smaller apertures than wild-type controls upon FC treatment both under dark and light conditions. Despite this, FC-induced stomatal aperture in *alix-1* plants exceeded that of light-exposed wild-type controls (Figure 19, right graph), indicating that *alix-1* stomata are not mechanically restricted. These results suggest that the increased closeness in *alix-1* stomata is likely due to constitutive induction of signaling pathways that promote stomatal closure rather than to a major defect in vacuolar dynamics.

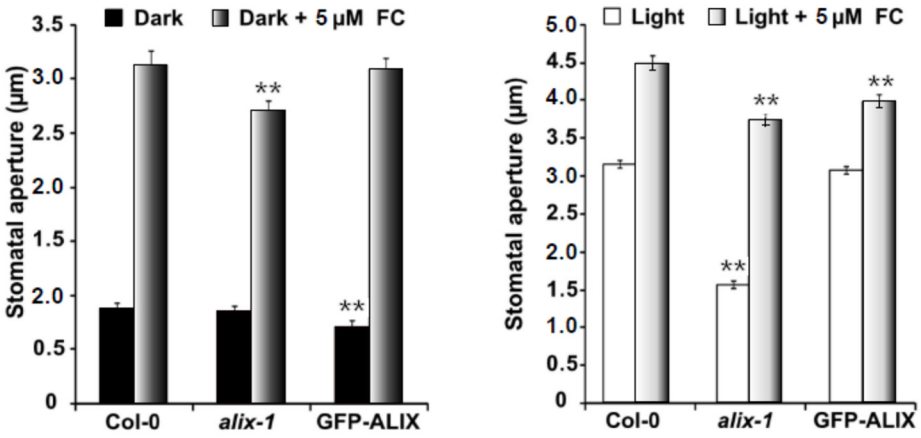

Figure 19. ***alix-1*** **vacuoles at guard cells are mechanically functional**

Stomatal aperture measurements in response to fusicoccin (FC) in dark- and light-treated leaves of wild-type (Col-0), GFP-ALIX, and *alix-1* plants. Values shown are averages ± SE from three replicates (n=70 in each replicate).

*p < 0.05; **p < 0.01 (Student's *t*-test) with resp'ct'to the wild-type in the same experimental conditions

4.5. Stomata are hypersensitive to ABA in alix-1 mutants

The observation that ALIX acts as a negative regulator of ABA responses prompted us to examine whether ALIX could be playing a similar role in controlling stomatal movement in response to ABA. First, we checked by confocal microscopy whether ALIX was localized in guard cells by visualizing GFP-ALIX driven by its own promoter (Figure 20). We could observe that ALIX was located in the cytosol and vesicle-like compartments of guard cells, indicating that ALIX function is extended to this specific cell type.

Next, we performed analysis of stomatal closure in response to different concentrations of ABA in *alix-1* mutants, wild-type (Col-0), and GFP-ALIX complemented lines. Our results showed that *alix-1* stomata were highly sensitive to low ABA concentrations, compared to the controls (Figure 21A). In fact, *alix-1* plants started to close their stomata at a concentration of 10nM ABA (by 27.5% relative to light-treated *alix-1* leaves) whereas wild-type and complemented lines remained open and only started to close them when treated with 1 µM ABA. This result indicates that ALIX function modulates ABA perception and/or signaling to control stomatal movement.

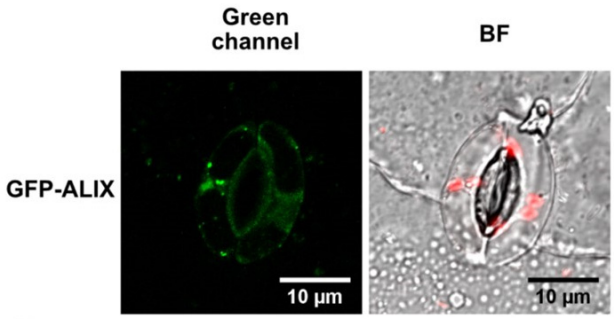

Figure 20. ALIX is located in guard cells
Confocal fluorescence images showing GFP-ALIX localization in the cytoplasm and punctuate structures of wild-type guard cells. Bar=10 µm.

According to our results, *alix-1* mutants show increased sensitivity to ABA and higher endogenous concentration of the ABA hormone; therefore, we speculated that *alix-1* plants may display constitutive ABA responses under non-stress conditions. To test this notion, we analyzed by RT-qPCR the transcript levels of two ABA responsive genes in *alix-1*, wild-type and GFP-ALIX seedlings grown under optimal conditions.

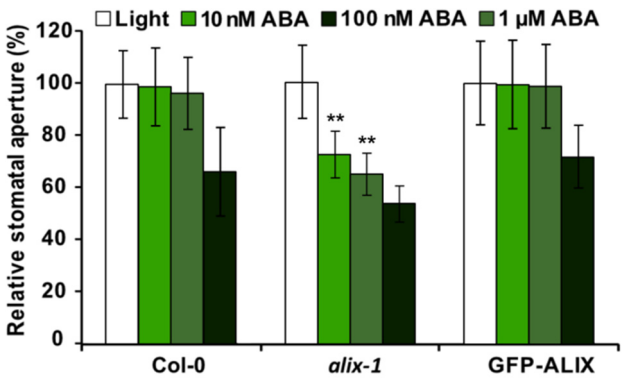

Figure 21. Hypersensitivity to ABA in alix-1 stomata
Analysis of stomatal closure in response to different concentrations of ABA in *alix-1* mutant, wild-type (Col-0), and GFP-ALIX/*alix-1* (labeled as GFP-ALIX) lines. Data are presented as percentage relative to each genotype under light conditions (100% stomatal aperture). Values shown are averages ± SE from three replicates (n=70 in each replicate).

We could observe that compared to the controls, *alix-1* mutants displayed increased expression of ABI1 (that encodes a PP2C-type phosphatase; Saez et al., 2006), and decreased expression of MYB60 (which encodes a guard cell-specific transcripcion factor that controls stomatal closure; Cominelli et al., 2005) under non-inductive conditions (Figure 22). These evidences suggest that *alix-1* mutation increases plant sensitivity to endogenous ABA levels.

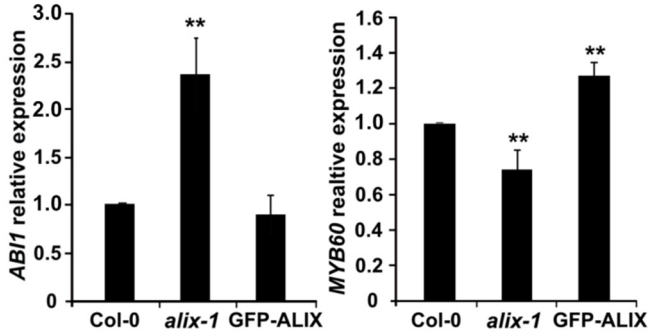

Figure 22. *alix-1* mutation increases ABA sensitivity of plants under non-stress conditions
RT-qPCR-analysis of the expression of ABA responsive genes *ABI1* and *MYB60* in soil-grown *alix-1* mutants, wild-type (Col-0), and GFP-ALIX/*alix-1* plants (GFP-ALIX).
**$p < 0.01$ (Student's *t*-test) with respect to the wild-type in the same experimental conditions. Data are means of three biological replicates with two technical replicates per sample. Error bars represent SD.

4.6. Trafficking and vacuolar degradation of ABA receptors are impaired in *alix-1* mutants.

Next, we aimed to gain insights on the molecular basis underlying the altered ABA responses observed in the *alix-1* mutants. Since it has been previously reported that other members of the ESCRT machinery participate in the trafficking of PYL proteins which are associated with the plasma membrane (Belda-Palazon et al., 2016; Yu et al., 2016), we first studied whether ALIX could be also involved in the trafficking of membrane associated PYLs. To do so, we introgressed a *35S:GFP-PYL4* transgene (Belda-Palazon et al., 2016) into the *alix-1* mutant background, and we analyzed by confocal microscopy if there were changes in the subcellular localization of the resulting GFP-PYL4 fusion between wild-type and *alix-1* seedlings treated or not with wortmannin (WM; an inhibitor of protein cargo trafficking to vacuoles that causes enlargement of MVBs ;Fernández-Borja et al., 1999). Under normal conditions, GFP-

PYL4 fusion mainly localize in the nucleus, cytosol and sorting endosomes of wild-type and *alix-1* plants (Figure 23; Bueso et al., 2014). However upon WM treatment of wild-type plants, GFP-PYL4 fluorescence appeared inside enlarged endosomal structures that were stained with LysoTracker Red, an acidophilic dye that allows to label and track lytic compartments in the late endocytic pathway (Belda-Palazon et al., 2016; Figure 23).

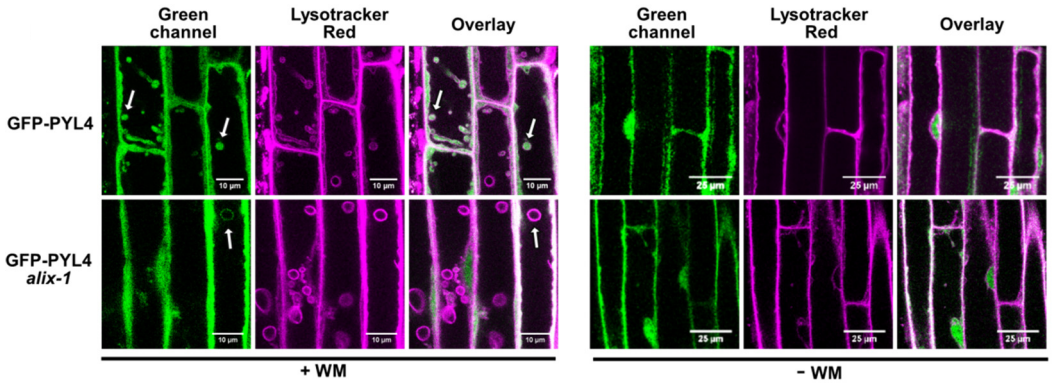

Figure 23. *alix-1* mutation affects the internalization of PYL4 to MVBs

Confocal images of wild-type (Col-0) and *alix-1* mutant root cells expressing GFP-PYL4 upon treatment or not with wortmannin (WM) and stained with LysoTracker Red. Bars= 10 and 25 µm. Arrows indicate representative WM- enlarged vesicles

Interestingly, we observed that in the *alix-1* mutants treated with WM, the number of LysoTracker Red-stained compartments containing GFP-PYL4 signal was highly reduced compared to those in wild-type controls, and, occasionally, GFP-PYL4 signal appeared decorating the membrane of these enlarged vesicles, which could not be appreciated in wild-type controls (Figure 23). This result indicates that the *alix-1* mutation might be interfering with the incorporation of the ABA receptors into MVB, likely impairing their degradation at the vacuole. To evaluate this hypothesis, we performed immunoblot analysis to compare endogenous PYL4 in the wild-type and in the *alix-1* mutants. We could observe increased accumulation of PYL4 in the *alix-1* mutant background compared to wild-type control when plants were grown in media containing 0.3 µM ABA (Figure 24A).

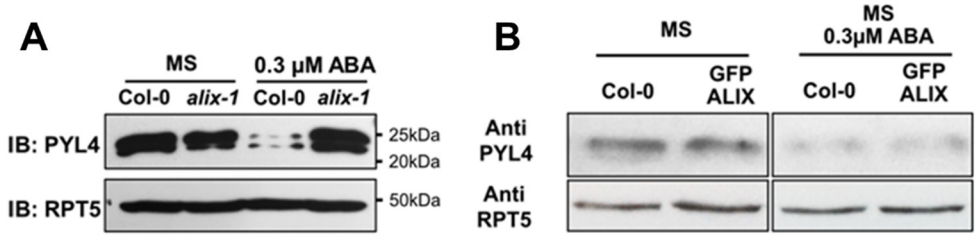

Figure 24. ***alix-1*** **mutations affects PYL4 accumulation upon ABA treatment**
(A) Immunoblot showing accumulation of endogenous PYL4 in wild-type (Col-0) and *alix-1* seedlings grown in the presence or absence of 0.3 µM ABA. Anti-RPT5 was used as loading control.
(B) Immunoblot showing accumulation of endogenous PYL4 in wild-type (Col-0) and GFP-ALIX/*alix-1* seedlings grown in MS or MS with 0.3 µM ABA for 6 days. Anti-RPT5 was used as loading control.

However, we could not observe differences in PYL4 abundance between the complemented line GFP-ALIX and the wild type (Figure 24B). These results indicate that ALIX activity to control PYL4 homeostasis is enhanced in response to ABA, probably reflecting a negative feedback mechanism to control PYL4 abundance. To discard the possibility that the different protein levels observed in the wild-type and the *alix-1* mutants were due to differences in *PYL4* gene expression, we performed RT-qPCR analysis, that revealed no significant differences between the genotypes (Figure 25A). This indicates that ALIX is acting at the posttranscriptional level to control PYL4 abundance. To further substantiate this hypothesis, we evaluated the degradation rate of PYL4 in both wild-type and *alix-1* backgrounds treated during 8 hours with the protein synthesis inhibitor cycloheximide (CHX), which precludes any effect due to changes in gene expression between genotypes. Upon treatment with CHX, we could observed a decline in PYL4 levels over time in the wild-type whereas this decrease was delayed in the *alix-1* mutants (figure 25B).

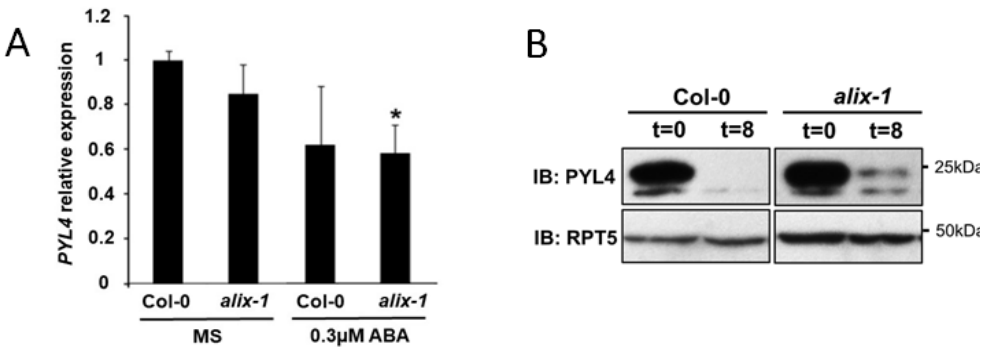

Figure 25. Diufferences in PYL4 transcript levels are not responsible of differences in protein levels between wild-type and *alix-1* mutant plants

(A) Expression levels of *PYL4*. *PYL4* expression levels do not change in wild-type (Col-0) and *alix-1* when grown under the same conditions (MS or MS with 0.3 µM ABA). * $p < 0.05$ (Student's *t*-test) with respect to the wild-type Col-0 grown in MS. In all cases, data are means of three biological replicates with two technical replicates each. Error bars represent SD.

(B) Immunoblot analyses of PYL4 levels in 8-d-old wild-type (Col-0) and *alix-1* seedlings treated with 50 µM CHX for 8 hours. Anti-RPT5 was used as loading control.

Next, we wanted to test whether defective ALIX function impairs sorting and degradation of PYL4 to the vacuole. To do so we analyzed the vacuolar delivery of a GFP-PYL4 fusion in the WT and *alix-1* background. This assay is based on the properties of the GFP, which is more stable in low pH environments (such as the vacuolar lumen) compared to other proteins. Then, when a GFP fusion protein is delivered to the vacuole for degradation, the GFP lasts longer in the vacuolar lumen rendering a degradative product (termed as GFP core) that allows to indirectly measure the levels of vacuolar arrival of the GFP fusion (daSilva et al., 2005; Scheuring et al., 2012). Therefore, we analized the ratio of GFP-PYL4 fusion and GFP core in the wild-type and *alix-1* mutant backgrounds. According to a role for ALIX in vacuolar destabilization of PYL4, we could observe that the GFP-PYL4/GFP core ratio was much higher in the *alix-1* mutant background compared to the wild-type, indicating that *alix-1* mutation is preventing a correct delivery of PYL4 to the vacuole (Figure 26)

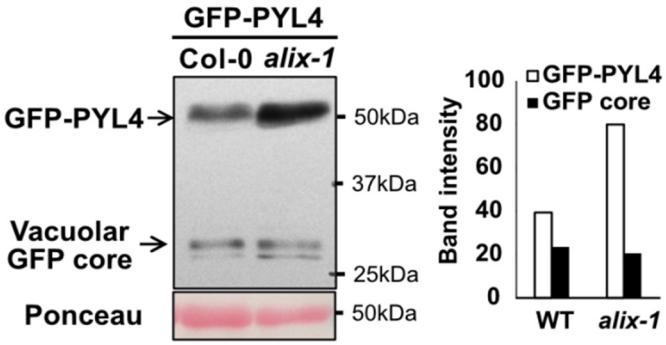

Figure 26. *alix-1* mutation impairs vacuolar delivery
Immunoblot analysis to track the vacuolar delivery of GFP-PYL4 in the wild-type (Col-0) and *alix-1* backgrounds. Anti-GFP was used in immunoblots to detect GFP-PYL4 and the GFP-core signal. Band intensity was quantified using Fiji (ImageJ 1.52i). Ponceau staining was used as loading control.

In order to test whether the *alix-1* mutation affects PYL4 levels at specific cell compartments, we analyzed PYL4 abundance at distinct subcellular fractions in wild-type and *alix-1* mutant plants. Noteworthily, *alix-1* mutation resulted in increased abundance of PYL4 in both cytosolic and microsomal fractions treated or not with ABA (Figure27).

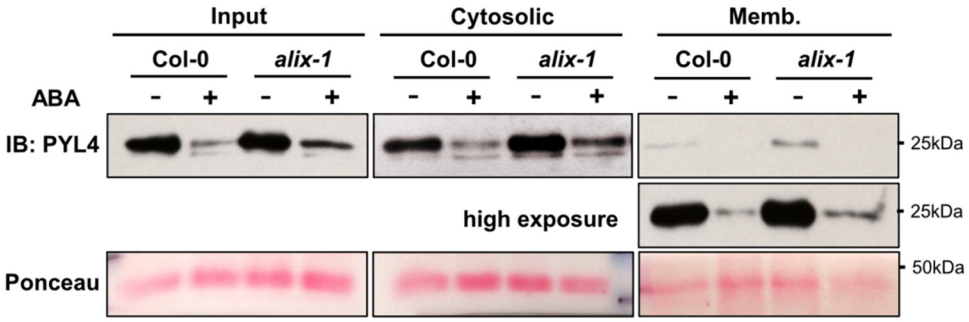

Figure 27. alix-1 mutants display increased PYL4 levels in both cytosolic and microsomal fractions
Isolation of microsomes from postnuclear fractions (Input) of 8-d-old wild-type (Col-0) or *alix-1* seedlings treated or not with ABA for 3 hours. Endogenous anti-PYL4 was used to evaluate PYL4 abundance in the cytosolic and microsomal (Memb.) fractions. Ponceau staining was used as loading control.

To test the possibility that disrupted ALIX function could be affecting the distribution of PYLs among other subcellular compartments such as the nucleus, we isolated nuclei

from *alix-1* and wild-type plants treated or not with ABA. The results showed that the *alix-1* mutantion had no effect on the nuclear pool of PYL4 (Figure 28).

Throughout our immunoblot analyses of endogenous PYL4 abundance, we noticed a secondary band of lower molecular weight. We found out that the lower band corresponded to PYR1 by using single *pyr1, pyl4* and quadruple *pyl* mutant (*pyr1 pyl4 pyl5 pyl8*; Figure 29).

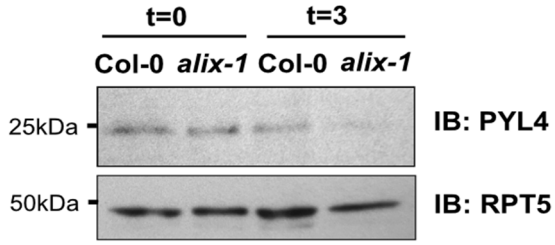

Figure 28. *alix-1* mutation do not alter PYL4 nuclear pool
Immunoblot analysis of PYL4 levels in nuclear protein extracts from 8-d-old wild-type (Col-0) or *alix-1* seedlings treated or not with ABA for 3 hours. Anti-RPT5 was used as loading control.

Interestingly, *alix-1* mutation did not display noticeable defects in the accumulation of PYR1 under the conditions tested, These results suggest that, although ALIX is able to interact with several ABA receptors, it differentially modulates their abundance, having a larger impact only on a subset of these receptors, including PYL4. Other possibility is that partial loss of function of ALIX in *alix-1* plants might not be sufficient to alter PYR1 homeostasis.

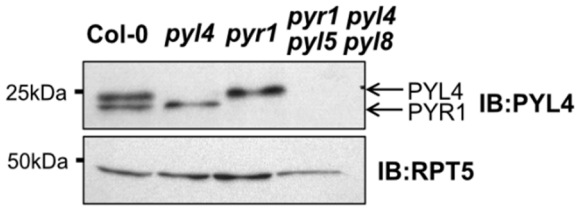

Figure 29. Lower band detected by anti-PYL4 corresponds to PYR1
Immunoblot to test the specificity of anti-PYL4. Protein extracts from 8-d-old wild-type (Col-0), single mutants *pyr1* and *pyl4* and quadruple mutant *pyr1 pyl4 pyl5 pyl8* were used. Arrows indicate the position of endogenous PYR1 and PYL4 proteins in the immunoblot. Anti-RPT5 was used as loading control

4.7. ABA hypersensitivity of *alix-1* mutants largely depends on ABA receptor function

To test whether increased accumulation of PYLs is the main cause for ABA hypersensitivity in *alix-1* mutants, we evaluated if the removal of ABA receptors was able to suppress the phenotypes observed in the *alix-1* mutants. To do so, we generated a pentuple *pyr1 pyl1 pyl4 pyl5 pyl8* mutant (termed *pent* here for simplicity) in the *alix-1* background (Figure 30) and we analyzed several ABA-related phenotypes in comparison to the pentuple mutant and wild-type controls.

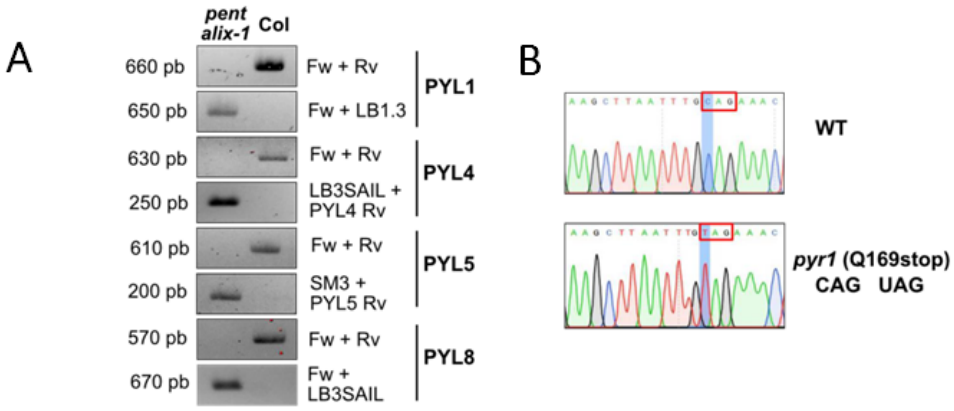

Figure 30. Genotyping of a pentuple *pyr1 pyl1 pyl4 pyl5 pyl8* mutant in the *alix-1* background (*pent alix-1*).

Single PYL mutants do not have severe phenotypic defects due to functional redundancy, however, the pentuple mutant we used has been reported to severely impair ABA perception and therefore plant responses to this hormone (Antoni et al., 2013). As shown previously (figure 14C), *alix-1* mutant plants exhibited increased ABA-mediated inhibition of seedling establishment; this phenotype was fully suppressed in the pentuple mutant background (*pent alix-1*; figure 31). In these analyses we included as a control another complemented line harboring a construct containing the *ALIX* genomic region (*gALIX/alix-1;* Cardona-López et al., 2015), which fully complemented *alix-1* phenotypic defects, further supporting our previous results for *alix-1* mutation as a cause of hypersensitivity to ABA.

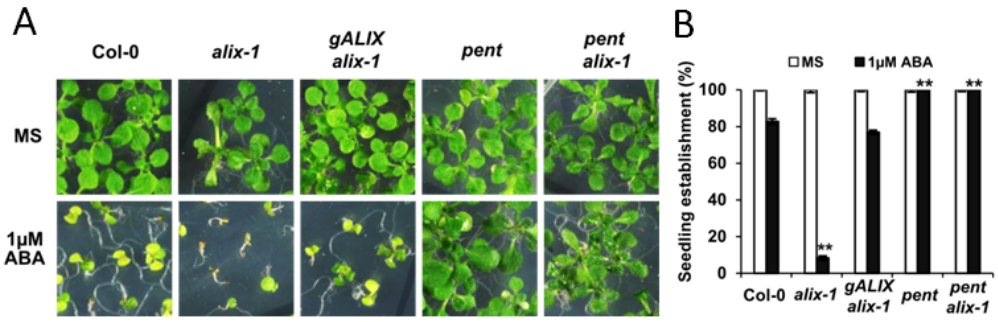

Figure 31. Increased ABA-mediated inhibition of seedling establishment displayed by alix-1 mutants is suppressed pent background

(A) Representative photographs of 15-d-old wild type (Col-0), *alix-1*, complemented line *gALIX/alix-1* and pentuple *pyr1 pyl1 pyl4 pyl5 pyl8* in wild type (*pent*) or *alix-1* (*pent alix-1*) backgrounds grown in the presence of 1 µM ABA.

(B) ABA-mediated inhibition of seedling establishment (emergence of the first true leaves) of the same genotypes analyzed in (A) that were grown in medium lacking or supplemented with 1 µM ABA. Data are means of three biological replicates (n=20 in each replicate). Error bars represent SD. MS medium (MS) was used as a control in all assays. $*p < 0.05$; $**p < 0.01$ (Student's *t*-test) with respect to the wild type in the same experimental conditions.

We also evaluated ABA responses, such as water loss and heat dissipation at the plant adult stage. In all instances, the *pent alix-1* mutants suppressed the defects displayed by the *alix-1* mutants (Figure 32). These results indicate that increased abundance of PYLs is largely responsible of the enhanced stomatal closure in *alix-1* mutants. According to this notion, when we analyzed stomatal closure in response to different concentrations of ABA, in *alix-1* mutants, wild-type (Col-0), *pent* mutants, and *pent alix-1* plants, we could observe that the high sensitivity of *alix-1* stomata to low concentrations of ABA was abolished when ABA perception was hampered (figure 33). Indeed, the stomatal aperture defects found in non-treated *alix-1* plants were also suppressed in *pent alix-1* background, further supporting the notion that *alix-1* stomata are fully operative but highly sensitive to endogenous ABA levels.

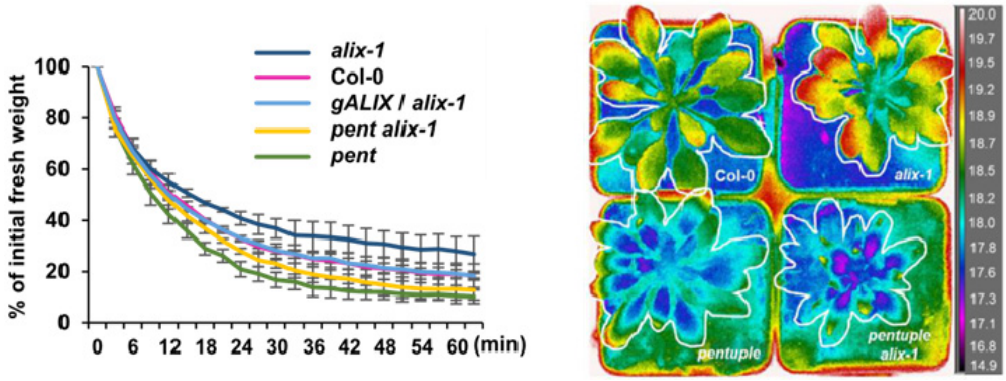

Figure 32. *pent alix-1* mutant suppress the reduced water loss and increased foliar temperature displayed by *alix-1* plants

(A) Kinetics of the loss of fresh weight in 15-d-old seedlings of wild type (Col-0), *alix-1*, complemented line *gALIX/alix-1* and pentuple *pyr1 pyl1 pyl4 pyl5 pyl8* in wild type (*pent*) or *alix-1* (*pent alix-1*) backgrounds. Plants were exposed for 60 minutes to the drying environment of a laminar flow hood. Values shown are averages ± SE from three replicates (n=15 in each replicate).
(B) Analysis of foliar temperature of 40-day-old wild-type (Col-0), *alix-1*, *pent* and *pent alix-1* plants using infra-red (IR) imaging. Correspondence between false colors and temperatures (°C) in IR images is shown.

To evaluate the contribution of ALIX-dependent control of PYL abundance on plant adaptation to ABA-related stresses, such as drought, we performed long term assays in adult plants subjected to water deprivation. We used the same genotypes as in the stomatal closure assays. Our findings show that after 20 days of water starvation, wild-type plants (both Col-0 and *gALIX: alix-1)* and *pentuple* mutants, were completely dry, whereas *alix-1* mutants showed no signs of dehydratation. However *pent alix-1* mutants displayed an intermediate phenotype, starting to show some signs of dehydratation (Figure 34).

These results indicate that although increased abundance of PYLs largely explains the ABA hypersensitivity of *alix-1* mutants, ALIX must have other functions in regulating other drought processes that might be independent of ABA or rely on different ABA signaling components.

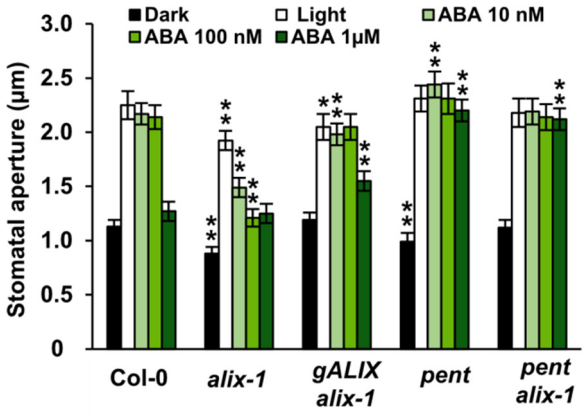

Figure 33. ABA-hypersensitivity of *alix-1* stomata is recovered in *pent alix-1* mutants

Analysis of stomatal closure in response to different concentrations of ABA in the same genotypes analyzed in wild type (Col-0), *alix-1*, complemented line *gALIX*/*alix-1* and pentuple *pyr1 pyl1 pyl4 pyl5 pyl8* in wild type (*pent*) or *alix-1* (*pent alix-1*) backgrounds. Values shown are averages ± SE from three replicates (n=100 in each replicate). *$p < 0.05$; **$p < 0.01$ (Student's *t*-test) with respect to the wild type in the same experimental conditions.

Figure 34. *alix-1* mutants are highly tolerant to drought

Representative photographs of 40-d-old grown under short day conditions wild type (Col-0), *alix-1*, complemented line *gALIX*/*alix-1* and pentuple *pyr1 pyl1 pyl4 pyl5 pyl8* in wild type (*pent*) or *alix-1* (*pent alix-1*) backgrounds before and after 20d of water deprivation.

4.8. *alix-1* mutation limits ALIX ability to interact with ABA receptors and ESCRT components

In a previous study it was shown that the *alix-1* mutation which causes a substitution of the Gly260 for an Asp, reduces the ability of the resulting mutant protein (ALIX-1) to

interact with the ESCRT-III component SNF7/VPS32 (Cardona-López et al., 2015; Dr. Laura Cuyas' thesis). Based on this result, we aimed to test whether *alix-1* mutation also affects the interactions of ALIX with ABA receptors. To do so, we performed yeast two hybrid assays using as prey either the Bro1 domain or a Bro1 version containing the *alix-1* mutation (Bro1mut). As it occurred with SNF7/VPS23, we could observe that the mutant version displayed reduced interaction with all four PYL receptors tested compared with the wild-type versions (Figure 35). To demonstrate that this reduced interaction ability was not due to lower accumulation of the mutant protein fusion, we extracted soluble proteins from the yeast cotransformants and performed western blot analysis. We could observe no differences in protein fusion abundance for baits or preys. Indeed, in some cases the abundance of the mutant protein fusion was even higher than that of the wild-type ALIX version (Figure 36).

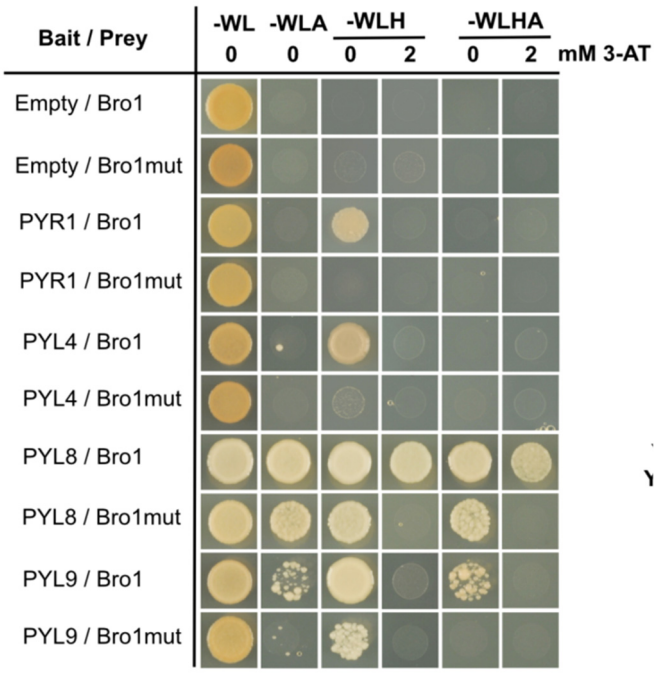

Figure 35. *alix-1* mutation impairs ALIX interaction with PYLs in Y2H
Yeast two-hybrid assays for the interaction between the Bro1 domain of ALIX or a variant containing the *alix-1* mutation (Bro1mut) and PYL ABA receptors. Transformed yeast cells were grown in SD-WL medium as a transformation control and in SD-WL media lacking adenine (WLA), histidine (WLH) or both (WLHA) for interaction assays. 3-amino-1,2,4-triazole (3AT; 2mM) was added to better visualize positive interactions. Empty vectors were used as negative controls.

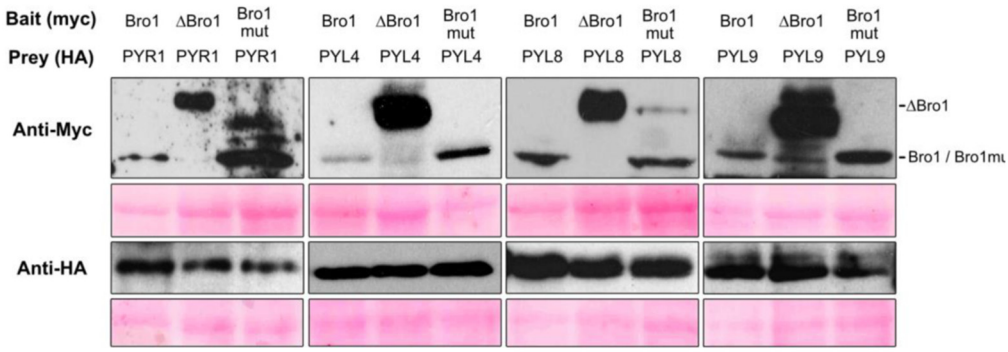

Figure 36. Expression analysis of bait and prey fusions used in yeast-two hybrid assays

Total protein extracts from yeast clones expressing bait and prey fusions as indicated were immunoblotted using anti-myc (detects baits) and anti-HA (detects preys) antibodies. Ponceau staining of membranes was used as loading control.

Next, we checked whether impaired ALIX-PYL interaction by the *alix-1* mutation could also be observed in planta. To do so, we performed BiFC experiments expressing either wild-type ALIX or ALIX-1 mutant protein fusions together with PYL4, as a representative member of the PYL family fused to the N- or C-terminal fragments of the YFP. According to the results obtained in the Y2H assays, confocal fluorescence imaging showed interaction between wild-type ALIX and PYL4 in MVBs (Figure 37). However, when we co-infiltrated the ALIX-1 mutant version with PYL4 fusion, the interaction was severely reduced (16% of that observed for ALIX-PYL4; Figure 37, right panel) as shown by quantitative analysis from Z-stacking sections. As we did in the Y2H assays, we assessed protein levels of the two corresponding YFP fusions in the co-infiltrated leaves to discard an effect of lower protein fusion abundance. We could verify that reduced ALIX-1/PYL4 interaction is not due to a lower accumulation of the mutant protein fusion in *N. benthamiana* leaves (Figure 38), further indicating an effect of *alix-1* mutation in the interaction ability of ALIX with protein cargos.

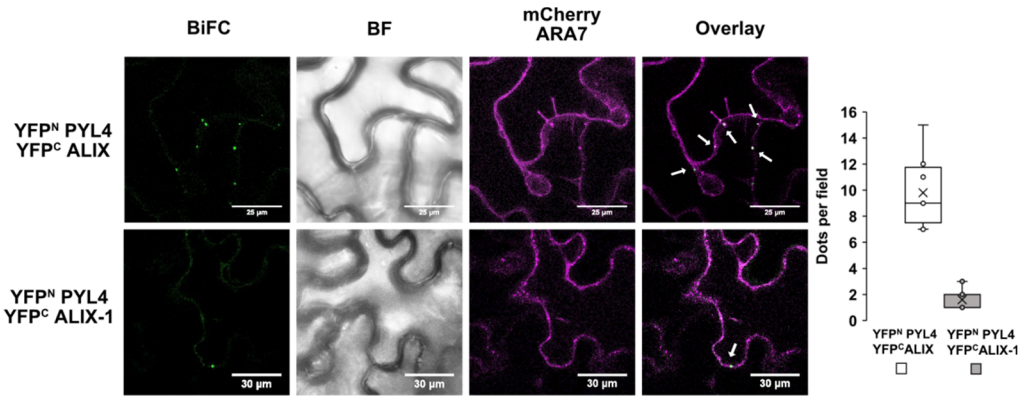

Figure 37. ***alix-1*** **mutation impairs the interaction of ALIX with PYL4 in vivo**
Colocalization of YFP fluorescence by ALIX/PYL4 or ALIX-1/PYL4 interaction with mCherry-ARA7-labelled MVBs is indicated by arrows in the Overlay. Bright-field (BF) images of the corresponding leaf areas are also shown. The numbers of intracellular punctae per leaf section (y-axis; dots per 50x50 µm field) agroinfiltrated with each construct combination (x-axis) are quantified. Results were obtained from 10 fields from five biological replicates (2 fields/replicate).

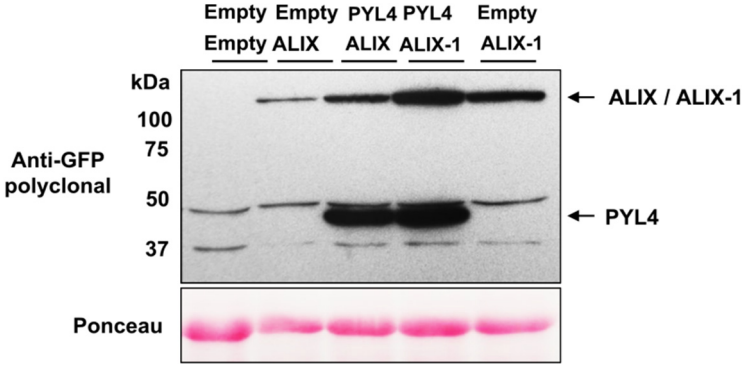

Figure 38. Expression analysis of PYL4, ALIX and ALIX-1 protein fusions used in the BiFC assays
Protein extracts from *Nicotiana benthamiana* leaves agroinfiltrated with the indicated construct combinations were immunoblotted using polyclonal anti-GFP, detecting both YFP-C and YFP-N protein fusions. The position of bands corresponding to wild-type and ALIX-1 mutant versions of ALIX, and that of PYL4 fused to YFP fragments are shown. Ponceau staining of the membrane was used as loading control.

Two recent studies have revealed that sorting and delivery of ABA receptors for their vacuolar degradation is mediated by components of the ESCRT machinery, i.e. FYVE1 and VPS23A, and that these two proteins interact with each other (Belda-Palazon et al., 2016; Shen et al., 2016; Yu et al., 2016). Moreover, it was found that both FYVE1 and VPS23A are able to physically bind to ALIX in vivo (Shen et al., 2016; Yu et al., 2016). We aimed to test whether *alix-1* mutation also affects such interactions. To achieve this, we performed BiFC in vivo analysis selecting VPS23A as a representative component of the ESCRT-I complex. Interaction with VPS23A was greatly hampered when the ALIX-1 mutant version, instead of wild-type ALIX, was co-expressed in *N. benthamiana*, as observed by quantitative analysis from Z-stacking sections of ALIX/VPS23A and ALIX-1/VPS23A agroinfiltrated leaf cells (Figure 39). As shown in figure 40, the reduced interaction observed in the BiFC assays was not due to lower accumulation of the mutant protein, indeed we could observe even higher levels of ALIX-1 protein.

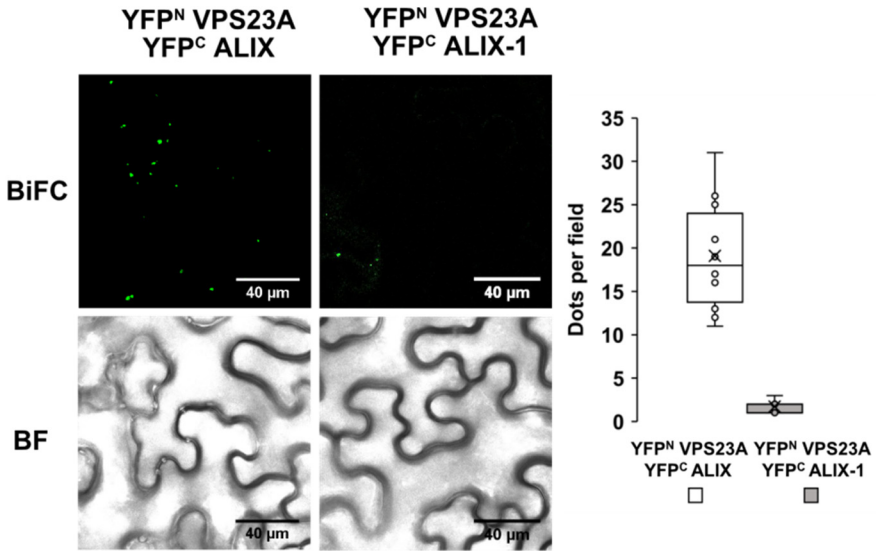

Figure 39. *alix-1* mutation impairs ALIX interaction with VPS23A in vivo

BiFC assays showing impaired interaction of an ALIX version containing the *alix-1* mutation (ALIX-1) with VPS23A. Bars = 40 µm. Bright-field (BF) images of the corresponding leaf areas are shown. The numbers of intracellular punctae per leaf section (y-axis; dots per 50x50 µm field) agroinfiltrated with each construct combination (x-axes) are quantified. Results were obtained from 10 fields from five biological replicates (2 fields/replicate).

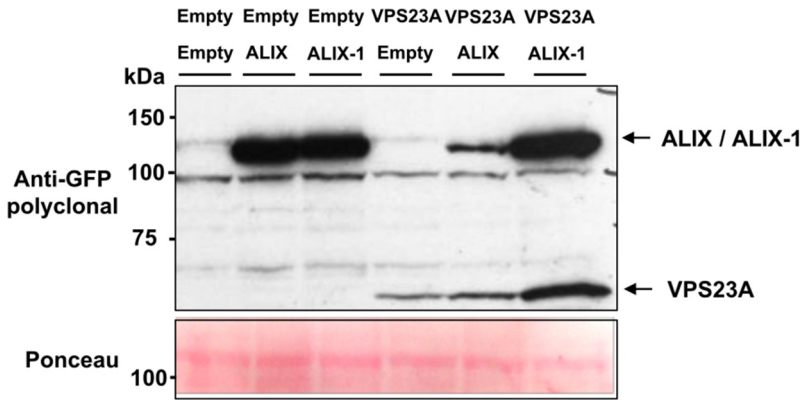

Figure 40. Expression analysis of VPS23A, ALIX and ALIX-1 protein fusions used in the BiFC assays
Protein extracts from *Nicotiana benthamiana* leaves agroinfiltrated with the indicated construct combinations were immunoblotted using polyclonal anti-GFP antibody to detect YFP-C (fused to VPS23A, ALIX or ALIX-1) or YFP-N (fused to ALIX or ALIX-1) protein fusions. Ponceau staining of the membrane was used as loading control.

In previous studies it has been reported that ALIX homologues from different organisms form dimers and this ability is essential for their activity (Pires et al., 2009; Fisher et al., 2009; Cardona-López et al., 2015). We took advantage of this ability to test the functionality of our ALIX-1 BiFC constructs. Therefore, we analyzed ALIX/ALIX-1 dimerization levels by BiFC. The quantitative analysis revealed that although ALIX-1 interaction with wild-type ALIX is reduced (43.7% of that shown by ALIX/ALIX constructs; figure 41), it is not as hampered as the interaction of ALIX-1 with PYL4 (16% compared to the ALIX with PYL4 interaction) or ALIX-1 with VPS23A (8.9% compared to the ALIX/VPS23A interaction). Again, we evaluated protein levels in the co-infiltrated *Nicotiana benthamiana* leaves, and we observed no significant differences in protein fusion levels between all constructs tested(Figure 42). These results show that the ALIX-1 BiFC constructs retain differential protein-protein interaction abilities and that reduced interaction of ALIX-1 with PYL4 and VPS23A is not due to full dysfunctionality of ALIX-1 fusions.

Overall, reduced physical interaction of ALIX-1 mutant protein with PYL receptors and a known ESCRT-I component mediating their trafficking (i.e. VPS23A), together with decreased ALIX-1 dimerization capability, provides an explanation at the molecular

level for defects in sorting and vacuolar degradation of ABA receptors in the Arabidopsis *alix-1* mutants.

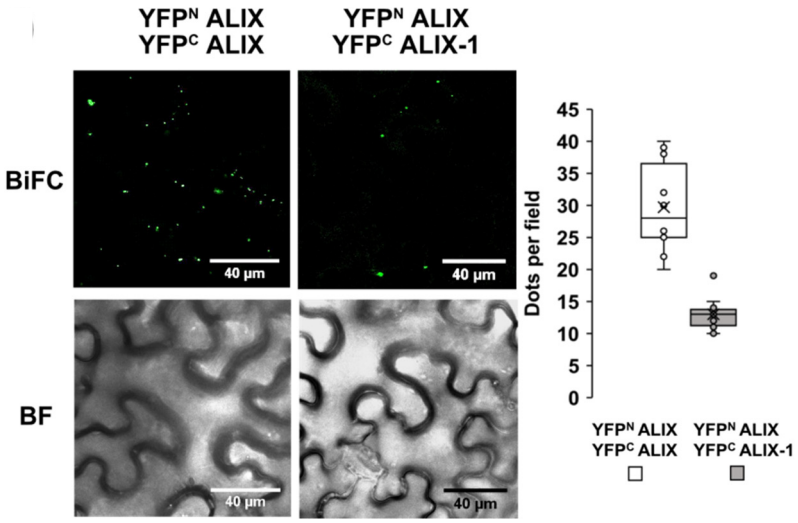

Figure 41. *alix-1* mutation partially impairs ALIX/ALIX dimerization in vivo

BiFC assays showing impaired dimerization of ALIX wild-type protein with an ALIX version containing the *alix-1* mutation (ALIX-1). Bars = 40 µm. Bright-field (BF) images of the corresponding leaf areas are shown. The numbers of intracellular punctae per leaf section (y-axis; dots per 50x50 µm field) agroinfiltrated with each construct combination (x-axes) are quantified. Results were obtained from 10 fields from five biological replicates (2 fields/replicate).

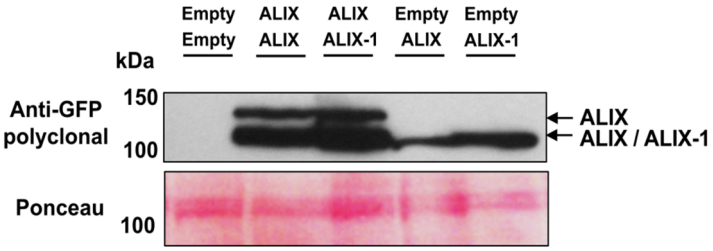

Figure 42. Expression analysis of ALIX and ALIX-1 protein fusions used in the BiFC assays

Protein extracts from *Nicotiana benthamiana* leaves agroinfiltrated with the indicated construct combinations were immunoblotted using polyclonal anti-GFP antibody to detect YFP-C (fused to ALIX) or YFP-N (fused to ALIX-1) protein fusions. Ponceau staining of the membrane was used as loading control.

5. DISCUSSION

ALIX homologues play essential roles in key processes in yeast and animal systems. However our knowledge in plants is much more limited. Previous studies from our lab and those from others have demonstrated the relevance of ALIX in the endosomal pathways and in the trafficking of cargo proteins such as PHT1 and BRI1 (Cardona-López et al., 2014). However the involvement of ALIX in other processes and in the trafficking of other cargos remained elusive. In this work we have discovered that ALIX plays an essential role in controlling ABA receptor abundance, by facilitating their sorting to the vacuole for degradation, likely participating in a desensitizing mechanism.

5.1. ALIX directly interact with PYLs

ALIX V-domain (comprising the coiled coil domains) has been described as a ubiquitin-binding domain that enables ALIX to interact with ubiquitinated protein cargos, a feature that is conserved in its homologs from other organisms (Fisher et al., 2007; Dowlatshahi et al., 2012; Keren-Kaplan et al., 2013; Pashkova et al., 2013; Kalinowska et al., 2015). However, in the case of PYL receptors, ALIX is able to directly interact with them, as we have demonstrated in our Y2H, PD and BiFC assays. It has been recently described that the ESCRT-I components VPS23A and FYVE1 are also able to directly interact with un-modified ABA receptors (Belda-Palazon et al., 2016; Yu et al., 2016; García-León et al., 2019). These interactions seem to be mediated by additional motifs other than their ubiquitin-binding domains, which could reflect a role for FYVE1, VPS23A and ALIX in ubiquitin-independent sorting of protein cargos. Indeed, previous studies show that cargo sorting into the MVB pathway, particularly in the case of soluble proteins, can occur in the absence of cargo ubiquitination just by physical interaction of cargos with components of any ESCRT complex (Mageswaran et al., 2014). Indeed, examples of mammalian ALIX-mediated ubiquitin-independent ESCRT-III/MVB sorting have been described (Dores et al., 2012, 2016), a process that might be extended to Arabidopsis ALIX when promoting trafficking of PYLs.

Physical interaction of FYVE1 with PYLs was found to be mediated by its N-terminal portion, a 200 aa-long intrinsically disordered region (IDR) that contains Pro- and Gln-rich sequences (Belda-Palazon et al., 2016). Upon binding to partners, IDR regions can adopt metastable conformations that allow molecular recognition of targets with low

affinity (Ward et al., 2004). Thus, the IDR region of FYVE1 might fold onto PYL proteins and stabilize their association (Belda-Palazon et al., 2016). Similarly, ALIX contains a Pro-rich IDR region at its C-terminal portion that likely enables interaction of the ALIX ΔBro1 domain with PYL proteins, as shown by Y2H assays. Noteworthy, in these assays we also identified interaction with PYLs through the Bro1 domain of ALIX, suggesting that different ALIX domains ensure recognition and binding of PYL proteins as an ubiquitin-independent "sorting signal" for entry into the ILVs.

It is especially relevant the fact that a pool of soluble proteins, the PYL ABA receptors, are able to transiently associate to the PM and undergo endocytosis and vacuolar degradation. It has been described the existence of soluble proteins that reach the vacuole helped by VSR (VACUOLAR SORTING RECEPTOR) proteins that travel with them through the endomembrane system (Kang et al., 2012). Nevertheless, the fate of these proteins that are targeted to the vacuole is not for degradation, they are storage proteins, like sporamin or aleurin, or lytic proteases that reside in the vacuole, such as amylases (Kang et al., 2014; Lee et al., 2013). Therefore, the participation of ALIX, together with the already described role of VPS23A and FYVE, in the vacuolar degradation of PYLs provides more evidences that support a new mechanism of degradation for soluble proteins never described before in any other system.

5.2. Role of ALIX in the trafficking of ABA receptors

Levels of the distinct ABA signaling components have to be properly regulated to ensure appropriate responses to ABA. Thus, plants need desensitization mechanisms to turn off ABA signaling to allow for example germination or normal plant growth once abiotic stress is relieved (Antoni et al., 2011; Irigoyen et al., 2014; Castillo et al., 2015; Munemasa et al., 2015). Recently, novel mechanisms to control the abundance and or activity of ABA signaling components associated to membranes have been described. These mechanisms include ubiquitination of ABA receptors at the plasma membrane by the E3 ligase RSL1 and their trafficking to the vacuole for degradation mediated by ESCRT-I subunits (i.e. VPS23A and FYVE1; Shen et al., 2016; Yu et al., 2016). In this study we have added a new player to this mechanism, the ESCRT-III associated component ALIX, which is able to physically interact with PYLs, VPS23A and FYVE1 in vivo (Shen et al., 2016; Yu et al., 2016; García-León et al., 2019), further supporting the notion that a canonical ESCRT pathway mediates vesicle trafficking of ABA receptors.

In this process ALIX modulates PYL4 abundance at the cytoplasm, participating in the plant desensitization mechanisms against this hormone, repressing ABA-triggered developmental (i.e. seed germination, seedling establishment, and root growth) and water deficiency-responses (stomatal closure). Indeed, we found that PYL4 turnover is enhanced in response to ABA which indicates that ALIX participates in an ABA-triggered negative feedback mechanism that may help to temporally restrict PYL4 function, allowing pulsed responses to ABA. This role of ABA has been previously reported for other membrane-associated ABA components such as the ion channel KAT1. When ABA levels are high, KAT1 endocytosis is enhanced to sequester it from the membrane to tightly control stomatal movements (Sutter et al., 2007).

Interestingly, ABA may have opposed roles in the desensitization mechanisms depending on the subcellular compartment and the process to be regulated. For instance, in the above mentioned mechanism, ABA triggers membrane-associated ABA receptor degradation, whereas in the nucleus, ABA protects PYL8 from degradation by inhibiting CRL4 E3 ubiquitin ligases that target it for ubiquitination via 26S proteasome (Belda-Palazon et al., 2018; Irigoyen et al., 2014). The latter one is especially important to break seed dormancy when endogenous ABA levels decrease. The antagonistic effect of ABA on the abundance of PYLs in separate cell compartments indicates independent modulation of different responses to this hormone.

5.3. Effects of the *alix-1* mutation

In this study we have unraveled the molecular basis that explains, at a great extent, the phenotypic defects observed in the *alix-1* mutants. In this context, we have shown that ALIX-PYL interaction was severely reduced in both Y2H and BiFC assays when an ALIX version containing the *alix-1* mutation was used. *Alix-1* mutation leads to substitution of non-charged Gly260 for Asp, a charged amino acid, which likely affects the structure of a tetratricopeptide pocket embedded into the Bro1 domain, resulting in altered Bro1 conformation and impaired protein–protein interaction ability. Weakened interaction of ALIX-1 with PYLs should limit internalization of the latter into ILVs, producing an accumulation of PYLs in different compartments due to its hampered degradation. In fact, it has been previously reported that increased PYL4 abundance (as in HA-PYL4 overexpressing plants) is sufficient to increase plant sensitivity to ABA (Pizzio et al., 2013). However, our data showed that *alix-1* mutants display a more severe phenotype in the presence of the hormone than HA-PYL4 overexpressing plants (Figure 2). Since ALIX protein interacts with other members of the PYL family, including

PYR1, PYL5, 8 and 9 in vesicle compartments in planta (Figure 1 and Supplemental Movies 2 to 5), it is very likely that ALIX has a general role in the control of the abundance of PYLs acting in close proximity to membranes. Indeed, *alix-1* mutation not only hampers ALIX-PYL interaction, but also affects the ability to interact with ESCRT-III component SNF7 (Cardona-López et al., 2015), ESCRT-I subunit VPS23A, and, to a lesser extent, with wild-type protein ALIX (this study; García-León et al., 2019) which could be altering trafficking of protein cargos, including ABA receptors. Thus, our data support a model in which ALIX contributes to the function of ESCRT-I and ESCRT-III complexes, allowing recognition and clustering of cargo proteins on the MVB surface (Odorizzi 2006; Belda-Palazon et al., 2016). The fact that ALIX is able to interact with components of both ESCRT-I (i.e. VPS23A and FYVE) and ESCRT-III (SNF7) brings the hypothesis that ALIX could be acting as a bridge among ESCRT complexes, helping to transfer cargos from ESCRT-I to –III complexes, avoiding their diffusion from areas of concentration at the MVB surface. Future studies should test this hypothesis using known targets of the ESCRT machinery, including integral membrane proteins. Additional effects due to impaired ALIX function, such as reduced ILV formation at MVBs and defective cargo processing by AMSH proteins (Kalinowska et al., 2015; Shen et al., 2016), cannot be disregarded as they may contribute to the inadequate vacuolar turnover of PYLs in *alix-1* mutants. Future work should address the molecular details underlying specific recognition of PYLs, including identification of PYL motifs targeted by ALIX domains. Such studies will help us to understand whether similar protein–protein interaction domains mediate binding of ALIX to other ABA pathway components identified in our studies, such as CAR proteins or the PP2C-type ABI1.

Besides PYLs accumulation, we have found that *alix-1* mutants have altered vacuolar biogenesis and increased PA and ABA levels which could be also contributing to the hypersensitive phenotype of the *alix-1* mutants. It has been previously reported that as occurs with *alix-1,* many ABA response mutants display altered hormonal levels, suggesting some kind of feedback regulation (Filkenstein, 2013). It has been demonstrated that drought stress stimulates de novo ABA biosynthesis. In this context, increased PYL abundance in *alix-1* plants, might be constitutively signaling and inducing the expression of ABA biosynthetic genes in a positive feedback loop.

In this work, we have shown that reduced PYL function in the *pent alix-1* plants suppresses most of the ABA hypersensitive phenotypes observed in the *alix-1* mutants. Nevertheless, the elimination of PYR1, PYL1, PYL4, PYL5 and PYL8 is not sufficient to complement all the phenotypes of the *alix-1* mutants, especially the ones related to

stomatal movements. For instance, *pent alix-1* mutants display higher resistance to drought when compared to *pent* mutants and wild-type plants. PYL2 has been reported to be the most important ABA receptor for ABA-induced stomatal closure. Indeed, loss of function of *PYL2* gene has been shown to be sufficient to cause ABA-stomata insensitivity (Dittrich et al., 2019), whereas overexpression of PYL2 has been proved to be a powerful biotechnological tool to fight drought stress (Cao et al., 2017). In the *pent* background, PYL2 is functional. Since *alix-1* plants have a defect in trafficking and degradation of PYLs, they might be failing to degrade PYL2, causing its accumulation, which would produce a similar effect to that of PYL2 overexpression for plant tolerance to drought.

In addition, recent studies have shown that PYL2 acts as an important PA receptor, being able to sense PA to trigger responses against long-term drought stress. Therefore, increased levels of PA together with the potential higher PYL2 levels in the *alix-1* mutants provides a framework to explain the stomatal hypersensitivity to ABA of the *alix-1* mutants. Future studies will address this hypothesis using single *pyl2* mutants in *alix-1* mutant background to determine if *pyl2* mutation is sufficient to complement the stomatal hypersensitivity of the *alix-1* mutants.

According to our current knowledge, additional Bro1-domain proteins might influence trafficking of ABA receptors mediated by the plant ESCRT machineries. Thus, it has been recently shown that the plant-specific protein BRAF competes with FYVE1 for binding to VPS23A at MVBs. In this way, BRAF1 negatively regulates FYVE1 recruitment to the MVB surface, which should impact internalization of cargos into ILVs and their vacuolar turnover (Shen et al., 2018). Yet, it remains to be tested whether BRAF function affects the accumulation of membrane-associated PYLs and whether it can be counteracted by ALIX in order to balance ABA receptor abundance according to the environmental conditions.

To sum up, based on our data and current literature, we propose a model in which ALIX, as part of a general ESCRT-machinery/MVB pathway, acts as a negative regulator of ABA responses, including stomatal closure. This role involves ALIX-mediated trafficking of membrane-associated ABA receptors for vacuolar degradation, process that is enhanced in the presence of ABA. (Figure 43). Deciphering the exact molecular basis of the processes controlled by ALIX should help to unveil new possible targets to fight against drought stress in plants.

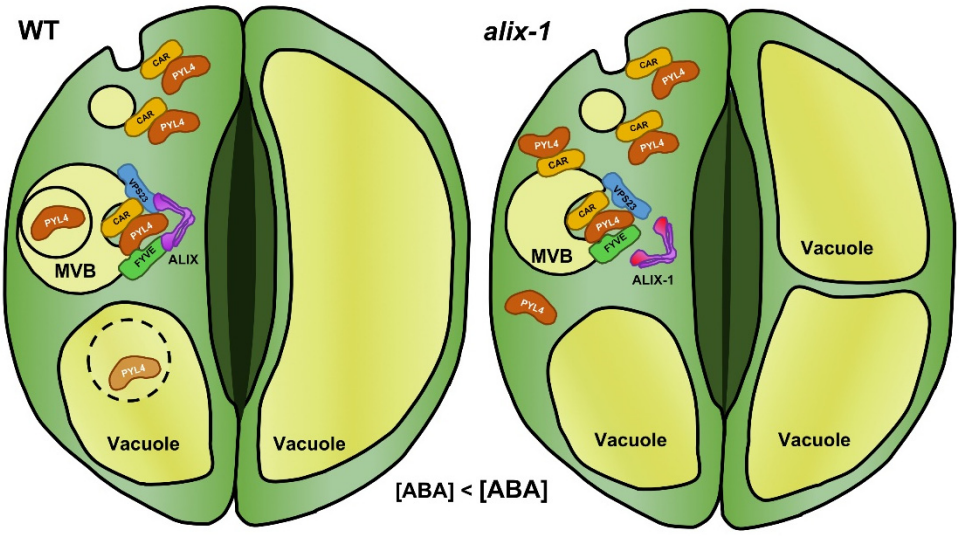

Figure 43. Model for the role of ALIX in the endosomal trafficking of ABA receptors
Soluble PYL4 proteins transiently bind to the plasma membrane via interaction with calcium-binding CAR proteins undergoing subsequent endosomal trafficking for vacuolar degradation. MVB sorting of ABA receptors is mediated by the ESCRT machinery aided by ALIX. Vacuolar proteolysis of PYL4 is enhanced in the presence of ABA, likely as a desensitizing mechanism to this hormone. *Alix-1* mutation impairs the interaction with PYL4 and the ESCRT-I component VPS23A, hampering the internalization of PYL4 into intraluminal vesicles in MVBs. Thus, *alix-1* leads to the accumulation of cytosolic and membrane-associated PYL4 that, together with increased ABA content in this mutant, increases sensitivity to ABA. Exacerbated response to ABA, together with vacuolar defects inherent to the *alix-1* mutation, causes higher stomatal closure compared to wild type plants.

5.4. Proposed roles of ALIX in other cellular processes

Based on the results of this study we propose two different plant cell processes in which ALIX could be involved. These are:

ALIX as a functional component of different ESCRT complexes

Plants lack of homologues for the canonical ESCRT-0 heterodimer complex present in opisthokonta. Nevertheless it has been proposed that specific plant components such as TOLs, FYVE1, ALIX and SH3P2 could play a similar role to ESCRT-0 in opisthokonta (Mosesso et al., 2019). In our TAP assays, we could co-precipitate together with ALIX the SH3 domain-containing protein SH3P2. Since ALIX also interacts with FYVE1, VPS23A and AMSH3, we propose that ALIX together with FYVE1 and SH3P2 could fulfill together all the characteristics of the canonical ESCRT-0 heterodimer complex,

including its ability to bind ubiquitin, to associate with the PM and to interact with DUBs, ESCRT-I components and clathrin (Nagel et al., 2017). The evidences supporting this hypothesis are:

- All FYVE1, SH3P2 and ALIX are able to bind Ub, specially K63 ubiquitin chains
- Both FYVE1 through its FYVE domain and SH3P2 through its BAR (Bin-Amphiphysin-Rvs) domain are able to bind phospholipids, positioning them close to membranes.
- Both SH3P2 and ALIX are able to interact with the DUB AMSH3 likely cooperating to its recruitment to the PM.
- SH3P2 is associated to CCV (clathrin coated vesicles), colocalizes with clathrin light chain-labelled structures and co-immunoprecipitates with clathrin heavy chains (Mosesso et al., 2019). Despite these evidences for SH3P2, ALIX and FYVE interaction or colocalization with CCVs has not been demonstrated yet.

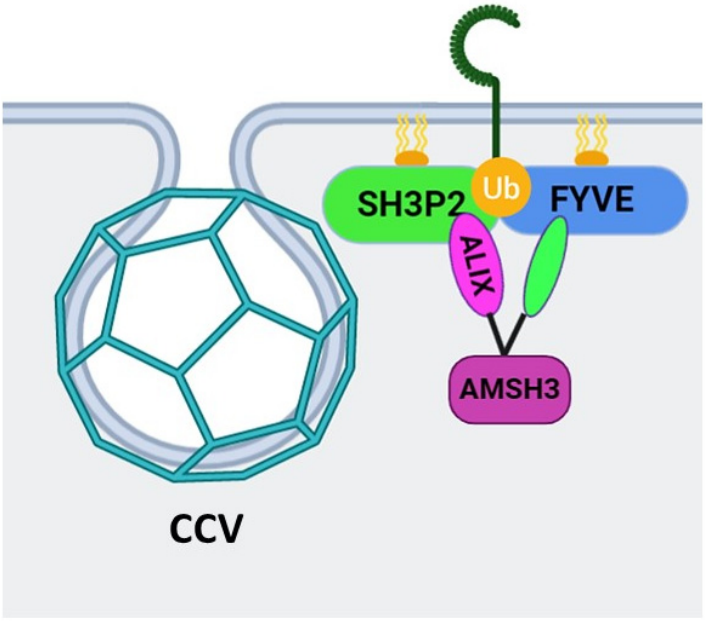

Figure 44. Proposed ESCRT-0-like model
SH3P2 and FYVE1 would recruit ALIX to the PM, where they would cooperate to recognize ubiquitinated cargoes. There they would recruit ESCRT-I and AMSH3 to iniciate cargo sorting

Based on these facts, we propose that ALIX might play different roles within the ESCRT pathway. Thus, at early stages of cargo recognition, ALIX could be recruited by FYVE1 and SH3P2 to the PM, where they will likely act as a ESCRT-0-like platform. There, they

might associate with AMSH DUBs and with the ESCRT-I subunit VPS23A to orchestrate cargo sorting (Figure 44).

Additionally, based on the concentric circle hypothesis (Nickerson et al., 2007), in which ESCRT-I, -II and -III components would assemble in circles around ESCRT-0, we propose that ALIX could be bridging the ESCRT-I and ESCRT-III complexes, helping to transfer Ub-cargos between different ESCRT components to facilitate their sorting.

Potential role of ALIX in miRNA processing

Studies in *Drosophila* and human cells have added new roles to the ESCRT machinery in the RNA biology. In *Drosophila* it has been found that members of the ESCRT-II are essential for transport and subcellular location of the mRNA bicoid to the anterior pole of the fruit fly egg (Irion & St Johnston, 2007). Other important new role of the ESCRT machinery is to participate in gene silencing. In animals GW-bodies, also named as mRNA P-bodies (processing bodies), have been described to be non-membranous cytoplasmic ribonucleoprotein foci (Yu et al., 2019) that congregate proteins related to miRNA (microRNA) post-translational silencing and mRNA decay. However, although the exact mechanism is not clear yet, it has been shown that some population of MVBs/endosomes, where the ESCRT machinery resides, are enriched in miRNAs, miRNA-targeted mRNAs and members of the miRNA machinery, including AGO proteins, all components of the RISC complex. Mutations in the ESCRT machinery reduce efficiency of miRNA-mediated gene silencing and produce accumulation of RISC components (Gibbings et al., 2009). Indeed, ALIX is able to bind AGO2 and miRNAs during extracellular vesicle (EV) biogenesis. In fact, ALIX knockdown does not affect the number of Evs released but severely decreases the amount of miRNAs in these EVs suggesting that ALIX has a key role in miRNA enrichment during EV formation (Iavello et al., 2016).

In plants, a function of the ESCRT machinery in mRNA-related processes is just starting to emerge. In the interactome of VPS2.2, RNA binding proteins have been found, suggesting a possible role of ESCRT machinery in mRNA biology (Ibl et al., 2012). Supporting this function, we have found in our TAP assays a significant enrichment in proteins related to the mRNA biology, especially related to mRNA processing, regulation of translation and cytoplasmic mRNA processing body (P-body) assembly. Among them, some proteins have a role in abiotic stress responses. For instance, APUM5 (Pumilio homolog 5) acts as a post-transcriptional negative regulator of abiotic stress responsive genes (Huh et al., 2014). Additionally, Arabidopsis RH8 (DEAD-box

ATP-dependent RNA helicase8) is able to interact with PP2CA at the nucleus, inhibiting its phosphatase activity (Baek et al., 2018). Many of these mRNA regulators are localized in the nucleus.

ALIX has been described as a cytosolic protein. However the possibility that it shuttles to the nucleus, as occurs with the ESCRT-I component FYVE1/FREE1 can not be disregarded (Li et al., 2019). Indeed, interestingly, ALIX accumulates in the nucleus upon treatment with Leptomycin B (LMB), an inhibitor of protein nuclear export (Dr. Laura Cuyas thesis, data not published; figure 45), suggesting that although transiently, ALIX might regulate yet-to-be identified nuclear processes. Future studies should address this appealing hypothesis.

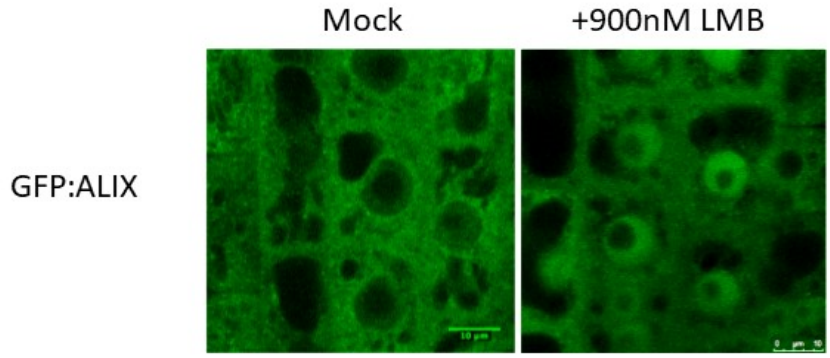

Figure 45. ALIX is also a nuclear protein
5 day-old GFP-ALIX seedlings were treated for 1 hour with 900 nM LMB. Confocal imaging showed that ALIX, which is normally located in cytosol and associated to membranes, was found in the nucleus after LMB addition. Bars: 10 µm.

In conclusion, ALIX is a multifunctional protein whose roles in plant biology are just starting to be unveiled. In this work we have discovered that ALIX participates in the regulation of the ABA signaling pathway and we provide new insights pointing to non-described functions of ALIX in plants.

6. CONCLUSIONS

I. ALIX directly interacts with ABA receptors, likely through an ubiquitin-independent mechanism.

II. The interaction between ALIX and ABA receptors occurs at MVBs.

III. *alix-1* mutation confers hypersensitivity to ABA in both seedling and adult plants.

IV. *alix-1* mutant plants display constitutive stomatal closure that is not due to general mechanic alterations in stomatal function. Increased stomatal closure reduces water loss and confers resistance to drought in *alix-1* mutant plants.

V. ALIX is a negative regulator of the abundance of ABA receptors mediating their degradation in the vacuole.

VI. ALIX function towards ABA receptors is enhanced in the presence of ABA, pointing to a negative feedback mechanism that controls the levels of specific ABA receptors.

VII. Increased accumulation of ABA receptors in the *alix-1* mutants is the main factor underlying their hypersensitivity to ABA.

VIII. *alix-1* mutation hampers the interaction ability of the resulting ALIX-1 protein to homodimerize and to interact with ABA receptors and the ESCRT-I subunit VPS23A.

7. CONCLUSIONES

I. ALIX interacciona directamente con los receptors de ABA, probablemente a través de un mecanismo independiente de ubiquitina.

II. La interacción entre ALIX y los receptors de ABA ocurres en los MVB.

III. La mutación *alix-1* confiere hipersensibilidad al ABA tanto en plántula como en planta adulta.

IV. Las plantas mutantes *alix-1* muestran cierre estomático constitutive que no es debido a alteraciones mecánicas en la función estomática. Este cierre estomático intensificado reduce la pérdida de agua y confiere resistencia a sequía en los mutantes *alix-1*.

V. ALIX es un regulador negative de la abundancia de los receptors de ABA mediando su degradación en la vacuola.

VI. La función de ALIX hacia los receptors de ABA está incrementada en presencia de ABA, apuntando hacia un mecanismo de retroalimentación negative que controla los niveles de receptores de ABA específicos.

VII. El incremento en la acumulación de los receptors de ABA en los mutantes *alix-1* es la principal causa de la hipersensibilidad al ABA de estos mutantes.

VIII. La mutación *alix-1* disrumpe la capacidad de la proteína ALIX-1 para homodimerizar e interaccionar con los receptors de ABA y la subunidad del ESCRT-I VPS23A.

8. BIBLIOGRAPHY

Aitchitt, M., Ainsworth, C.C. & Thangavelu, M. (1993) Plant Mol Biol Rep 11: 317.

Antignani, V., Klocko, A.L., Bak, G., Chandrasekaran, S.D., Dunivin, T., Nielsen, E. (2015) Recruitment of PLANT U-BOX13 and the PI4Kβ1/β2 phosphatidylinositol-4 kinases by the small GTPase RabA4B plays important roles during salicylic acid-mediated plant defense signaling in Arabidopsis. The Plant Cell. 27, 243–261.

Antoni, R., Gonzalez-Guzman, M., Rodriguez, L., Peirats-Llobet, M., Pizzio, G.A., Fernandez, M.A., De Winne, N., De Jaeger, G., Dietrich, D., Bennett, M.J., Rodriguez, P.L. (2013). PYRABACTIN RESISTANCE1-LIKE8 plays an important role for the regulation of abscisic acid signaling in root. Plant Physiol. 161, 931-941.

Antoni, R., Rodriguez, L., Gonzalez-Guzman, M., Pizzio, G.A., Rodriguez, P.L. (2011). News on ABA transport, protein degradation, and ABFs/WRKYs in ABA signaling. Curr Opin Plant Biol. 14, 547-553.

Archana, J. –S., Christiane, V., Jeffrey, L. (2011) Abscisic acid signal off the STARTing block. 4 (4), 562-580.

Austin, B.P. and Waugh, D.S. (2012). Isolation of *Metarhizium anisopliae* carboxypeptidase A with native disulfide bonds from the cytosol of *Escherichia coli* BL21(DE3). Protein Expr Purif. 82,116-124.

Babst, M. (2005). A protein's final ESCRT. Traffic. 6, 2-9.

Babst, M., Katzmann, D.J., Estepa-Sabal, E.J., Meerloo, T., and Emr, S.D. (2002a). ESCRT-III: an endosome-associated heterooligomeric protein complex required for mvb sorting. Dev Cell. 3, 271-282.

Babst, M., Katzmann, D.J., Snyder, W.B., Wendland, B., and Emr, S.D. (2002b). Endosome-associated complex, ESCRT-II, recruits transport machinery for protein sorting at the multivesicular body. Dev Cell. 3, 283-289.

Baek, W., Lim, C. W., Lee, S. C. (2018) A DEAD-box RNA helicase, RH8, is critical for regulation of ABA 89ignaling and the drought stress response via inhibition of PP2CA activity. Plant, Cell and Environment. 41(7), 1593-1604.

Bar, M. & Avni, A. (2014) Endosomal trafficking and signaling in plant defense

responses. Curr Opin Plant Biol. 22, 86-92.

Barberon, M., Zelazny, E., Robert, S., Conéjéro, G., Curie, C., Friml, J., Vert, G. (2011) Monoubiquitin-dependent endocytosis of the IRON-REGULATED TRANSPORTER 1 (IRT1) transporter controls iron uptake in plants. Proc Natl Acad Sci USA. 108(32), 450-458.

Bauer, H., Ache, P., Lautner, S., Fromm, J., Hartung, W., Al-Rasheid, K.A., Sonnewald, S., Sonnewald, U., Kneitz, S., Lachmann, N., Mendel, R. R., Bittner, F., Hetherington, A. M., Hedrich, R. (2013) The stomatal response to reduced relative humidity requires guard cell-autonomous ABA synthesis. Curr Biol, 23,53-57.

Bayle, V., Arrighi, J.F., Creff, A., Nespoulous, C., Vialaret, J., Rossignol, M., Gonzalez, E., Paz-Ares, J., Nussaume, L. (2011) *Arabidopsis thaliana* high-affinity phosphate transporters exhibit multiple levels of posttranslational regulation. Plant Cell. 23: 1523-1535.

Becker, D. (1990). Binary vectors which allow the exchange of plant selectable markers and reporter genes. Nucleic Acids Res. 18: 203.

Belda-Palazon, B., Gonzalez-Garcia, M.P., Lozano-Juste, J., Coego, A., Antoni, R., Julian, J., Peirats-Llobet, M., Rodriguez, L., Berbel, A., Dietrich, D., Fernandez, M.A., Madueño, F., Bennett, M.J., Rodriguez, P.L. (2018) PYL8 mediates ABA perception in the root through non-cell-autonomous and ligand-stabilization-based mechanisms. Proc Natl Acad Sci USA. 115, E11857-E11863.

Belda-Palazon, B., Rodriguez, L., Fernandez, M.A., Castillo, M.C., Anderson, E.A., Gao, C., González-Guzmán, M., Peirats-Llobet, M., Zhao, Q., De Winne, N., Gevaert, K., De Jaeger, G., Jiang, L., Leon, J., Mullen, R.T., and Rodriguez, P.L. (2016). FYVE1/FREE1 Interacts with the PYL4 ABA Receptor and Mediates its Delivery to the Vacuolar Degradation Pathway. Plant Cell. 28, 2291-2311.

Bensmihen S, To A, Lambert G, Kroj T, Giraudat J, Parcy F (2004) Analysis of an activated ABI5 allele using a new selection method for transgenic Arabidopsis seeds. FEBS Lett 561: 127–131.

Book, A. J., Gladman, N. P., Sang-Sook, L., Scalf, M., Smith, L. M., Vierstra, R. D. (2010) Affinity purification of the Arabidopsis 26S proteasome reveals a diverse array of plant proteolytic complexes. 285 (13), 25554-25569.

Brandt, B., Brodsky, D. E., Xue, S., Negi, J., Iba, K., Kangasjärvi, J., Ghassemian, M., Stephan, A. B., Hu, H., Schroeder, J. (2012) Reconstitution of abscisic acid activation of SLAC1 anion channel by CPK6 and OST1 kinases and branched ABI1 PP2C phosphatase action. Proc Natl Acad Sci USA. 109(26), 10593-10598.

Brandt, B., Munemasa, S., Wang, C., Nguyen, D., Yong, T., Yang, P.G., Poretsky, E., Belknap, T.F., Waadt, R., Aleman, F., and Schroeder, J.I. (2015). Calcium specificity signaling mechanisms in abscisic acid signal transduction in Arabidopsis guard cells. eLife 4, e03599.

Bueso, E., Rodriguez, L., Lorenzo-Orts, L., Gonzalez-Guzman, M., Sayas, E., Muñoz-Bertomeu, J., Ibañez, C., Serrano, R., and Rodriguez, P.L. (2014). The single-subunit RING-type E3 ubiquitin ligase RSL1 targets PYL4 and PYR1 ABA receptors in plasma membrane to modulate abscisic acid signaling. Plant J. 80, 1057-1071.

Cai, Y., Zhuang, X., Gao, C., Wang, X., Jiang, L. (2014) The Arabidopsis endosomal sorting complex required for transport III regulates internal vesicle formation of the prevacuolar compartment and is required for plant development. Plant Physiology. 165, 1328-1343.

Cao, M. –J., Zhang, Y. –L., Liu, X., Huang, H., Zhou, X. E., Wang, W. –L., Zeng, A., Zhao, C. –Z., Si, T., Du, J., Wu, W. –W-., Wang, F. –X., Xu, H. E., Zhu, J. –K. (2017) Combining chemical and genetic approaches to increase drought resistance in plants. Nature communications. 8 (1183).

Cardona-López, X., Cuyas, L., Marín, E., Rajulu, C., Irigoyen, M.L., Gil, E., Puga, M.I., Bligny, R., Nussaume, L., Geldner, N., Paz-Ares, J., and Rubio V. (2015). ESCRT-III-Associated Protein ALIX Mediates High-Affinity Phosphate Transporter Trafficking to Maintain Phosphate Homeostasis in Arabidopsis. Plant Cell. 27, 2560-2581.

Castillo, M.C., Lozano-Juste, J., González-Guzmán, M., Rodriguez, L., Rodriguez, P.L., and León, J. (2015). Inactivation of PYR/PYL/ RCAR ABA receptors by tyrosine nitration may enable rapid inhibition of ABA signaling by nitric oxide in plants. Sci. Signal. 8, ra89.

Cominelli, E., Galbiati, M., Vavasseur, A., Conti, L., Sala, T., Vuylsteke, M., Leonhardt, N., Dellaporta, S.L., Tonelli, C. (2005). A guard-cell-specific MYB transcription factor regulates stomatal movements and plant drought tolerance. Curr Biol. 15, 1196-1200.

Conibear, E. (2002). An ESCRT into the endosome. Mol Cell. 10, 215-216.

Cui, Y., Shen, J., Gao, C., Zhuang, X., Wang, J., Jiang, L. (2016) Biogenesis of Plant Prevacuolar Multivesicular Bodies. Mol Plant. 9, 774-786.

Curtis, M.D., Grossniklaus, U. (2003). A gateway cloning vector set for high-throughput functional analysis of genes in planta. Plant Physiol. 133: 462–469.

Cutler, S.R., Rodriguez, P.L., Finkelstein, R.R., and Abrams, S.R. (2010). Abscisic acid: Emergence of a core signaling network. Annu. Rev. Plant Biol. 61, 651-679.

daSilva, L.L., Taylor, J.P., Hadlington, J.L., Hanton, S.L., Snowden, C.J., Fox, S.J., Foresti, O., Brandizzi, F., and Denecke, J. (2005). Receptor salvage from the prevacuolar compartment is essential for efficient vacuolar protein targeting. Plant Cell 17, 132-148.

Demir, F., Horntrich, C., Blachutzik, J.O., Scherzer, S., Reinders, Y., Kierszniowska, S., Schulze, W.X., Harms, G.S., Hedrich, R., Geiger, D., and Kreuzer, I. (2013). Arabidopsis nanodomain- delimited ABA signaling pathway regulates the anion channel SLAH3. Proc Natl Acad Sci USA 110, 8296-8301.

Diettrich, M., Mueller, H. M., Bauer, H., Peirats-Llobet, M., Rodriguez, P. L., Geilfus, C. –M., Carpentier, S. C., Al Rasheid, K. A. S., Kollist, H., Merilo, E., Herrmann, J., Müller, T., Ache, P., Hetherington, A. M., Hedrich, R. (2019) The role of Arabidopsis ABA receptors from the PYR/PYL/RCAR family in stomatal acclimation and closure signal integration. Nature Plants. 5, 1002-1011.

Dores, M.R., Chen, B., Lin, H., Soh, U.J., Paing, M.M., Montagne, W.A., Meerloo, T., Trejo, J. (2012). ALIX binds a YPX(3)L motif of the GPCR PAR1 and mediates ubiquitin-independent ESCRT-III/MVB sorting. J. Cell Biol. 197, 407-419.

Dores, M.R., Grimsey, N.J., Mendez, F., Trejo, J. (2016). ALIX regulates the ubiquitin-independent lysosomal sorting of the P2Y1 purinergic receptor via a YPX3L motif. PloS One 11, e0157587.

Dowlatshahi, D.P., Sandrin, V., Vivona, S., Shaler, T.A., Kaiser, S.E., Melandri, F., Sundquist, W.I., Kopito, R.R. (2012). ALIX is a Lys63-specific polyubiquitin binding protein that functions in retrovirus budding. Dev Cell. 23, 1247-1254.

Dubeaux, G., Vert, G. (2017). Zooming into plant ubiquitin-mediated endocytosis. Curr

Opin Plant Biol. 40, 56-62.

Eckardt, N. (2005) Brassinosteroid Perception and Signaling: Heterodimerization and Phosphorylation of Receptor-Like Kinases BRI1 and BAK1. The Plant Cell. 17, 1638-1640.

Erwig, J., Ghareeb, H., Kopischke, M., Hacke, R., Matei, A., Petutschnig, E., Lipka, V. (2017) Chitin-induced and CHITIN ELICITOR RECEPTOR KINASE1 (CERK1) phosphorylation-dependent endocytosis of Arabidopsis thaliana LYSIN MOTIF-CONTAINING RECEPTOR-LIKE KINASE5 (LYK5). The New phytologist 215. 382-396.

Fernández-Arbaizar, A., Regalado, J.J., and Lorenzo, O. (2012). Isolation and characterization of novel mutant loci suppressing the ABA hypersensitivity of the Arabidopsis coronatine insensitive 1-16 (coi1-16) mutant during germination and seedling growth. Plant Cell Physiol. 53, 53–63.

Fernandez-Borja, M., Wubbolts, R., Calafat, J., Janssen, H., Divecha, N., Dusseljee, S., and Neefjes, J. (1999). Multivesicular body morphogenesis requires phosphatidyl-inositol 3-kinase activity. Curr. Biol. 9, 55-58.

Finkelstein, R. (2013) Abscisic acid synthesis and response. Arabidopsis Book. 11: e0166.

Fisher, R.D., Chung, H.Y., Zhai, Q., Robinson, H., Sundquist, W.I., and Hill, C.P. (2007). Structural and biochemical studies of ALIX/ AIP1 and its role in retrovirus budding. Cell 128, 841-852.

Fisher, R.D., Chung, H.Y.,Zhai, Q., Robinson, H., Sundquist, W.I., Hill, C.P. Structural and biochemical studies of ALIX/AIP1 and its role in retrovirus budding (2007). Cell. 128, 841-852

Foiani, M., Marini, F., Gamba, D., Lucchini, G., and Plevani, P.(1994). The B subunit of the DNA polymerase alpha-primase complex in Saccharomyces cerevisiae executes an essential function at the initial stage of DNA replication. Mol. Cell. Biol. 14, 923-933.

Frémont, S., Echard, A. (2018) Membrane traffic in the late steps of cytokinesis. Current Biology, 28(8), 458-470.

Fujii, H., Chinnusamy, V., Rodrigues, A., Rubio, S., Antoni, R., Park, S.Y., Cutler, S.R., Sheen, J., Rodriguez, P.L., and Zhu, J.K. (2009). In vitro reconstitution of an abscisic

acid 94ignaling pathway. Nature 462, 660-664.

Fujita, Y., Fujita, M., Shinozaki, K., Yamaguchi-Shinozaki, K. (2011) ABA-mediated transcriptional regulation in response to osmotic stress in plants. Journal of Plant Research. 124 (4), 509-525.

Fujita, Y., Nakashima, K., Yoshida, T., Katagiri, T., Kidokoro, S., Kanamori, N., Umezawa, T., Fujita, M., Maruyama, K., Ishiyama, K., et al (2009) Three SnRK2 protein kinases are the main positive regulators of abscisic acid signaling in response to water stress in Arabidopsis. Plant Cell Physiol 50, 2123-2132.

Gao, C., Luo, M., Zhao, Q., Yang, R., Cui, Y., Zeng, Y., Xia, J. and, Jiang, L. (2014). A unique plant ESCRT component, FREE1, regulates multivesicular body protein sorting and plant growth. Curr Biol. 24, 2556-2563.

Gao, C., Zhuang, X., Cui, Y., Fu, X., He, Y., Zhao, Q., Zeng, Y., Shen, J., Luo, M., and Jiang, L. (2015). Dual roles of an Arabidopsis ESCRT component FREE1 in regulating vacuolar protein transport and autophagic degradation. Proc Natl Acad Sci USA 112, 1886-1891.

Gao, C., Zhuang, X., Shen, J., Jiang, L. (2017) Plant ESCRT complexes: Moving Beyond Endosomal Sorting. Trends in Plant Sciences. 22:11, 986-998.

García-León, M., Cuyas, L., Abd El-Moneim, D., Rodriguez, L., Belda-Palazon, B., Sánchez-Quant, E., Fernández, Y., Roux, B., Zamarreño, A. M., Garcia-Mina, J. M., Nussaume, L., Rodriguez, P.L., Paz-Ares, J., Leonhardt, N., Rubio, V. (2019) Arabidopsis ALIX regulates stomatal aperture and turnover of ABA receptors.Plant Cell.

García-León, M., Iniesto, E., Rubio, V. (2018) Tandem affinity purification of protein complexes from Arabidopsis cell cultures. Two-Hybrid Systems. Methods in Molecular Biology. Vol: 1794 (21), 297-310.

Geiger, D. Scherzer, S., Mumm, P., Stange, A., Marten, I., Bauer, H., Ache, P., Matschi, S., Liese, A., Al-Rasheid, K.A., et al (2009). Activity of guard cell anion channel SLAC1 is controlled by drought-stress signaling kinase- phosphatase pair. Proc Natl Acad Sci USA 106, 21425-21430.

Geldner, N., Dénervaud-Tendon, V., Hyman, D.L., Mayer, U., Stierhof, Y.D., and Chory, J. (2009). Rapid, combinatorial analy- sis of membrane compartments in intact plants

with a multicolor marker set. Plant J. 59, 169-178.

Gibbings, D. J., Ciaudo, C., Erhardt, M., Voinnet, O. (2009) Multivesicular bodies associate with components of miRNA effector complexes and modulate miRNA activity. Nat. Cell Biol. 11, 1143–1149.

Gonzalez-Guzman, M., Pizzio, G.A., Antoni, R., Vera-Sirera, F., Merilo, E., Bassel, G.W., Fernandez, M.A., Holdsworth, M.J., Perez-Amador, M.A., Kollist, H., and Rodriguez, P.L. (2012). Arabidopsis PYR/PYL/RCAR receptors play a major role in quanti- tative regulation of stomatal aperture and transcriptional response to abscisic acid. Plant Cell 24, 2483-2496.

Groothuis, T. AM., Dantuma, N. P., Neefjes, J., Salomons, F. A. (2006) Ubiquitin crosstalk coneecting cellular processes. Cell. Division. 1, 21.

Gruenberg, J., and Stenmark, H. (2004). The biogenesis of multivesicular endosomes. Nat Rev Mol Cell Biol. 5, 317-323.

Heard, W., Sklenar, J., Tome, D.F., Robatzek, S., Jones, A.M. (2015) Identification of regulatory and cargo proteins of endosomal and secretory pathways in Arabidopsis thaliana by proteomic dissection. Mol. Cell. Proteom. 14,1796-1813.

Helander, J., Vaidya, A., Cutler, S. (2016) Chemical manipulation of plant water use. Bioorganic & Medicinal Chemistry. 24 (3) ,493-500.

Henne, W. M., Buchkovich, N. J., Zhao, Y., Emr, S. D. (2012) The endosomal sorting complex ESCRT-II mediates the assembly and architecture of ESCRT-III helices. Cell. 151 (2), 356-371.

Henne, W.M., Buchkovich, N.J., and Emr, S.D. (2011). The ESCRT pathway. Dev Cell. 21, 77-91.

Henne, W.M., Stenmark, H., Emr, S.D. (2013). Molecular mechanisms of the membrane sculpting ESCRT pathway. Cold Spring Harb Perspect Biol 5, a016766.

Hsu, P. –K., Takashi, Y., Munemasa, S., Merilo, E., Laanemets, K., Waadt, R., Pater, D., Kollist, H., Schroeder, J. I. (2018) Abscisic acid-independent stomatal CO_2 and ABA signaling downstream of OST1 kinase. Proc Natl Acad Sci USA. 115(42), 9971-9980.

Hua, D., Wang, C., He, J., Liao, H., Duan, Y., Zhu, Z., Guo, Y., Chen, Z., Gong, Z. (2012) A plasma membrane receptor kinase, GHR1, mediates abscisic acid- and hydrogen

peroxide- regulated stomatal movement in Arabidopsis. Plant Cell. 24(6), 2546-2561.

Huh, S. U., Paek, K. –H. (2014) APUM5, encoding a Pumilio RNA binding protein, negatively regulates abiotic stress responsive gene expression. BMC Plant Biology. 14: 75.

Hyangju, K., Kim, S. Y., Song, K., Sohn, E. J., Lee, Y., Lee, D. W., Hara-Nishimura, I., Hwang, I. (2012) Trafficking of Vacuolar Proteins: The Crucial Role of *Arabidopsis* Vacuolar Protein Sorting 29 in Recycling Vacuolar Sorting Receptor. Plant Cell. 24 (12), 5058-5073.

Iavello, A., Frech, V. S., Gai, C., Deregibus, M. C., Quesenberry, P. J., & Camussi, G. (2016). Role of Alix in miRNA packaging during extracellular vesicle biogenesis. *International journal of molecular medicine*. *37*(4), 958–966.

Ibl, V., Csaszar, E., Schlager, N., Neubert, S., Spitzer, C., Hauser, M. –T. (2012) Interactome of the plant-specific ESCRT-III component VPS2.2 in Arabidopsis thaliana. J Proteome Res. 11(1), 397–411.

Ibl, V., Csaszar, E., Schlager, N., Neubert, S., Spitzer, C., Hauser, M. –T. (2012) Interactome of the plant-specific ESCRT-III component AtVPS2.2 in Arabidopsis thaliana. J. Proteome Res. 111, 397-411. 8.

Ichioka, F., Kobayashi, R., Katoh, K., Shibata, H., Maki, M. (2008) Brox, a novel farnesylated Bro1 domain-containing protein that associates with charged multivesicular body protein 4 (CHMP4). The FEBS jounal. 275(4), 682-675.

Ichioka, F., Takaya, E., Suzuki, H., Kajigaya, S., Buchman, V. L., Shibata, H., Maki, M. (2007) HD-PTP and Alix share some membrane-traffic related proteins that interact with their Bro1 domains or proline-rich regions. Arch. Biochem Biophys. 457 (2), 142-149.

Irigoyen, M.L., Iniesto, E., Rodriguez, L., Puga, M.I., Yanagawa, Y., Pick, E., Strickland, E., Paz-Ares, J., Wei, N., De Jaeger, G., Rodriguez, P.L., Deng, X.W., and Rubio, V. (2014). Targeted degradation of abscisic acid receptors is mediated by the ubiquitin ligase substrate adaptor DDA1 in Arabidopsis. Plant Cell. 26, 712-728.

Irion, U., & St Johnston, D. (2007) bicoid RNA 96ignaling96on requires specific binding of an endosomal sorting complex. Nature. 445, 554–558.

Isono, E., Katsiarimpa, A., Muller, I.K., Anzenberger, F., Stierhof, Y.D., Geldner, N., Chory, J., and Schwechheimer, C. (2010). The deubiquitinating enzyme AMSH3 is required for intracellular trafficking and vacuole biogenesis in Arabidopsis thaliana. Plant Cell 22, 1826-1837.

Kalinowska, K., Isono, E. (2018) All roads lead to the vacuole-autophagic transport as part of the endomembrane trafficking network in plants. Journal of Experimental Botany. 69 (6), 1313-1324.

Kalinowska, K., Nagel, M.K., Goodman, K., Cuyas, L., Anzenberger, F., Alkofer, A., Paz-Ares, J., Braun, P., Rubio, V., Otegui, M.S., and Isono, E. (2015). Arabidopsis ALIX is required for the endosomal localization of the deubiquitinating enzyme AMSH3. Proc Natl Acad Sci USA 112, E5543-5551.

Kang, H., Hwang, I. (2014) Vacuolar sorting receptor-mediated trafficking of soluble vacuolar proteins in plant cells. Plants. 3(3), 392-408.

Kasai, K., Takano, J., Miwa, K., Toyoda, A., Fujiwara, T. (2011) High boron-induced ubiquitination regulates vacuolar sorting of the BOR1 borate transporter in Arabidopsis thaliana. J Biol Chem. 286,6175-6183.

Katsiarimpa, A., Anzenberger, F., Schlager, N., Neubert, S., Hauser, M.T., Schwechheimer, C., and Isono E. (2011). The Arabidopsis deubiquitinating enzyme AMSH3 interacts with ESCRT-III subunits and regulates their localization. Plant Cell 23, 3026-2040.

Katzmann, D.J., Babst, M., and Emr, S.D. (2001). Ubiquitin-dependent sorting into the multivesicular body pathway requires the function of a conserved endosomal protein sorting complex, ESCRT-I. Cell 106, 145-155.

Kelly, B. T., Owen, D. J. (2011) Endocytic sorting of transmembrane protein cargo. Curr Opin Cell Biol. 23(4), 404-412.

Keren-Kaplan, T., Attali, I., Estrin, M., Kuo, L.S., Farkash, E., Jerabek-Willemsen, M., Blutraich, N., Artzi, S., Peri, A., Freed, E.O., Wolfson, H.J., and Prag, G. (2013). Structure-based in silico identification of ubiquitin-binding domains provides insights into the ALIX-V:ubiquitin complex and retrovirus budding. EMBO J. 32, 538-551.

Kim, J., Sitaraman, S., Hierro, A., Beach, B. M., Odorizzi, G., Hurley, J. H. (2005) Structural basis for endosomal targeting by the Bro1 domain. Developmental Cell.

8(6), 937-947.

Kim, T.H., Böhmer, M., Hu, H., Nishimura, N., Schroeder, J.I. (2010). Guard cell signal transduction network: advances in understanding abscisic acid, CO2, and Ca2+ signaling.vAnnu Rev Plant Biol. 61, 561-591.

Kolb, C., Nagel, M.K., Kalinowska, K., Hagmann, J., Ichikawa, M., Anzenberger, F., Alkofer, A., Sato, M.H., Braun, P., and Isono, E. (2015). FYVE1 Is Essential for Vacuole Biogenesis and Intracellular Trafficking in Arabidopsis. Plant Physiol. 167, 1361-1373.

Kong, L., Cheng, J., Zhu, Y., Ding, Y., Meng, J., Chen, Z., Xie, Q. Guo, Y., Li, J., Yang, S., Gong, Z. (2015) Degradation of the ABA co-receptor ABI1 by PUB12/13 U-box E3 ligases. Nat. Commun. 6, 8630.

Kyuuma, M., Kikuchi, K., Kojima, K., Sugawara, Y., Sato, M., Mano, N., Goto, J., Takeshita, T., Yamamoto, A., Sugamura, K., and Tanaka, N. (2007). AMSH, an ESCRT-III associated enzyme, deubi- quitinates cargo on MVB/late endosomes. Cell Struct. Funct. 31, 159-172.

Lee, S.C., Lan, W., Buchanan, B.B., and Luan, S. (2009). A protein kinase-phosphatase pair interacts with an ion channel to regulate ABA signaling in plant guard cells. Proc Natl Acad Sci USA 106, 21419-21424.

Lee, Y., Jang, M., Song, K., Kang, H., Lee, M. H., Lee, D. W., Zouhar, J., Rojo, E., Sohn, E. J., Hwang, I. (2013) Functional identification of sorting receptors involved in trafficking of soluble lytic vacuolar proteins in vegetative cells of Arabidopsis. 161(1) 121-133.

Leitner, J., Petrášek, J., Tomanov, K., Retzer, K., Pařezová, M., Korbei, B., Bachmair, A., Zažímalová, E., Luschnig, C. (2012). Lysine63-linked ubiquitination of PIN2 auxin carrier protein governs hormonally controlled adaptation of Arabidopsis root growth. Proc. Natl. Acad. Sci. USA. 109: 8322–8327.

Li, D., Zhang, L., Li, X., Kong, X., Wang, X., Li, Y., Liu, Z., Wang, J., Li, X., Yang, Y. (2018). AtRAE1 is involved in degradation of ABA receptor RCAR1 and negatively regulates ABA signalling in Arabidopsis. Plant Cell Environ. 41, 231-244.

Li, H., Li, Y., Zhao, Q., Li, T., Wei, J., Li, B., Shen, W., Yang, C., Zeng, Y., Rodriguez, P. L., Zhao, Y., Jiang, L., Wang, X., Gao, C. (2019) The plant ESCRT component FREE1 shuttles to the nucleus to attenuate abscisic acid signaling. Nature Plants. 5, 512-524.

Li, Y., Zhang, L., Li, D., Liu, Z., Wang, J., Li, X., and Yang, Y. (2016). The Arabidopsis F-box E3 ligase RIFP1 plays a negative role in abscisic acid signalling by facilitating ABA receptor RCAR3 degradation. Plant Cell Environ. 39, 571-582.

Liu, X.L., Covington, M.F., Fankhauser, C., Chory, J., and Wagner, D.R. (2001). ELF3 encodes a circadian clock-regulated nuclear protein that functions in an Arabidopsis PHYB signal transduction pathway. Plant Cell. 13, 1293-1304.

Lu, D., Lin, W., Gao, X., Wu, S., Cheng, C., Avila, J., Heese, A., Devarenne, T. P., He, P., Shan, L. (2011) Direct ubiquitination of pattern recognition receptor FLS2 attenuates plant innate immunity. Science. 332(6036): 1439-1442.

Luhtala, N., and Odorizzi, G. (2004). Bro1 coordinates deubiquitination in the multivesicular body pathway by recruiting Doa4 to endosomes. J. Cell Biol. 166, 717-729.

Luo, J., Shen, G., Yan, J., He, C., Zhang, H. (2006) AtCHIP functions as an E3 ubiquitin ligase of protein phosphatase 2A subunits and alters plant response to abscisic acid treatment. Plant J. 46, 649–657.

Luthala, N., Odorizzi, G. (2004) Bro1 coordinates deubiquitination in the multivesicular body pathway by recruiting Doa4 to endosomes. Journal of Cell Biology. 166(5), 717.

Ma, Y., Cao, J., He, J., Qiaoqiao, C., Xufeng, L., Yang, Y. (2018) Molecular mechanism for the regulation of ABA homeostasis during plant development and stress responses. Int J Mol Sci. 19(11): 3643.

Ma, Y., Szostkiewicz, I., Korte, A., Moes, D., Yang, Y., Christmann, A., Grill, E. (2009). Regulators of PP2C phosphatase activity function as abscisic acid sensors. Science. 324, 1064–1068.

MacGurn, J.A., Hsu, P.C., and Emr, S.D. (2012). Ubiquitin and membrane protein turnover: from cradle to grave. Annu Rev Biochem. 81, 231-259.

Mageswaran, S.K., Dixon, M.G., Curtiss, M., Keener, J.P., Babst M. (2014). Binding to any ESCRT can mediate ubiquitin-independent cargo sorting. Traffic 15, 212-229.

Marhavý P., Bielach A., Abas L., Abuzeineh A., Duclercq J., Tanaka H., Pařezová M., Petrášek J., Friml J., Kleine-Vehn J., et al. (2011). Cytokinin modulates endocytic trafficking of PIN1 auxin efflux carrier to control plant organogenesis. Dev. Cell 21,

796-80.

Mäser, P., Leonhardt, N., Schroeder, J. I. (2003) The Clickable Guard Cell: Electronically Linked Model of Guard Cell Signal Transduction Pathways. The Arabidopsis book. 32(1).

Mattei, S., Klein, G., Satre, M., Aubry, L. (2006) Trafficking and developmental signaling: ALIX at the crossroads. European Journal of Cell Biology. 85(9-10), 925-936.

Mayers, J. R., Wang, L., Pramanik, J., Johnson, A., Sarkeshik, A., Wang, Y., Saengsawang, W., Yates, J. R., Audhya, A. (2013) Regulation of ubiquitin-dependent cargo sorting by multiple endocytic adaptors at the plasma membrane. Proc Natl Acad Sci USA 110, 11857–11862.

McCullough, J., Fisher, R. D., Whitby, F. G., Sundquist, W. I., Hill, C.P. (2008) ALIX-CHMP4 interactions in the human ESCRT pathway. Proc Natl Acad Sci USA. 105 (22) 7687-7691.

McMahon, H.T., Boucrot, E. (2011) Molecular mechanism and physiological functions of clathrin-mediated endocytosis. Nat. Rev. Mol. Cell Biol. 12, 517–533.

McNatt, M.W., McKittrick, I., West, M., and Odorizzi, G. (2007). Direct binding to Rsp5 mediates ubiquitin-independent sorting of Sna3 via the multivesicular body pathway. Mol Biol Cell 18, 697-706.

Merlot, S., Leonhardt, N., Fenzi, F., Valon, C., Costa, M., Piette, L., Vavasseur A, Genty, B., Boivin, K., Müller, A., Giraudat, J., and Leung, J. (2007). Constitutive activation of a plasma membrane H(+)-ATPase prevents abscisic acid-mediated stomatal closure. EMBO J. 26, 3216-3226.

Merlot., Mustilli, A.C., Genty, B., North, H., Lefebvre, V., Sotta, B., Vavasseur, A., and Giraudat, J. (2002). Use of infrared thermal imaging to isolate Arabidopsis mutants defective in stomatal regulation. Plant J. 30, 601-609.

Missotten, M., Nichols, A., Rieger, K., and Sadoul, R. (1999). Alix, a novel mouse protein undergoing calcium-dependent interaction with the apoptosis-linked-gene 2 (ALG-2) protein. Cell Death Differ. 6, 124-129.

Mosesso, N., Nagel, M.-K., Isono, E. (2019). Ubiquitin recognition in endocytic trafficking – with or without ESCRT-0. Journal of Cell Science. 132(16).

Munemasa, S., Hauser, F., Park, J., Waadt, R., Brandt, B., and Schroeder, J.I. (2015). Mechanisms of abscisic acid-mediated control of stomatal aperture. Curr Opin Plant Biol. 28, 154-162.

Murashige, T., and Skoog, F. (1962). A revised medium for rapid growth and bio assays with tobacco tissue cultures. Physiol Plant. 15, 473-497.

Murphy, J. E., Padilla, B. E., Hasdemir, B., Cottrell, G. S., Bunnett, N. W. (2009) Endosomes: A legitimate platform for the 101ignaling train. Proc Natl Acad Sci USA 106, 17615-17622.

Murrow, L., Malhotra, R., Debnath, J. (2015) ATG12-ATG3 interacts with ALIX to promote basal autophagic flux and late endosome function. Nature Cell Biology. 17, 300-310.

Nagel, M. –K., Kalinowska, K., Vogel, K., Reynolds, G. D., Wu, Z., Anzenberger, F., Ichikawa, M., Tsutsumi, C., Sato, M. H., Kuster, B., Bednarek, S. Y., Isono, E. (2017) Arabidopsis SH3P2 binds ubiquitin and ESCRT-I. Proc Natl Acad Sci USA. 114 (34) 7197-7204.

Nakashima, K., and Yamaguchi-Shinozaki, K. (2013). ABA signaling in stress-response and seed development. Plant Cell Rep. 32, 959-970.

Nemhauser, J.L., Hong, F., Chory, J. (2006) Different plant hormones regulate similar processes through largely nonoverlapping transcriptional responses. Cell 126, 467–475.

Nickerson, D.P., Russell, M.R., and Odorizzi, G. (2007). A concentric circle model of multivesicular body cargo sorting. EMBO Rep. 8, 644-650.

Nishimura, K., Matsunami, E., Yoshida, S., Kohata, S., Yamauchi, J., Jisaka, M., Nagaya, T., Yokota K., Nakagawa, T. (2016) The tyrosine-sorting motif of the vacuolar sorting receptor VSR4 from Arabidopsis thaliana, which is involved in the interaction between VSR4 and AP1M2, μ1-adaptin type 2 of clathrin adaptor complex 1 subunits, participates in the post-Golgi sorting of VSR4. Bioscience, Biotechnology, and Biochemistry, 80(4), 694-705.

Odorizzi, G. (2006). The multiple personalities of Alix. J. Cell Sci. 119, 3025-3032.

Otegui, M. & Reyes, F. C. (2010) Endosomes in Plants. Nature Education 3(9):23.

Paciorek, T., Zažímalová, E., Ruthardt, N., Petrášek, J., Stierhof, Y-D., Kleine-Vehn, J., Morris, D. A., Emans, N., Jürgens, G., Geldner, N., Friml, J. (2005) Auxin inhibits endocytosis and promotes its own efflux from cells. Nature 435, 1251-1256.

Paez-Valencia, J., Goodman, K., and Otegui, M.S. (2016). Endocytosis and Endosomal Trafficking in Plants. Annu Rev Plant Biol. 67, 309-335.

Park, S.Y., Fung, P., Nishimura, N., Jensen, D.R., Fujii, H., Zhao, Y., Lumba, S., Santiago, J., Rodrigues, A., Chow, T.F.F., Alfred, S.E., Bonetta, D., Finkelstein, R., Provart, N.J., Desveaux, D., Rodriguez, P.L., McCourt, P., Zhu, J.K., Schroeder, J.I., Volkman, B.F., Cutler, S.R. (2009) Abscisic Acid Inhibits Type 2C Protein Phosphatases via the PYR/PYL Family of START Proteins. Science. 324, 1068-1071.

Pashkova, N., Gakhar, L., Winistorfer, S.C., Sunshine, A.B., Rich, M., Dunham, M.J., Yu, L., Piper, R.C. (2013). The yeast Alix homolog Bro1 functions as a ubiquitin receptor for protein sorting into multivesicular endosomes. Dev Cell. 25, 520-533.

Peirats-Llobet, M., Han, S.K., Gonzalez-Guzman, M., Jeong, C.W., Rodriguez, L., Belda-Palazon, B., Wagner, D. et al. (2016) A direct link between abscisic acid sensing and the chromatin-remodeling ATPase BRAHMA via core ABA signaling pathway components. Mol. Plant. 9, 136–147.

Pires, R., Hartlieb, B., Signor, L., Schoehn, G., Lata, S., Roessle, M., Moriscot, C., Popov, S., Hinz, A., Jamin, M., Boyer, V., Sadoul, R., Forest, E., Svergun, D.I., Göttlinger, H.G., Weissenhorn, W. (2009) A crescent-shaped ALIX dimer targets ESCRT-III CHMP4 filaments. Structure. 17(6), 843-856.

Pizzio, G.A., Rodriguez, L., Antoni, R., Gonzalez-Guzman, M., Yunta, C., Merilo, E., Kollist, H., Albert, A., and Rodriguez, P.L. (2013). The PYL4 A194T mutant uncovers a key role of PYR1-LIKE4/PROTEIN PHOSPHATASE 2CA interaction for abscisic acid signaling and plant drought resistance. Plant Physiol. 163, 441-455.

Popov, S., Popova, E., Inoue, M., Göttlinger, H. G. (2008). Human immunodeficiency virus type 1 Gag engages the Bro1 domain of ALIX/AIP1 through the nucleocapsid. Journal of virology. 82(3), 1389–1398.

Puga, M.I., Mateos, I., Charukesi, R., Wang, Z., Franco-Zorrilla, J.M., de Lorenzo, L., Irigoyen, M.L., Masiero, S., Bustos, R., Rodríguez, J., Leyva, A., Rubio, V., Sommer, H., and Paz-Ares, J. (2014) SPX1 is a phosphate-dependent inhibitor of Phosphate

Starvation Response 1 in Arabidopsis. Proc Natl Acad Sci USA 111, 14947-14952.

Reggiori, F., and Pelham, H.R. (2001). Sorting of proteins into multi- vesicular bodies: Ubiquitin-dependent and –independent targeting. EMBO J. 20, 5176-5186.

Reyes, F.C., Buono, R., Otegui, M.S. (2011) Plant endosomal trafficking pathways. Current Opinion in Plant Biology. 14, 666-673.

Reyes, F.C., Buono, R.A., Roschzttardtz, H., Di Rubbo, S., Yeun, L.H., Russinova, E., Otegui, M.S. (2014). A novel endosomal sorting complex required for transport (ESCRT) component in Arabidopsis thaliana controls cell expansion and development. J Biol Chem. 289, 4980-4988.

Richardson, L.G., Howard, A.S., Khuu, N., Gidda, S.K., McCartney, A., Morphy, B.J., and Mullen, R.T. (2011). Protein-Protein Interaction Network and Subcellular Localization of the Arabidopsis Thaliana ESCRT Machinery. Front Plant Sci. 2, 20.

Richter, S., Geldner, N., Schrader, J., Wolters, H., Stierhof, Y.D., Rios, G., Koncz, C., Robinson, D. G., Jürgens, D. (2007) Functional diversification of closely related ARF-GEFs in protein secretion and recycling. Nature 448, 488-92

Robatzek, S., Chinchilla, D., Boller, T. (2006) Ligand-induced endocytosis of the pattern recognition receptor FLS2 in Arabidopsis. Genes and Dev. 20, 537-546.

Rodriguez, L., Gonzalez-Guzman, M., Diaz, M., Rodrigues, A., Izquierdo-Garcia, A.C., Peirats-Llobet, M., Fernandez, M.A., Antoni, R., Fernandez, D., Marquez, J.A., Mulet, J.M., Albert, A., Rodriguez, P.L. (2014). C2-domain abscisic acid-related proteins mediate the interaction of PYR/PYL/RCAR abscisic acid receptors with the plasma membrane and regulate abscisic acid sensitivity in Arabidopsis. Plant Cell. 26, 4802-4820.

Rodríguez, P. –L. (2016) Abscisic Acid Catabolism Generates Phaseic Acid, a Molecule Able to Activate a Subset of ABA Receptors. Molecular Plant. 9, 1448-1450.

Rubio, S., Rodrigues, A., Saez, A., Dizon, M.B., Galle, A., Kim, T.H., Santiago, J., Flexas, J., Schroeder, J.I., and Rodriguez, P.L. (2009). Triple loss of function of protein phosphatases type 2C leads to partial constitutive response to endogenous abscisic acid. Plant Physiol. 150, 1345-1355.

Saez, A., Robert, N., Maktabi, M.H., Schroeder, J.I., Serrano, R., and Rodriguez, P.L. (2006). Enhancement of abscisic acid sensitivity and reduction of water consumption in Arabidopsis by combined inactivation of the protein phosphatases type 2C ABI1 and HAB1. Plant Physiol. 141, 1389-1399.

Sambrook J, Fritsch EF, Maniatis T (1989) Molecular cloning: A Laboratory Manual. 2nd edition. Cold Spring Harbor Laboratory Press, N.Y.

Sancho-Andrés, G., Soriano-Ortega, E., Gao, C., Bernabé-Orts, J. M., Narasimhan, M., Müller, A. O., Tejos, R., Jiang, L., Friml, J., Marcote, M. J. (2016) Sorting Motifs Involved in the Trafficking and Localization of the PIN1 Auxin Efflux Carrier. Plant physiology, 171(3), 1965–1982.

Santelia, D., and Lawson, T. (2016). Rethinking Guard Cell Metabolism. Plant Physiol. 172, 1371-1392.

Sato, A., Sato, Y., Fukao, Y., Fujiwara, M., Umezawa, T., Shinozaki, K., Hibi, T. et al. (2009) Threonine at position 306 of the KAT1 potassium channel is essential for channel activity and is a target site for ABA-activated SnRK2/ OST1/SnRK2.6 protein kinase. Biochem. J. 424, 439–448.

Sato, T., Maekawa, S., Yasuda, S., Yamaguchi, J. (2011) Carbon and nitrogen metabolism regulated bu the ubiquitin-proteasome system. Plant signaling and behavior. 6(10), 1465-1468.

Scheuring, D., Künzl, F., Viotti, C., Yan, M.S., Jiang, L., Schellmann, S., Robinson, D.G., and Pimpl, P. (2012). Ubiquitin initiates sorting of Golgi and plasma membrane proteins into the vacuolar degradation pathway. BMC Plant Biol. 12, 164.

Schroeder, J. I., Allen, G. J., Hugouvieux, V., Kwak, J. M., Waner, D. (2001) Guard cell signal transduction. Annu. Rev. Plant. Physiol. Plant Mol. Biol. 52, 627-658.

Schroeder, J.I., Raschke, K., Neher, E. (1987) Voltage dependence of K+ channels in guard-cell protoplasts. Proc Natl Acad Sci USA 84: 4108.

Sharma, B., Joshi, D., Yadav, P. K., Gupta, A. K., Bhatt, T. K. (2016) Role of ubiquitin-mediated degradation system in plant biology. Front Plant Sci. 7, 806.

Sheard, L. B., Zheng, N. (2009) Signal advance for abscisic acid. Nature 462, 575-576.

Shen, J., Gao, C., Zhao, Q., Lin, Y., Wang, X., Zhuang, X., and Jiang, L. (2016). AtBRO1 Functions in ESCRT-I complex to regulate multivesicular body protein sorting. Mol Plant. 9, 760-763.

Shen, J., Zhao, Q., Wang, X., Gao, C., Zhu, Y., Zeng, Y., and Jiang, L. (2018). A plant Bro1 domain protein BRAF regulates multivesicular body biogenesis and membrane protein homeostasis. Nat Commun. 9, 3784.

Shields, S.B., and Piper, R.C. (2011) How ubiquitin functions with ESCRTs. Traffic 12, 1306–1317.

Sierla, M., Waszczak, C., Vahisalu, T., Kangasjärvi, J. (2016) Reactive oxygen species in the regulation of stomatal movements. Plant Physiol. 171(3): 1569-1580.

Spallek, T., Beck, M., Ben Khaled, S., Salomon, S., Bourdais, G., Schellmann, S., Robatzek, S. (2013) ESCRT-I mediates FLS2 endosomal sorting and plant immunity. PloS Genetics. 9(12).

Sparkes, I.A., Runions, J., Kearns, A., and Hawes, C. (2006). Rapid, transient expression of fluorescent fusion proteins in tobacco plants and generation of stably transformed plants. Nat Protoc. 1, 2019-2025.

Spitzer, C., Schellmann, S., Sabovljevic, A., Shahriari, M., Keshavaiah, C., Bechtold, N., Herzog, M., Müller, S., Hanisch, F.G. and Hülskamp, M. (2006). The Arabidopsis *elch* mutant reveals functions of an ESCRT component in cytokinesis. Development 133, 4679-4689.

Spitzer, C., Schellmann, S., Sabovljevic, A., Shahriari, M., Keshavaiah, C., Bechtold, N., Herzog, M., Müller, S., Hanisch, F. –G., Hülskamp, M. (2006) The *Arabidopsis elch* mutant reveals functions of an ESCRT component in cytokinesis. 133, 4679-4689.

Squire, G.R., and Mansfield, T.A. (1972). Studies of the mechanism of action of fusicoccin, the fungal toxin that induces wilting, and its interaction with abscisic acid. Planta 105, 71-78.

Stone, S. L. (2019) Role of the ubiquitin proteasome system in plant response to abiotic stress. International review of cell and molecular biology. 343, chapter 3, 65-110.

Sun, S., Sun, L., Zhou, X., Wu, C., Wang, R., Lin, S. –H., Kuang, J. (2016) Phosphorylation-Dependent Activation of the ESCRT Function of ALIX in Cytokinetic

Abscission and Retroviral Budding. Developmental cell. 36(3), 331-343.

Sutter, J. –U., Sieben, C., Hartel, A., Eisenach, C., Thiel, G., Blatt, M. R. (2007) Abscisic acid triggers the endocytosis of the Arabidopsis KAT1 K^+ channel and its recycling to the plasma membrane. Current Biology. 17, 1396-1402.

Swaminathan, S., Amerik, A.Y., and Hochstrasser, M. (1999). The Doa4 deubiquitinating enzyme is required for ubiquitin homeostasis in yeast. Mol Biol Cell 10, 2583-2594.

Takahashi, F., Suzuki, T., Osakabe, Y., Betsuyaku, S., Kondo, Y., Dohmae, N., Fukuda, H., Yamaguchi-Shinozaki, K., Shinozaki, K. (2018). A small peptide modulates stomatal control via abscisic acid in long-distance signaling. Nature. 556(7700), 235–238.

Takano, J., Tanaka, M., Toyoda, A., Miwa, K., Kasai, K., Fuji, K., Onouchi, H., Naito, S., Fujiwara, T. (2010) Polar localization and degradation of Arabidopsis boron transporters through distinct trafficking pathways. Proc Natl Acad Sci USA. 107, 5220-5225.

To, A., Valon, C., Savino, G., Guilleminot, J., Devic, M., Giraudat, J. and Parcy, F. (2006). A network of local and redundant gene regulation governs Ara- bidopsis seed maturation. Plant Cell 18, 1642-1651.

Tuteja, N. (2007) Abscisic acid and abiotic stress signaling. Plants signaling and behavior. 2(3), 135-138.

Van Leene, J., Eeckhout, D., Persiau, G., Van De Slijke, E., Geerinck, J., Van Isterdael, G., Witters, E., De Jaeger, G. (2011) Isolation of transcription factor complexes from Arabidopsis cell suspension cultures by tandem affinity purification. Methods Mol Biol 754:195–218.

Van Leene, J., Witters, E., Inzé, D., De Jaeger, G. (2008) Boosting tandem affinity purification of plant protein complexes. Trends Plant Sci. 13: 517-520.

Vierstra, R. D. (2009) The ubiquitin-26S proteasome system at the nexus of plant biology. Nature Reviews Molecular Cell Biology. 10, 385-397.

Voinnet, O. (2003). RNA silencing bridging the gaps in wheat extracts. Trends Plant Sci. 8, 307-309.

Wang, P., Zhao, Y., Li, Z., Hsu, C. C., Liu, X., Fu, L., Hou, Y. J., Du, Y., Xie, S., Zhang, C., Gao, J., Cao, M., Huang, X., Zhu, Y., Tang, K., Wang, X., Tao, W. A., Xiong, Y., Zhu, J. K. (2018) Reciprocal Regulation of the TOR Kinase and ABA Receptor Balances Plant Growth and Stress Response. Molecular Cell. 69(1), 100-112.

Wang, X., Kota, U., He, K., Blackburn, K., LI, J., Goshe, M. B., Huber, S. C., Clouse, S. D. (2008) Sequential transphosphorylation of the BRI1/BAK1 receptor kinase complex impacts early events in brassinosteroid signaling. Dev Cell. 15, 220-235.

Ward, J.J., Sodhi, J.S., McGuffin, L.J., Buxton, B.F., and Jones, D.T. (2004). Prediction and functional analysis of native disorder in proteins from the three kingdoms of life. J. Mol Biol. 337, 635-645.

Weigel D, Glazebrook J (2002) Arabidopsis: A Laboratory Manual. CSHL Press.

Wemmer, M., Azmi, I., West, M., Davies, B., Katzmann, D., and Odorizzi, G. (2011). Bro1 binding to Snf7 regulates ESCRT-III membrane scission activity in yeast. J. Cell Biol. 192, 295-306.

Weng, J. –K., Ye, M., Li, B., Noel, J. P. (2016) Co-evolution of hormone metabolism and signaling networks expands plant adaptive plasticity. Cell. 166 (4), 881-893.

Winter, V., and Hauser, M.T. (2006). Exploring the ESCRTing machinery in eukaryotes. Trends Plant Sci. 11, 115-123.

Wright, M.H., Berlin, I., and Nash, P.D. (2011). Regulation of endocytic sorting by ESCRT-DUB-mediated deubiquitination. Cell Biochem Biophys. 60, 39-46.

Wu, Q., Zhang, X., Peirats-Llobet, M., Belda-Palazon, B., Wang, X., Cui, S., Yu, X., Rodriguez, P. L., An, C. (2016) Ubiquitin Ligases RGLG1 and RGLG5 Regulate Abscisic Acid Signaling by Controlling the Turnover of Phosphatase PP2CA. Plant Cell. 28, 2178–2198.

Yang, W., Zhang, W., Wang, X. (2017) Post-translational control of ABA signaling: the roles of protein phosphorylation and ubiquitination. Plant Biotech Journal. 15, 4-14.

Yoshinari, A., Fujimoto, M., Ueda, T., Inada, N., Naito, S., Takano, J. (2016) DRP1-Dependent Endocytosis is Essential for Polar Localization and Boron-Induced Degradation of the Borate Transporter BOR1 in Arabidopsis thaliana. Plant and Cell Physiology. 57, (9), 1985–2000.

Yu, F., Lou, L., Tian, M., Li, Q., Ding, Y., Cao, X., Wu, Y., Belda-Palazon, B., Rodriguez, P.L., Yang, S., and Xie, Q. (2016). ESCRT-I Component VPS23A Affects ABA Signaling by Recognizing ABA Receptors for Endosomal Degradation. Mol Plant. 9, 1570-1582.

Yu, X., Li, B., Jang, G. –J., Jiang, S., Jiang, D., Jang, J. –C., Wu, S. –H., Shan, L., He, P. (2019) Orchestration of processing body dynamics and mRNA decay in Arabidopsis immunity. Cell Reports. 28(8), 2194-2205.

Zhou, J., Liu, D., Wang, P., Ma, X., Lin, W., Chen, S., Mishev, K., Lu, D., Kumar, R., Vanhoutte, I., Meng, X., He, P., Russinova, E., Shan, L. (2018) Regulation of Arabidopsis brassinosteroid receptor BRI1 endocytosis and degradation by plant U-box PUB12/PUB13-mediated ubiquitination. Proc Natl Acad Sci USA. 115(8), 1906-1915.

9. SUPPLEMENTARY MATERIAL

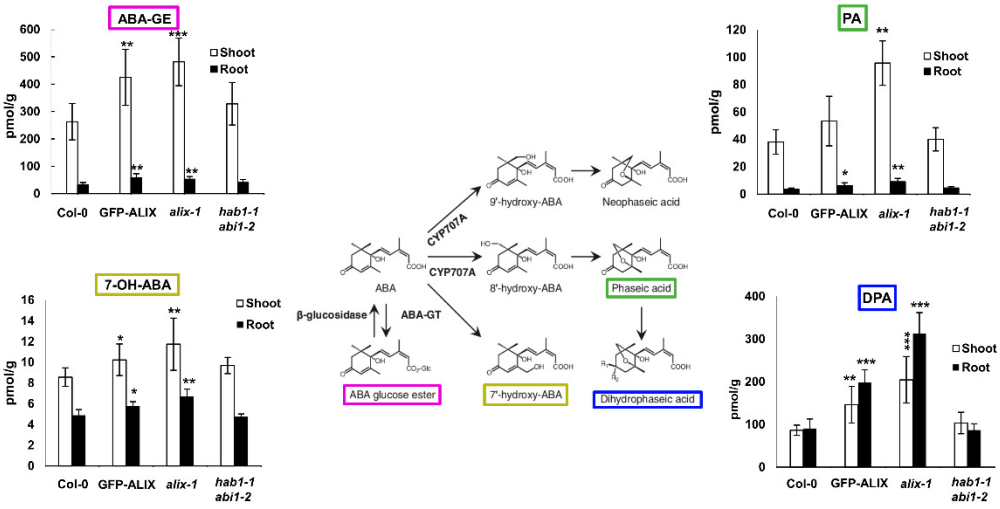

Supplemental figure 1. ABA catabolite levels are increased in *alix-1* mutants.

ABA-GE, DPA, PA and 7-OH-ABA concentration (pmol/g) was measures in shoot and roots of 14-d-old seedlings for wild-type (Col-0), GFP-ALIX and *alix-1* mutant. *hab1-1 abi1-2* mutants were used as the ABA hypersensitive control.

*p < 0.05; **p < 0.01 (Student's t-test) with respect to the wild –type in the same experimental conditions. Error bars represent SD.

Abbreviatures correspond to ABA-GE, ABA glucose-esther; DPA, dihydroxyphaseic acid; PA, phaseic acid.

Supplemental movie 1-5

Table 6. Lists of proteins identified as interacting with full length ALIX or ALIX fragments in yeast two hybrid assays.

The protein name and/or description found in The Arabidopsis Information Resource (TAIR; https://www.arabidopsis.org), functional categorization according to MapMan (http://mapman.gabipd.org/es/mapman), the Arabidopsis Genome Initiative (AGI) accession number, and the number of clones isolated for each protein are shown. Columns on the right indicate the conditions in which yeast clones were able to grow and an estimation of the strength of each interaction based on yeast growth under selective auxotrophies and presence of 3-amino-1,2,4-triazole (3-AT; being XXX the strongest interaction).

(A) Proteins that interact with full length ALIX

Identified proteins			Nº of clones	WL	WLA	WLH 0.5 mM 3-AT	WLAH 0.5 mM 3-AT
Function	Name	AGI					
Apoptosis	ATBAG3	AT5G07220	5	XX	XX	XX	XX
Chloroplast organization	NFU1	AT4G01940	1	XX	XX	X	X
Cyanase	CYANASE, CYN, MEE5.3	AT3G23490	1	XX		XX	X
Endomembrane system	Guanine nucleotide signalin family BIG1	AT4G38200	3	XX	XX	XX	XX
	Pentatricopeptide (PPR) repeat-containing protein	AT2G02150	2	XX	XX		
Electron carrier activity	Rieske (2Fe-2S) domain-containing protein	AT1G71500	1	XX	XX		X
Hidrolase	Heteroglycan Glucosidase 1 (HGL1)	AT3G23640	2	XX	XX	X	X
Kinase	AKIN10	AT3G01090	1	XX	XX	XX	XX
Photorespiration	Glycine decarboxylase complex H protein.	AT2G35370	1	XX		X	X
Signalosome	CSN5A (COP-9 subunity)	AT1G71230	3	XX		XX	XX
Molecular funtion unknown	F-Box family protein	AT5G56420	1	XX	XX	XX	XX
	Meprin and TRAF homology domain-containing protein	AT3G20370	11	XX	X		X
	NLI interacting factor	AT3G29760	1	XX		XX	X
	Unknown protein	AT1G53380	1	XX		XX	

(B) Proteins that interact with the Bro1 domain (1-143 aa)								
Identified proteins				Nº of clones	WL	WLA	WLH 0.5 mM 3-AT	WLAH 0.5 mM 3-AT
Function		Name	AGI					
Arginine metabolism		Arginase (putative)	AT4G08870	2	XX	XX	XX	XX
		Type I protein arginine methyltransferase	AT1G04870	1	XX	XX	XX	XX
Calcium binding		CAR8; C2 domain-containing protein;	AT1G23140	1	XX	XX	XX	XX
		CAR1; C2 domain-containing protein	AT5G37740	1	XX	XX	XX	XX
		CaLB domain family protein	AT1G07310	1	XX	X	XX	X
Cold tolerance		LOS2; copper ion binding	AT2G36530	1	XX	XX	XXX	XX
Electron carrier activity		Arabidopsis thaliana ATPC1	AT4G04640	1	XX	XXX	XXX	XXX
		Ferredoxin related	AT4G32590	2	XX	XX	XX	XX
		Respiratory burst oxidase (putative)	AT4G11230	1	XX	XX	XX	X
Endomembrane system		PHOSPHATIDYLINOSITOL 4-OH KINASE BETA1	AT5G64070	2	XX		XX	XX
Hormone response	ABA response	PYL9/ RCAR1 (ABA receptor)	AT1G01360	2	XX	XX	XX	XX
	Auxin response	IAA16; transcription factor	AT3G04730	2	XX	XX	XX	XX
Kinase		AKIN10	AT3G01090	1	XX	XX	XX	XX
mRNA processing		CSTF77, ATCSTF77	AT1G17760	1	XX	XX	XX	XX
Nitrate assimilation		ATGSR1; copper ion binding protein	AT5G37600	1	XX		XX	XX
Protein folding		DNAJ heat shock N-terminal domain-containing protein	AT2G01710	1	XX	XX	XX	XX
Protein Storage Vacuoling		SOYBEAN GENE REGULATED BY COLD-2	AT1G09070	10	XX	XX	XX	XX
Proton transport ATP synthase complex		ATP12 protein-related	AT5G40660	2	XX	XX	XX	XX
Pseudouridine synthase		Pseudouridine synthase family protein	AT1G56345	1	XX X	XXX	XXX	XXX
Signal recognition		signal recognition particle binding	AT2G18770	1	XX	XX	XX	XX
Translation		60S ribosomal protein L4/L1 (RPL4A)	AT3G09630	1	XX	XX	XX	XX
		60S ribosomal protein L4/L1 (RPL4D)	AT5G02870	1	XX	XX	XX	XX
Toxic catabolic process		ATGSTF14 | ATGSTF14; glutathione transferase	AT1G49860	2	XX	XX	XX	XX
Transcriptional regulation		NAD(P)-binding Rossmann-fold superfamily protein	AT4G35250	2	XX X	XXX	XXX	XXX
Transport channels		VDAC3, ATVDAC3	AT5G15090	4	XX	XX	XX	XX

(B) Proteins that interact with the Bro1 domain (1-143 aa)							
Identified proteins			Nº of clones	WL	WLA	WLH 0.5 mM 3-AT	WLAH 0.5 mM 3-AT
Function	Name	AGI					
Ubiquitin 112ignaling protein	UBQ1	AT3G52590	1	XX	XX	XX	XX
Molecular function unknown	Meprin and TRAF homology domain-containing protein	AT3G20360	1	XX	X	X	X
	Phosphoglycerate/bisphosphoglycerate mutase-related	AT1G09932	1	XX		XX	XXX
	Unknown protein	AT1G61170	1	XX	X	XX	X

(C) Proteins that interact with the ΔBro1 fragment (405-846 aa)							
Identified proteins			Nº of clones	WL	WLA	WLH 0.5 mM 3-AT	WLAH 0.5 mM 3-AT
Function	Name	AGI					
Calcium ion binding	Oxygen evolving enhancer 3 (PsbQ).	AT1G14150	1	XX	XX	XX	XX
Electron carrier activity	PETC, PGR1	AT4G03280	1	XX		XX	X
Endomembrane system	glycosyl hydrolase family protein 5 /signaling family protein	AT1G02310	1	XXX	XXX	XXX	XXX
Lipid metabolic process	Lipase class 3 family protein	AT5G18630	1	XX	XX	XX	XX
Gene silencing	ATSAHH1, DL3010W, EMB1395, HOG1	AT4G13940	1	XX	XX	XX	XX
Kinase	AKIN10	AT3G01090	1		XX	XX	XX
Phosphatydilinositol metabolic process	Phosphatidylinositol-4-phosphate 5-kinase family protein	AT1G71010	1	XX	XX	XX	XX
Photosynthesis	GAPA-1	AT3G26650	1	XX	XX	XX	X

(C) Proteins that interact with the ΔBro1 fragment (405-846 aa)							
Identified proteins			Nº of clones	WL	WLA	WLH 0.5 mM 3-AT	WLAH 0.5 mM 3-AT
Function	Name	AGI					
Protein Storage Vacuole targeting	SOYBEAN GENE REGULATED BY COLD-2	AT1G09070	2	XX	XX	XX	XX
Proteolisis	XBCP3 (xylem bark cysteine peptidase 3)	AT1G09850	2	XXX	XXX	XXX	XXX
SA response	ORG4 (OBP3-RESPONSIVE GENE 4)	AT2G06010	1	XX	XX	XX	XX
Translation	Dihydrouridine synthase family protein (tRNA)	AT4G38890	1	XX	XX	XX	XX
	Ribosomal protein S15 family protein	AT1G80620	1	XX	XX	XX	X
Ubiquitin 113ignaling protein	RUB1	AT1G31340	2	XX	XX	XX	XX
	UBQ1	AT3G52590	3	XX	XX	XX	XXX
	UBQ3	AT5G03240	1	XX	XX	X	XX
	UBQ6	AT2G47110	1	XX	XX	XX	XX
	UBQ10	AT4G05320	5	XX	XX	XX	XX
	UBQ11	AT4G05050	5	XX	XX	XX	XX
	UBQ14	AT4G02890	1	XX	XX	XX	XX
Molecular function unknown	Cadmium-responsive protein	AT4G19070	1	XX	XX	XX	XX
	Unknown protein	AT3G09860	1	XX	XX	XX	XX

Table 7. Lists of proteins identified as interacting with full length ALIX in tandem affinity purification assays (TAP)

Identified proteins		
Function	Name	AGI
cytoplasmic mRNA processing body assembly	PAT1H1	AT3G22270
	DEAD-box ATP-dependent RNA helicase 6;RH6	AT2G45810
	DEAD-box ATP-dependent RNA helicase 8;RH8	AT4G00660
regulation of translation	Polyadenylate-binding protein 5;PAB5	AT1G71770
	Polyadenylate-binding protein 2;PAB2	AT4G34110
	Pumilio homolog 5;APUM5	AT3G20250
	Pumilio homolog 6, chloroplastic;APUM6	AT4G25880
mRNA processing	Multiple organellar RNA editing factor 4, mitochondrial;MORF4	AT5G44780
	RNA-binding (RRM/RBD/RNP motifs) family protein;MNF13.1	AT5G40490
	PRP19B	AT2G33340
	RNA-binding (RRM/RBD/RNP motifs) family protein	AT3G07810
	Polyadenylate-binding protein RBP45B	AT1G11650
	RNA-binding protein 47C (RBP47C)	AT1G47490
	RNA-binding (RRM/RBD/RNP motifs)	AT3G07810
	RNA-binding (RRM/RBD/RNP motifs)	AT4G26650
	Proline-rich family protein;ELF5	AT5G62640
	Polyadenylate-binding protein RBP45A	AT5G54900
	Polyadenylate-binding protein RBP47C	AT1G47500
	Oligouridylate-binding protein 1A;UBP1A	AT1G54080
	Multiple organellar RNA editing factor 1;MORF1	AT4G20020
	RNA-binding (RRM/RBD/RNP motifs) family protein	AT1G22910
	DExH-box ATP-dependent RNA helicase DExH13	AT2G42270
mRNA binding	RNA-binding KH domain-containing protein	AT2G38610
	evolutionarily conserved C-terminal region 1 (ECT1)	AT3G03950
	evolutionarily conserved C-terminal region 10 (ECT10)	AT5G58190
	evolutionarily conserved C-terminal region 3 (ECT3)	AT5G61020
	evolutionarily conserved C-terminal region 4 (ECT4)	AT1G55500
	evolutionarily conserved C-terminal region 5 (ECT5)	AT3G13060
	evolutionarily conserved C-terminal region 6 (ECT6).	AT3G17330
	RNA-binding (RRM/RBD/RNP motifs) family protein	AT3G15010
	RNA-binding (RRM/RBD/RNP motifs) family protein	AT3G13224

Identified proteins		
Function	**Name**	**AGI**
	KH domain-containing protein	AT1G33680
	hydroxyproline-rich glycoprotein family protein	AT1G14710
damaged DNA binding	DNA repair metallo-beta-lactamase family protein	AT1G19025
nucleotide binding	P-loop containing nucleoside triphosphate hydrolases superfamily protein	AT4G24710
	Zinc finger C-x8-C-x5-C-x3-H type family protein	AT3G06410
	C2H2 and C2HC zinc fingers superfamily protein	AT3G05760
	Zinc finger C-x8-C-x5-C-x3-H type family protein	AT5G18550
	BRAT1 PARTNER 1, BRP1	AT3G15120
DNA-binding	G-BOX BINDING FACTOR 3, GBF3	AT2G46270
	basic helix-loop-helix (bHLH) DNA-binding superfamily protein	AT5G43175
	bromodomain and extraterminal domain protein 9 (BET9)	AT5G14270
	bromodomain and extraterminal domain protein 10 (BET10)	AT3G01770
	ANAC010; NAC domain containing protein 10 (NAC010)	AT1G28470
ATP binding	ABCF4, ATGCN4, ATP-BINDING CASSETTE F4	AT3G54540
	ABCC11; member of MRP subfamily	AT1G30420
	ACLB-1, ATP-CITRATE LYASE SUBUNIT B-1	AT3G06650
	ACLB-2, ATP CITRATE LYASE SUBUNIT B-2	AT5G49460
methyl-CpG-binding	ARABIDOPSIS THALIANA METHYL-CPG-BINDING DOMAIN 7, ATMBD7	AT5G59800
F-box/RNI-like superfamily protein	RNI-like superfamily protein	AT3G58890
Protein binding	GFS12, GREEN FLUORESCENT SEED 12	AT5G18525
	HEMC/RUG1	AT5G08280
	phospholipase D (PLDbeta)	AT2G42010
Zinc ion binding	gamma subunit of Mt ATP synthase (ATP3)	AT2G33040
Methyltransferase	LCMT1, LEUCINE CARBOXYL METHYL TRANSFERASE 1, SBI1, SUPPRESSOR OF BRI1	AT1G02100
	PRMT4b	AT3G06930
H+-ATPase	AHA10; belongs to H+-APTase gene family	AT1G17260
Dehydrogenase	6-phosphogluconate dehydrogenase family protein	AT1G64190
Leucin rich receptor (LRR)	Disease resistance protein (TIR-NBS-LRR class) family	AT2G16870
Metallochaperone activity	manganese tracking factor for mitochondrial SOD2 (MTM1)	AT4G27940
Kinase activity	Serine/threonine kinase (LRR)	AT5G01950

Identified proteins		
Function	**Name**	**AGI**
	Protein kinase capable of phosphorylating tyrosine, serine, and threonine residues	AT1G07570
FRIGIDA-like	FRIGIDA-like protein	AT3G22440
	FRIGIDA-like protein	AT5G48385
Endomembrane system	SNF7.2	AT2G19830
	Endosomal targeting BRO1-like domain-containing protein	AT1G15130
	SH3P2; SH3 domain-containing protein.	AT4G34660
	Calcium-dependent lipid-binding (CaLB domain) family protein	AT4G34150
	EXT12; Proline-rich extensin-like family protein (cell wall)	AT2G43150
	PELPK2; hydroxyproline-rich glycoprotein family protein (cell wall)	AT5G09520
Molecular function unknown	unknown protein	AT3G56250
	DNA topoisomerase 4 subunit B (DUF810)	AT4G11670
	unknown protein	AT3G56250
	MAK16 protein-related	AT1G23280
	Tetratricopeptide repeat (TPR)-like superfamily protein	AT4G39820
	DAW1, DUO1-ACTIVATED WD40 11.	AT4G35560
	ALKBH10A, ATALKBH10A oxidoreductase, 2OG-Fe(II) oxygenase family protein	AT2G48080
	Carboxylate clamp (CC)-tetratricopeptide repeat (TPR) proteins	AT5G10090

10. ANNEXES

- Arabidopsis ALIX regulates stomatal aperture and turnover of ABA receptors
- Tandem affinity purification of protein complexes from Arabidopsis cell cultures